

Review

Physics and technology considerations for the deuterium–tritium fuel cycle and conditions for tritium fuel self sufficiency

Mohamed Abdou^{1,*}, Marco Riva¹, Alice Ying¹, Christian Day², Alberto Loarte³, L.R. Baylor⁴, Paul Humrickhouse⁵, Thomas F. Fuerst⁵ and Seungyon Cho⁶

¹ University of California, Los Angeles (UCLA), United States of America

² Karlsruhe Institute of Technology (KIT), Germany

³ ITER Organization, Route de Vinon-sur-Verdon, CS90046, 13067 St Paul-lez-Durance, France

⁴ Oak Ridge National Laboratory (ORNL), United States of America

⁵ Idaho National Laboratory (INL), United States of America

⁶ National Fusion Research Institute (NFRI), Korea, Republic Of

E-mail: abdou@fusion.ucla.edu

Received 22 June 2020, revised 16 September 2020

Accepted for publication 7 October 2020

Published 23 November 2020



CrossMark

Abstract

The tritium aspects of the DT fuel cycle embody some of the most challenging feasibility and attractiveness issues in the development of fusion systems. The review and analyses in this paper provide important information to understand and quantify these challenges and to define the phase space of plasma physics and fusion technology parameters and features that must guide a serious R & D in the world fusion program. We focus in particular on components, issues and R & D necessary to satisfy three ‘principal requirements’: (1) achieving tritium self-sufficiency within the fusion system, (2) providing a tritium inventory for the initial start-up of a fusion facility, and (3) managing the safety and biological hazards of tritium. A primary conclusion is that the physics and technology state-of-the-art will not enable DEMO and future power plants to satisfy these principal requirements. We quantify goals and define specific areas and ideas for physics and technology R & D to meet these requirements. A powerful fuel cycle dynamics model was developed to calculate time-dependent tritium inventories and flow rates in all parts and components of the fuel cycle for different ranges of parameters and physics and technology conditions. Dynamics modeling analyses show that the key parameters affecting tritium inventories, tritium start-up inventory, and tritium self-sufficiency are the tritium burn fraction in the plasma (f_b), fueling efficiency (η_f), processing time of plasma exhaust in the inner fuel cycle (t_p), reactor availability factor (AF), reserve time (t_r) which determines the reserve tritium inventory needed in the storage system in order to keep the plant operational for time t_r in case of any malfunction of any part of the tritium processing system, and the doubling time (t_d). Results show that $\eta_f f_b > 2\%$ and processing time of 1–4 h are required to achieve tritium self-sufficiency with reasonable confidence. For $\eta_f f_b = 2\%$ and processing time of 4 h, the tritium start-up inventory required for a 3 GW fusion reactor is ~ 11 kg, while it is < 5 kg if $\eta_f f_b = 5\%$ and the processing time is 1 h. To achieve these stringent requirements, a serious R & D program in physics and technology is necessary. The EU-DEMO direct internal recycling concept that carries fuel

* Author to whom any correspondence should be addressed.

directly from the plasma exhaust gas to the fueling systems without going through the isotope separation system reduces the overall processing time and tritium inventories and has positive effects on the required tritium breeding ratio (TBR_R). A significant finding is the strong dependence of tritium self-sufficiency on the reactor availability factor. Simulations show that tritium self-sufficiency is: impossible if $AF < 10\%$ for any $\eta_i f_b$, possible if $AF > 30\%$ and $1\% \leq \eta_i f_b \leq 2\%$, and achievable with reasonable confidence if $AF > 50\%$ and $\eta_i f_b > 2\%$. These results are of particular concern in light of the low availability factor predicted for the near-term plasma-based experimental facilities (e.g. FNSF, VNS, CTF), and can have repercussions on tritium economy in DEMO reactors as well, unless significant advancements in RAMI are made. There is a linear dependency between the tritium start-up inventory and the fusion power. The required tritium start-up inventory for a fusion facility of 100 MW fusion power is as small as 1 kg. Since fusion power plants will have large powers for better economics, it is important to maintain a 'reserve' tritium inventory in the tritium storage system to continue to fuel the plasma and avoid plant shutdown in case of malfunctions of some parts of the tritium processing lines. But our results show that a reserve time as short as 24 h leads to unacceptable reserve and start-up inventory requirements. Therefore, high reliability and fast maintainability of all components in the fuel cycle are necessary in order to avoid the need for storing reserve tritium inventory sufficient for continued fusion facility operation for more than a few hours. The physics aspects of plasma fueling, tritium burn fraction, and particle and power exhaust are highly interrelated and complex, and predictions for DEMO and power reactors are highly uncertain because of lack of experiments with burning plasma. Fueling by pellet injection on the high field side of tokamak has evolved to be the preferred method to fuel a burning plasma. Extrapolation from the DIII-D penetration scaling shows fueling efficiency expected in DEMO to be $<25\%$, but such extrapolations are highly uncertain. The fueling efficiency of gas in a reactor relevant regime is expected to be extremely poor and not very useful for getting tritium into the core plasma efficiently. Gas fueling will nonetheless be useful for feedback control of the divertor operating parameters. Extensive modeling has been carried out to predict burn fraction, fueling requirements, and fueling efficiency for ITER, DEMO, and beyond. The fueling rate required to operate $Q = 10$ ITER plasmas in order to provide the required core fueling, helium exhaust and radiative divertor plasma conditions for acceptable divertor power loads was calculated. If this fueling is performed with a 50–50 DT mix, the tritium burn fraction in ITER would be $\sim 0.36\%$, which is too low to satisfy the self-sufficiency conditions derived from the dynamics modeling for fusion reactors. Extrapolation to DEMO using this approach would also yield similarly low burn fraction. Extensive analysis presented shows that specific features of edge neutral dynamics in ITER and fusion reactors, which are different from present experiments, open possibilities for optimization of tritium fueling and thus to improve the burn fraction. Using only tritium in pellet fueling of the plasma core, and only deuterium for edge density, divertor power load and ELM control results in significant increase of the burn fraction to 1.8–3.6%. These estimates are performed with physics models whose results cannot be fully validated for ITER and DEMO plasma conditions since these cannot be achieved in present tokamak experiments. Thus, several uncertainties remain regarding particle transport and scenario requirements in ITER and DEMO. The safety standard requirements for protection of the public and release guidelines for tritium have been reviewed. General safety approaches including minimizing tritium inventories, reducing tritium permeation through materials, and decontaminating material for waste disposal have been suggested.

Keywords: tritium, fuel cycle, self-sufficiency, tritium burn fraction, fueling efficiency, initial startup inventory, burning plasma

(Some figures may appear in colour only in the online journal)

Contents

1. Introduction	4	6. Plasma physics aspects of the tritium burn fraction and predictions for ITER and beyond	21
2. Outline description of the fuel cycle	4	6.1. Introduction and simple estimates of the tritium burn fraction in ITER	21
2.1. Inner fuel cycle: tritium storage, fueling, exhaust, fuel clean-up and processing systems	4	6.2. Refinement of the tritium burn fraction in ITER by sophisticated edge plasma and edge-core plasma integrated modeling	22
2.2. Outer fuel cycle: tritium extraction systems from blanket, plasma facing components, and coolant	5	6.2.1. Open physics/scenario integration issues impacting the prediction of the TBF in ITER	23
3. Dynamic fuel cycle models to determine time-dependent tritium flow rates and inventories, and perform self-sufficiency analysis and start-up assessment	6	6.3. Possible differences between ITER and DEMO impacting the TBF	25
3.1. Formulation of the dynamic model	6	6.4. Summary and conclusions for plasma physics aspects of the tritium burn fraction	26
3.2. Tritium self-sufficiency condition	6	7. Plasma fueling technology and predictions of fueling efficiency for ITER and DEMO based on experiments and modeling	27
3.3. The achievable tritium breeding ratio	7	7.1. Fueling technology background	27
3.4. Tritium burn fraction	8	7.2. Fueling efficiency data from tokamaks	28
3.5. Evaluation of start-up inventory and required TBR	9	7.3. Fueling of ITER and DEMO burning plasmas	29
3.6. Reactor availability factor modeling	10	7.4. Anticipated fueling efficiency and implications	30
3.7. Reference parameters for various subsystems in the fuel cycle	10	8. Tritium safety	30
4. Tritium inventories and tritium self-sufficiency analysis	11	8.1. Tritium hazards and regulations	30
4.1. Calculation of tritium inventory in various systems as function of key physics and technology parameters	11	8.2. Tritium permeation and management	32
4.2. Physics and technology parameters window for tritium self-sufficiency	12	9. Options for tritium fuel cycle technology for DEMO and required R & D	34
4.2.1. Effect of tritium burn fraction, fueling efficiency, and tritium processing time on tritium self-sufficiency	13	9.1. Vacuum pumping	34
4.2.2. Self-sufficiency analysis during different stages of nuclear fusion development: the effect of reactor availability factor	13	9.1.1. Fuel separation	35
4.2.3. Mitigation of TBR requirements via direct internal recycling	14	9.2. Fuel clean-up	36
4.2.4. Penetration of fusion energy into power market	15	9.3. Isotope separation system (ISS)	37
5. Calculation of the required tritium start-up inventory and assessment of the availability of external tritium supply for start-up of near- and long-term fusion facilities	15	9.3.1. Isotope rebalancing and protium removal (IRPR)	37
5.1. Availability of external tritium supply	16	9.4. Exhaust detritiation (EDS) and water detritiation system (WDS)	37
5.2. Dependence of tritium startup inventory on burn fraction, fueling efficiency and processing time	16	9.5. Coolant purification system (CPS)	38
5.3. Reduction of required tritium start-up inventory via direct internal recycling	17	9.6. Tritium extraction system (TES)	38
5.4. The necessity of high fuel cycle reliability to reduce the reserve inventory	17	9.7. Fueling system	39
5.5. Dependence of tritium start-up inventory on fusion power	18	10. Summary	39
5.6. Other remarks on tritium start-up inventory	19	Acknowledgments	42
		Appendix A. Mathematical formulation of the tritium fuel cycle dynamics model	45
		References	47

1. Introduction

The tritium aspects of the deuterium–tritium (DT) fuel cycle embody some of the most challenging feasibility and attractiveness issues in the development of fusion systems. The purpose of this paper is to review and analyze the DT fuel cycle with the goal to understand and quantify these challenges and to define the phase space of plasma physics and fusion technology parameters and features that must guide a serious R & D in the world fusion program.

The world effort on development of fusion energy systems is focused on the DT fuel cycle. Tritium is a dominant consideration in the development and operation of fusion systems for several key reasons. Although deuterium is naturally abundant in Earth's oceans, tritium is rare in nature because it is radioactive with a relatively short half-life of 12.32 years. Tritium can be generated by interaction of neutrons and lithium. However, tritium consumption in fusion systems is huge: 55.8 kg per 1000 MW fusion power per year. In contrast, tritium production in especially designed fission reactors is <0.5 kg per year. Furthermore, the tritium injection rate into the plasma must be a factor of 20 to 200 times the tritium consumption rate by fusion reactions because of the short particle confinement time in the plasma. In addition, processing of tritium from the plasma exhaust and other components of the fusion system involves processes that take significant time. Therefore, the amount of tritium to be managed in a fusion power plant is several orders of magnitude larger than the quantities of tritium that have been handled in fission reactors and other applications to date. These and other considerations clearly indicate that there are three major requirements that are critical for the successful development and safe operation of fusion facilities:

- (1) Achieving tritium self-sufficiency within the fusion system
- (2) Providing a tritium inventory for the initial start-up of a fusion facility
- (3) Managing the safety and biological hazards of tritium

Understanding, modeling, and analyzing these three major requirements are primary focuses in this paper. These three areas are very complex function of the physics and technology aspects of the fusion system. Of particular concern is that detailed analysis shows that extrapolation of the state-of-the-art in plasma physics and fusion technology to future DEMO and power plants require extensive programs of R & D whose outcome cannot be assured. These serious issues were addressed in a number of publications over the past three decades (see for example, references [1–15]). Although progress has been made in some areas, there are persistent challenges for which no solutions have yet been found. We hope that the careful, relatively detailed analysis in this paper can stimulate new ideas and approaches toward meeting the principal requirements of the DT fuel cycle.

In this paper, we also address the tritium issues and requirements for each step in the sequence of fusion development. Current scenarios for fusion development envision a number of near-term DT fusion development facilities, e.g. VNS, CTF,

FNSF, (see for example, references [4, 16]) followed by two or three DEMO facilities around the world that can demonstrate engineering feasibility, economic potential and safe operation. The success of DEMO would lead to a phase of power plant entry into the marketplace, which in turn would lead to a large number of fusion power plants that grow according to the normal growth rates of the electric power market. We elucidate the tritium issues and requirement for each step in the sequence of fusion facilities. One example is reliability and availability which will progress from low values in early fusion development facilities to much higher values in DEMO and still much higher in power plants. We show that availability has major impact on the ability to achieve tritium self-sufficiency.

Because of tritium radioactive decay and the time for processing tritium, dynamic modeling of the fuel cycle is used in this paper as the basis for calculating time-dependent tritium flow rates and inventories in various systems. The dynamic fuel cycle model was first introduced in 1986 [1]. We upgraded this dynamic model capability to investigate some parameters and system features not addressed previously.

This paper has ten sections. Section 2 provides a description of the overall fuel cycle including the inner and outer fuel cycles. Section 3 describes the formulation of a dynamic fuel cycle model to determine time-dependent tritium flow rates and inventories. Section 4 is devoted to calculations and analysis of the physics and technology parameters window for tritium self-sufficiency. Section 5 presents the results of the calculation of the required start-up tritium inventory as well as an assessment of the availability of external tritium supply for start-up of near- and long-term fusion facilities. Section 6 addresses the plasma physics aspects of the tritium burn fraction and predictions for ITER and beyond. Section 7 describes the plasma fueling technology and presents predictions of fueling efficiency for ITER and DEMO based on experiments and modeling. Section 8 summarizes tritium safety issues. Section 9 describes options for the DT fuel cycle technology for DEMO and required R & D. The paper concludes with a summary.

2. Outline description of the fuel cycle

The fuel cycle of a fusion reactor includes two sub-cycles: (1) the inner fuel cycle (IFC), i.e. plasma exhaust (vacuum pump), fuel clean-up, isotope separation, water detritiation, storage and management, and fueling systems, and (2) the outer fuel cycle (OFC), i.e. first wall, divertor, breeding zone (BZ), coolant processing and tritium extraction system. A schematic of a typical fusion fuel cycle and tritium flow rates is shown in the block diagram of figure 1. The next two subsections will discuss details of the inner and outer fuel cycles, respectively.

2.1. Inner fuel cycle: tritium storage, fueling, exhaust, fuel clean-up and processing systems

A tritium start-up inventory is necessary to start DT reactor operation. Tritium in the form of hydrides is initially stored in apposite metal beds (e.g. depleted uranium). The tritium

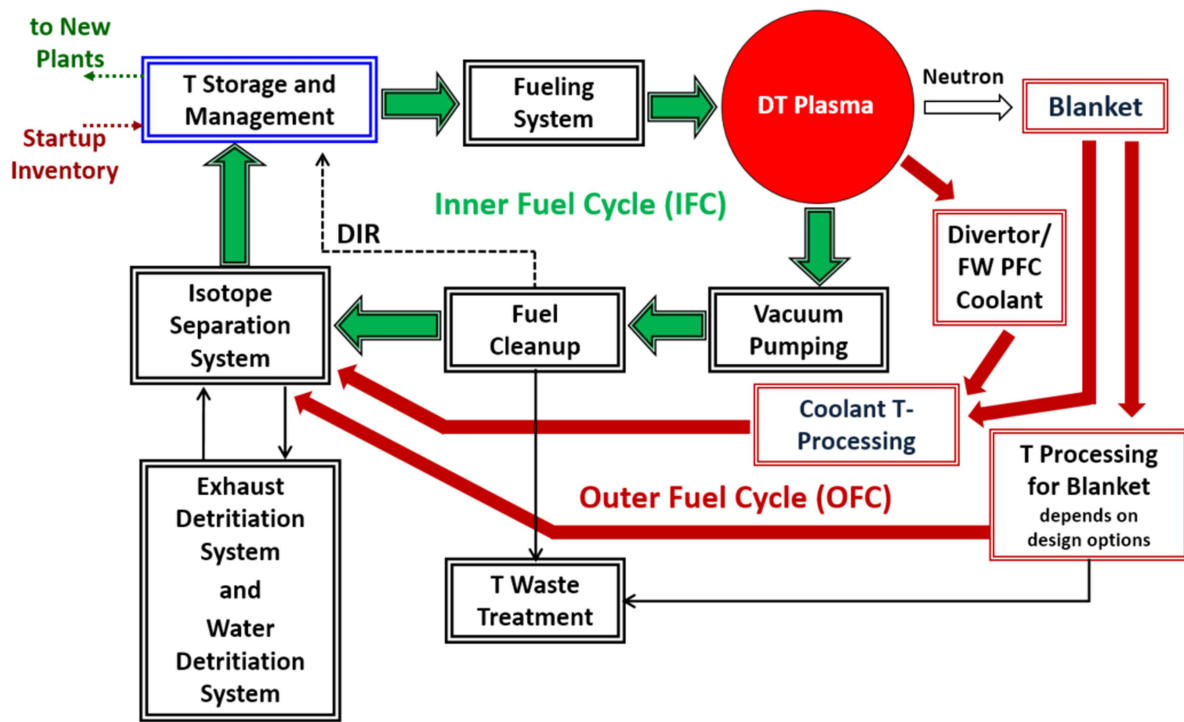


Figure 1. Schematic of main components of fusion inner and outer fuel cycles showing main tritium flow rates in fusion systems.

storage and management system is connected to the fueling system where D and T are prepared to fuel the plasma. Most common techniques are: (i) injection of frozen pellets at high speed—pellet velocity of $\sim 1000 \text{ m s}^{-1}$ is necessary to reach the plasma core more efficiently, and (ii) gas puffing. Note that only a fraction of the injected fuel particles proportional to the fueling efficiency reaches the plasma core whereas the remaining fraction of fuel is exhausted through the scrape-off layer (SOL) to the vacuum pumps, together with the unburned fraction of tritium from the plasma. The fraction of tritium that reaches the plasma and undergoes fusion reaction before it escapes the confinement is called tritium burn fraction (TBF). In other words, TBF is the probability that a tritium atom injected into the plasma will be consumed in a fusion reaction before it diffuses out of the plasma. In the IFC, tritium fluxes exhausted from the plasma through the vacuum pump are processed in order to obtain the adequate level of purity, physical form, and required DT ratio to fuel the plasma. In particular, exhausted fluxes from the plasma are pumped to the fuel clean-up compartments where plasma enhancement gases (PEG), e.g. Ar, Ne, N, etc, and helium ashes are separated from hydrogenic species with the use of diffusers, e.g. Pd–Ag alloy, and catalytic reactors with Pd membrane. After clean up, hydrogen isotopologues (H_2 , D_2 , T_2 , HD, HT, and DT) reach the isotope separation system (ISS). This is typically a set of differently sized cryogenic distillation columns which performs isotope separation exploiting a sensible difference in the boiling points of H_2 , and T_2 , respectively, 20 and 25 K. This technology is the most promising among the candidates (e.g. gas chromatography, thermal diffusion method, etc) because it can process large flow rates and maintain high separation factor, but has the downside of holding tritium for

long times (\sim hours) thus increasing the tritium inventory in the component. In order to maintain the discharge of tritium below the regulatory discharge limits (see section 8), the exhaust detritiation system (EDS) extracts tritium and converts it to tritiated water which is in turn fed to the water detritiation system (WDS) where tritium removal is performed through several chemical exchange columns (e.g. water vapor/HT). Finally, we added the direct internal recycling (DIR) line, proposed by the EU-DEMO team [6, 13, 14, 17, 30, 191], which carries pure fuel from the exhaust gas to the storage and management system and therefore helps to reduce tritium inventories in the IFC. Analyses of the DIR provided in sections 4 and 5 show the benefit of this technology on tritium self-sufficiency and start-up inventory reduction. A comprehensive description of the DIR process, the technology involved, and necessary R & D is provided in section 9.

2.2. Outer fuel cycle: tritium extraction systems from blanket, plasma facing components, and coolant

Two lines characterize the OFC: (i) tritium extraction system (TES) for the blanket and (ii) coolant purification system (CPS). Tritium generated in the BZs of blankets is released from lithium containing materials (ceramics, liquid metals, or molten salt) and carried to the TES unit where tritium is separated from its carrier, e.g. helium purge gas for ceramic breeders or eutectic lithium–lead for liquid metal concepts. The recovered tritium flows to the ISS in the IFC for further processing. High tritium fluxes from plasma, i.e. charge exchange neutrals (CXN) and ions, are implanted into plasma facing components (PFCs), i.e. first wall and divertor, generating tritium build-up inventory. Driven by concentration and thermal gradients, part of this tritium diffuses through

structural material of PFCs and permeates to coolant channels. Thus, the coolant with some tritium content reaches the heat exchanger and the CPS units which monitor and control tritium amount in coolant which has implications to safety, e.g. tritium permeation from coolant loop to reactor buildings and environment. Finally, the hydrogenic species recovered by the CPS units flow to the ISS in the inner part of the fuel cycle.

3. Dynamic fuel cycle models to determine time-dependent tritium flow rates and inventories, and perform self-sufficiency analysis and start-up assessment

Because of the relatively short half-life of tritium radioactive decay and the relatively long time for processing tritium, dynamic modeling of the fuel cycle is essential for calculating time-dependent tritium flow rates and inventories in various systems. The dynamic fuel cycle model was first introduced in 1986 [1] and further improved in 2015 [3] and in 2020 [5]. For this paper, we upgraded this dynamic model capability to investigate some additional parameters and system features not addressed previously. This section describes the model, which is the basis for analysis in section 4 of tritium inventories and self-sufficiency and in section 5 on the required start up inventory.

3.1. Formulation of the dynamic model

The approach used in the fuel cycle modeling follows the resident time method proposed in reference [1] and adopted later by many researchers (e.g. references [2–5, 7–11]). The overall fusion fuel cycle is described by a system of time-dependent zero-dimensional ordinary differential equations (ODEs). Each component i is characterized by a typical tritium residence time (τ_i) characteristic of the technology, a tritium inventory (I_i), a tritium flow rate from component j to component i (I_j/τ_j) _{i} and $j \neq i$, and a tritium flow rate out of component i (I_i/τ_i). We include a tritium source term (S_i) for component i (tritium generation is typically only in blankets). Tritium losses are modeled as non-radioactive losses (ε_i) and losses due to radioactive decay (λ is the tritium decay rate) in each component.

Thus, we can derive the system of ODEs describing the fuel cycle in the form:

$$\frac{dI_i}{dt} = \sum_{j \neq i} \left(\frac{I_j}{\tau_j} \right)_i - (1 + \varepsilon_i) \frac{I_i}{\tau_i} - \lambda I_i + S_i \quad (3.1)$$

In this work, we use the upgraded fuel cycle model to obtain a system of ODEs representing the fuel cycle by applying equation (3.1) to every fuel cycle compartment. A detailed schematic of the fuel cycle and the system of ODEs (equations (A.1)–(A.12)) obtained is given in the appendix A. Refer to reference [5] for further detail.

The model tracks tritium inventory build-up and tritium flow rates into and out of the fuel cycle components. The performance of each component is modeled by a number of characteristic parameters (e.g. residence and processing times,

tritium extraction and fueling efficiency, etc) representative of each technology. No effort is spent to solve any transport phenomena and/or chemical balance in detail with typical numerical method used for dimensional modeling. Instead, our modeling technique can be classified as system-level simulation (SLS), i.e. a simulation where the level of detail is adjusted to the practical simulation of large and complex systems, which comprehends various components that are usually not completely defined. Thus, the model does not require a detailed knowledge of each part of the system and can serve as a precious tool to investigate the performance of the overall system in the early stages of conceptual design. This choice allows overcoming some challenging issues of fuel cycle modeling:

- (a) Self-sufficiency analysis requires a computational technique which ensures simulations of reactor performances over a reactor lifetime, i.e. ~ 30 years. Thus, the computational technique must ensure acceptable computational times;
- (b) Several components of fuel cycle system are still in conceptual design phase. Therefore, detailed modeling may not be practical. Modeling of components as black boxes, with an associated residence time, is more practical and yields results useful to understanding the overall system behavior and the importance of certain components and parameters.

Our model may also be used for sensitivity analyses and gives helpful information back to the system level designers, e.g. on acceptable residence times, and hence directly influence technology choices. Note that detailed models of fuel cycle components, where constitutive governing equations are numerically solved, exist in literature, e.g. for the helium coolant ceramic reflector test blanket module (HCCR-TBM) [5, 22–25]. Further advancement of OFC modeling was shown in [26, 27], where the authors integrated the detailed model to system level in order to represent typical tritium streams. Despite the improvements in the computational technique used for this kind of modeling, high fidelity models require a significant computational power. Thus, simulations are possible only on short time scales, e.g. a few days, and, therefore, unpractical for extending the analysis over reactor's lifetime. However, the higher fidelity of these models provides various data, e.g. processing times, permeation rates, losses to environment, etc, which can constitute precious input to maintain high accuracy in residence time models, which embrace longer time scales.

3.2. Tritium self-sufficiency condition

Tritium must be generated in sufficient quantities and extracted efficiently to ensure tritium self-sufficiency. According to references [1–4], the tritium self-sufficiency condition is defined as:

$$TBR_A \geq TBR_R \quad (3.2)$$

The self-sufficiency condition is met if the achievable TBR (TBR_A) is greater than or equal to the required TBR (TBR_R). The achievable TBR is how much tritium can actually be produced per fusion neutron in the blanket in practical fusion

system. A description of the achievable TBR is presented in section 3.3. The required TBR is the tritium breeding ratio which is required in order to have a self-sufficient fuel cycle. TBR_R must exceed unity by a margin sufficient to:

- (a) Compensate for tritium losses by radioactive decay (5.47% per year) during time between production and use, and during fusion system shutdown;
- (b) Supply tritium inventory for start-up of other reactors (for a specified doubling time);
- (c) Provide a ‘reserve’ inventory necessary for continued reactor operation under certain conditions, e.g. a failure in a tritium processing system (this ‘reserve’ inventory will be part of the inventory stored in the tritium storage and management system).

Attaining tritium self-sufficiency is absolutely necessary for DT fusion energy systems to be feasible, since tritium is not a natural element present in nature and resources from production in non-fusion facilities are extremely limited. Furthermore, achieving tritium self-sufficiency depends on complex interactions of plasma physics and fusion technology parameters. In addition, DT fusion reactors require an initial tritium start-up inventory in order to start operation. This is necessary because there is a time lag between tritium production and usage due to a characteristic time needed for tritium processing in the fuel cycle components, i.e. the tritium processing time, and because of the initial tritium inventory build-up in components of the fuel cycle. Large start-up inventory is of concern since there is no practical external resources of tritium: current reserves are irrelevant in a temporal horizon of 20–30 years or longer as tritium quickly decays (half-life 12.32 years), and tritium production in fission reactors and/or accelerator seems economically prohibitive (further details regarding tritium sources is given in section 5). In order to operate fusion reactors, e.g. the DEMO reactors designed by different countries, the required tritium start-up inventory must be minimized. Furthermore, low initial inventory reduces the risk associated with high amounts of radioactive material, as explained in section 8.

3.3. The achievable tritium breeding ratio

The achievable TBR is the amount of tritium that can be produced per fusion neutron in the blanket in practical fusion system. The achievable TBR is a function of technology, material and physics design, and operating conditions. A comprehensive analysis of the many aspects of the achievable TBR was made by Abdou *et al* in reference [1]. Subsequently, a large number of integral experiments for fusion blanket neutronics was conducted using DT neutrons at the fusion neutronics source facility as part of a 10 years collaborative program between the Japanese Atomic Energy Institute and USA [34]. These integral experiments enabled quantitative evaluation of the uncertainties in predicting the achievable TBR due to calculation methods, codes, and nuclear data. Additional detailed neutronics calculations of the impact of various materials, design options, and physics and technology choices on the achievable TBR were reported in reference [3]. There have

been many calculations of tritium breeding by many authors over many years, but references [1, 3, 34] represent the state-of-the-art evaluation of the achievable TBR and associated uncertainties, which we will summarize briefly below. Further advances in the state-of-the-art will not be possible prior to performing experiments in DT fusion facilities, as we will also explain below.

Analysis of current worldwide FW/blanket concepts shows that achievable TBR for the most detailed blanket system designs available is ≤ 1.15 [3]. But we must account for uncertainties. Uncertainties in calculating the achievable TBR are in *three areas*:

(i) *System definition.* Achievable TBR depends on many system parameters and design considerations that are not yet well defined (e.g. amount and configuration of structure, required FW thickness, using separate coolant and/or neutron multiplier, need for electric insulator, chamber penetrations, absorbing materials in plasma-stabilizing shells, divertors, and plasma heating/CD systems). No blanket has been built or tested yet. Available conceptual designs try to be optimistic to obtain high TBR, for example, by using very thin first wall of ~ 1 – 2.5 cm and minimizing the structure content in the blanket. In comparison, the ITER first wall design is ~ 7 cm thick, and TBR would be much less than unity if any future fusion system would use ITER-type FW. Note that up to 30% reduction in TBR could result from using 20% of the blanket volume for structure [3]. Physics requirements on the blanket in future fusion systems, such as presence of non-breeding materials for stabilizing shells, penetrations for heating, current drive, and other purposes, are not yet firmly established and can result in a substantial reduction in the achievable TBR.

(ii) *Modeling and calculation method.* There have been major advances in neutron transport calculation methods and codes since the early 1970s. Powerful Monte Carlo and discrete-ordinates (Sn) codes have been developed based on significant improvements in the methods and utilizing the tremendous progress in speed, storage capacity, and faster data handling of modern computers. These advances enabled simulation of neutron transport in blankets in 3D geometry with considerable details not possible 20 years ago, (see for example, reference [18–20]). Furthermore, CAD-based interface programs have been developed to achieve the bi-directional conversion between commercial CAD systems and the neutron transport simulation codes (see for example, reference [38]). These interface programs resulted in major improvements in describing the geometry and material composition in various zones of the blanket. This automation of the interface also reduced the human effort and errors in preparing large input files to the transport codes. A number of scientists recently utilized all these advances to perform 3D neutron and photon transport calculation for the blanket and shield in considerable detail (see for example, reference [39]). Therefore, the capabilities to calculate 3D nuclear responses such as nuclear heating and tritium production in blanket modules and sectors are very advanced today, compared to the state-of-the-art in other areas of fusion research such as plasma physics and simulation of liquid metal MHD multiple effects in blankets.

While accurate modeling of the FW/blanket is the dominant factor, all other chamber components (e.g. divertor, rf antennas, penetrations and concomitant structure for heating and current drive, module-to-module connections, stabilizing shells) will have an impact on the TBR. Therefore, very detailed 3D modeling is necessary for calculating the achievable TBR. This should accurately reflect the detailed chamber geometry and configuration including all components with detailed design and material distribution. In addition, the accurate neutron source profile in the plasma which depends on the details of the spatial profile of fusion reaction rate in the plasma, will have an impact on the TBR. Also, peaking at the magnetic axis at mid-plane of a toroidal facility will affect the distribution of tritium breeding in the inboard and outboard blankets.

While the neutronics methods and codes available today are very advanced, there are still uncertainties in calculating the achievable TBR. Human and computational resources required to simulate all the complexities of the detailed chamber geometry and configuration, including all components with detailed design and material distribution and heterogeneity and accurate neutron source profile, are still very large. Therefore, modelers have to introduce approximations to make the required human and computational resources manageable. This introduces uncertainties. For example, neglecting heterogeneity effects results in errors up to $\sim 10\%$ in predicting the TBR.

(iii) *Nuclear data.* The uncertainties in the achievable TBR associated with nuclear data are primarily due to uncertainties in the measured cross sections and energy and angle distributions of secondary neutrons. Another uncertainty arises from processing the cross sections into multi-group data libraries. However, this uncertainty can be greatly reduced by relying on continuous energy cross section data or using a fine energy group structure. Many cross section sensitivity/uncertainty analyses have been performed to provide an estimate of the uncertainty in the calculated TBR in different blanket concepts and where values in the range of 2%–6% were found [35]. Nuclear data for fusion applications have been under continuous improvement since the early 1970s.

As indicated above, a comprehensive program of integral experiments for fusion blanket neutronics was performed [34]. Large differences between calculations and experiments were found, and a safety factor of >1.1 to 1.2 was recommended to be applied to calculated TBR to assure high confidence in tritium breeding. Another series of integral experiments was subsequently made [36, 37], and the analysis showed that calculation of the tritium production rate overestimated the experimental value by an average factor of ~ 1.14 . While there is uncertainty of $\sim 5\%$ in measuring the tritium production rate in the mock up assemblies, the large overestimation from the calculation is alarming.

It is clear from the above that there are considerable uncertainties in calculating the achievable TBR. References [1, 3, 34, 35] investigated the sources of these uncertainties and methods to quantify them. Reference [1] proposed a sophisticated ‘statistical’ approach to estimate the range of ‘total uncertainties’ in calculating the achievable TBR when

all the effects of different uncertainties are combined. We will not describe such complex statistical approach here.

In summary, the best estimate of the achievable TBR for the most detailed blanket system designs available is ≤ 1.15 . But there is uncertainty of $\sim 10\%$ between integral experiments and calculations that cannot be resolved until we build and operate a practical blanket system in a DT fusion facility. Another way to state this is that there is a high confidence that an achievable TBR of 1.05 can be obtained, but there is less confidence that an achievable TBR of 1.15 can be realized. It is important to note that the 10% margin we use here does not account for uncertainties due to major changes in design definition, which can be large.

When can we accurately predict, verify, and validate achievable TBR?

This is an important question. The answer is that such accurate prediction will be possible only after we have:

- (a) Detailed, accurate definition of the design of the in-vessel components (PFC, first wall/blanket, penetrations, etc). This can be realized only after actual blankets are built and tested in the real fusion nuclear environment.
- (b) Prototypical and accurate integral neutronics experiments:
 1. This can be achieved only in a DT-plasma-based facility
 2. Note that current integral experiments are limited to point neutron source with $S < 5 \times 10^{12} \text{ n s}^{-1}$. These point neutron sources do not allow (a) accurate simulation of angular neutron flux and (b) complex geometry with subsystem details and heterogeneity.

Analysis has shown that at least a ‘full sector’ testing in a fusion facility is required for accurate measurement of achievable TBR. The reason is that uncertainties in extrapolation in the poloidal direction from testing of a module is larger than the required accuracy.

3.4. Tritium burn fraction

The TBF (f_b) is a measure of the amount of tritium burned in the plasma before confinement is lost and particles diffuse out of the plasma and into the SOL. It is defined as the ratio of the tritium burning rate (\dot{N}^-) to the tritium fueling rate (\dot{T}_f) as shown in equation (3.3):

$$f_b = \frac{\dot{N}^-}{\dot{T}_f} \quad (3.3)$$

The tritium fueling rate (\dot{T}_f) is the fraction of tritium injection rate (\dot{T}_i) that has entered and penetrated the plasma. In particular, the fueling efficiency is defined as the ratio of the tritium fueling rate to the tritium injection rate:

$$\eta_f = \frac{\dot{T}_f}{\dot{T}_i} \quad (3.4)$$

Combining equations (3.3) and (3.4), we obtain an expression for the tritium injection rate as:

$$\dot{T}_i = \frac{\dot{T}_f}{\eta_f} = \frac{\dot{N}^-}{\eta_f f_b} \quad (3.5)$$

Thus, in order to minimize the tritium injection rate, one needs to maximize the tritium fueling efficiency and burn fraction. Assuming a 50%–50% DT mixture, where tritium and deuterium plasma density is $n_T = n_D = n$, a simplified expression for f_b can be derived as:

$$f_b = \frac{\langle \sigma v \rangle n \tau^*}{2 + \langle \sigma v \rangle n \tau^*} \quad (3.6)$$

Where $\langle \sigma v \rangle$ the averaged product of energy-dependent cross section (σ) for the DT reaction, (v) the velocity, and τ^* the effective particle confinement time, which is defined as:

$$\tau^* \cong \frac{\tau}{1 - R} \quad (3.7)$$

where τ the confinement time and R is the recycling coefficient (from the edge). Since the 1980s, reactor studies assumed $R = 0.95$, with no theoretical or experimental evidence, in order to obtain very high f_b , e.g. 30%–40% and make their conceptual design attractive. However, as described in sections 6 and 7, recent experimental results showed that neutral fueling from recycling is highly inefficient ($R \sim 0$). This means that the expected values of burn fraction are very low, for example, ITER has an estimated burn fraction of 0.36% if the maximum capacity for fueling is used with 50-50 DT mix in the fuel (see section 6 for possible improvements on this value resulting from ITER operation itself). Another conclusion is that gas fueling is not efficient due to poor neutral penetration, and therefore, pellet fueling is needed as it has the potential for achieving high fueling efficiency. ITER is planning to use pellet fueling. Our results presented in section 4.2 show that with extrapolation from plasma physics and technology parameters, i.e. burn fraction of 0.36% for ITER at maximum capacity for fueling with 50-50 DT mix in the fuel and pellet fueling efficiency of 25%, tritium fuel self-sufficiency cannot be attained and the required tritium start-up inventory is unobtainable (order of tens of kilograms for a 3 GW reactor). Therefore, intense research and innovative ideas by plasma physicists to substantially increase the burn fraction to 5% are required for the feasibility of DT fusion, or at least 2% if substantial advances in tritium processing technology can be realized. This paper explores technology options, design choices, and plasma physics parameters in order to determine the phase space of tritium self-sufficiency and provide fuel cycle R & D guidance. Section 6 addresses the plasma physics aspects of the TBF in ITER and suggests directions for R & D for future improvements. Section 7 presents plasma fueling technology and provides predictions for fueling efficiency in ITER, DEMO, and beyond with present technology.

3.5. Evaluation of start-up inventory and required TBR

The tritium storage system dynamics has been accurately described by Kuan and Abdou in reference [2]. The tritium inventory initially contained in the storage system (I_S^0) characterizes the start-up inventory. As reactor operation begins,

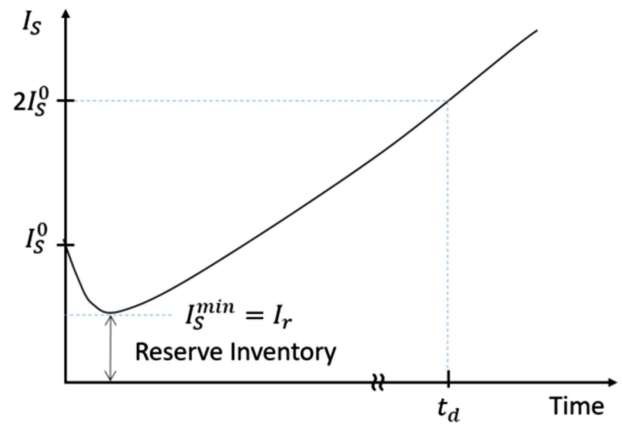


Figure 2. Qualitative description of the storage system tritium inventory dynamics.

the tritium inventory in the storage decreases, as tritium is provided to the fueling system and, ultimately, to the plasma. Thus, the storage inventory reaches a minimum and starts to increase as a result of the extraction and accumulation of tritium coming from the OFC (i.e. in blankets and TESs) and due to the recirculation of tritium processed in the IFC, as shown in figure 2.

An important consideration is that the storage inventory must include a ‘reserve’ inventory (I_r) in order to allow continuous reactor operation in case of any malfunctions due to random failures in a part of any tritium processing line. This reserve inventory is critical to ensure a high level of plant reliability and availability, which has direct implications for the competitiveness of fusion technology. In this work, we specify the minimum storage inventory as:

$$I_S^{\min} = I_r \quad (3.8)$$

$$I_r = \frac{\dot{N}^-}{\eta_f f_b} t_r q \quad (3.9)$$

where t_r is the reserve time, i.e. the period of tritium supply kept in ‘reserve’ inventory in the storage system to maintain the plasma and the power plant operational in case of any malfunction in a part (q) of any tritium processing system. This implies that the storage system is able to provide the necessary tritium injection rate to the plasma ($\dot{N}^- / \eta_f f_b$, where \dot{N}^- is the tritium burning rate in the plasma, η_f is the fueling efficiency, and f_b the TBF) in case of failure of a fraction of the system (q) for a certain reserve time (t_r). The burn fraction and fueling efficiency concepts are described in detail in section 4. After a doubling time (t_d) the storage system inventory reaches a value equal to twice the initial inventory:

$$I_S(t_d) = 2I_S^0 \quad (3.10)$$

Thus, in a doubling time, the reactor generates a sufficient start-up inventory to start a second reactor. Here, we assume that this second reactor is characterized by the same technology and representative parameters of the original first reactor, hence the same start-up inventory is needed. However, this assumption is conservative since in times of $\sim t_d$ (which is several years) technology may advance, and thus lower

start-up inventory may be sufficient. Note that an alternative definition of equation (3.10) was adopted in various previous researches (references [6–9]) as $I_S(t_d) = I_S^0 + I_S^{\min}$. However, equation (3.10) is slightly more conservative (see TBR_R values reported in table 2 of reference [6]), which is appropriate at this state of knowledge of fusion technology.

The required TBR (TBR_R) and the tritium start-up inventory (I_S^0) are mutually dependent, and neither of them is known in the beginning of the calculation. Therefore, the code calculates the required TBR and tritium start-up inventory through iterations. Given the weak dependency of start-up inventory on required TBR, convergence with a degree of accuracy of 0.01% is found for equation (3.10) in a few iterations.

3.6. Reactor availability factor modeling

In order to account for ordinary periodical maintenance and/or unexpected shutdown due to random failures, we introduced in the model an overall reactor duty or availability factor (AF), which was originally defined in reference [16] and can be written as:

$$AF = \frac{MTBF}{MTBF + MTTR} = \frac{1}{1 + \frac{MTTR}{MTBF}} \quad (3.11)$$

where MTBF is the mean time between failures (plasma on) and MTTR the mean time to repair (plasma off). A ‘switch operation’ which turns the plasma on and off according to the MTBF and MTTR periods is implemented in the numerical model in order to account for the availability factor of the fusion system. Therefore, in our model the availability factor is calculated using a time-averaged approach based on the alternation of periods of MTBF and MTTR, where these two parameters are predefined constants. Furthermore, pulsed operational mode based on burn-dwell time cycle is lumped into the availability factor calculation. Note that this time-averaged approach may be not fully representative of cases when the availability factor is particularly low, for instance due to a failure event which requires several months of reactor shut down. However, this formulation allows to describe the overall effect of the availability factor on tritium self-sufficiency, and shows the importance of the subject of RAMI. Other models which consider a statistical outage approach to treat the reactor availability factor are available in references [13, 167].

Analyses have shown that in order to obtain an overall availability factor > 50% for a DEMO reactor, the blanket and divertor components shall each require $MTBF > 10$ years and $MTTR < 2$ weeks, giving an availability factor for each of the blanket and divertor of $\sim 87\%$ [4, 16, 21]. Extrapolation from other technologies, e.g. aerospace and fission industry, shows expected MTBF for fusion blankets/divertor as short as hours to days, and MTTR of several months, strongly indicating a huge difference between requirements and expectations.

Two fundamental reasons which lead to short MTBF, long MTTR, and low expected availability in current concepts of fusion confinement systems can be explained as follows. The first reason resides in the necessary choice of locating the blanket/FW/divertor inside the vacuum vessel, which is a low fault

tolerance domain and requires immediate shutdown in case of various failures (e.g. coolant leak). Furthermore, due to limited physical space and other considerations, no redundancy is possible. Long MTTR is due to the difficulties in accessing to nuclear components inside the vacuum vessel. Repair and replacement require breaking the vacuum seal, many connects/disconnects, and many operations in the limited access space of tokamaks, stellarators, and other ‘toroidal/closed’ configurations. Note that the decision to insert the blanket inside the vacuum vessel is necessary to protect the vacuum vessel, which must be robust and cannot be in high radiation/temperature/stress state facing the plasma. The second reason is the large surface area of the first wall, which results in high failure rate for a given unit failure rate per unit length of piping, welds, and joints, determining short MTBF.

Low availability factors could have tremendous consequences on tritium economy and self-sufficiency: during the reactor downtime (i.e. during the MTTR) tritium production in blankets is interrupted whilst tritium is continuously lost by radioactive decay. Thus, the TBR requirements could become more demanding in case of low availability factor. In particular, in the fusion development pathway, there are three different stages of reactor development:

- (a) Near term plasma-based experimental facilities (e.g. FNSF, VNS, CTF, etc);
- (b) Demonstration (DEMO) reactors (e.g. EU-DEMO, K-DEMO, etc);
- (c) Power reactors.

These facilities will have different performance, reliability, and availability. Near-term facilities are expected to have an availability factor < 30%, and DEMO is planned to reach availability of $\sim 30\%–50\%$ [16, 31], whereas high availability factors (> 80%) are needed in future commercial fusion power plants to ensure competitiveness and establishment of fusion technology as a reliable energy source. In this study, we perform self-sufficiency analysis to assess the effect of availability factors on required TBR for the different stages of fusion technology and suggest ideas to enable compensation for shortfall in tritium breeding of near term devices.

3.7. Reference parameters for various subsystems in the fuel cycle

A literature survey was performed to determine a set of representative reference plasma and technology parameters to use in the analysis. These parameters are summarized in tables 1–3 (refer to the underlined value in case multiple parameters are shown for the same technology—some discrepancies were found among the data reported in literature for typical parameters used in fuel cycle analyses).

We did not select (underlined) a fueling system processing time in table 2 since the fueling system is not simulated in the model. However, the processing time of 4 h chosen for the fuel clean-up and ISS accounts for the fueling system processing time as well, i.e. we assume that 4 h is a reasonable estimate of the overall tritium processing time in the plasma exhaust of the

Table 1. Main parameters for the reference case.

Parameter	Value	Source/explanation
Tritium burning rate in the plasma (\dot{N}^-)	0.459 kg day ⁻¹	Burning rate for 3 GW fusion plant
Tritium burn fraction in the plasma (f_b)	0.36%	ITER at maximum capacity for fueling with 50-50 DT mix see section 6.1
	1.5%	Expected for first DEMOs [13]
Fueling efficiency (η_f)	25%	See section 7.2
Doubling time (t_d)	5 years	Abdou <i>et al</i> [1, 4]
Reserve time (t_r)	24 h	—
Fraction of the fuel cycle failing (q)	25%	—

Table 2. IFC processing times chosen for the reference case.

Component	Processing time	Source
Fuel clean-up and isotope separation system	1.3 h	Day <i>et al</i> [14]
	5 h	Coleman <i>et al</i> [13]
	0.1 day	Abdou <i>et al</i> [1]
	1–24 h	Abdou <i>et al</i> [4]
	<u>4 h</u>	<u>Chosen for analysis</u>
Water detritiation system	<u>1 h</u>	<u>Day <i>et al</i> [14]</u>
	20 h	Coleman <i>et al</i> [13]
Fueling system	20 min	Day <i>et al</i> [14]
	30 min	Coleman <i>et al</i> [13]

Table 3. OFC processing times (and residence times) chosen for the reference case.

Component	Processing time (or residence time)	Source
Breeding zone	10 days	Abdou <i>et al</i> [1]
	0.1–1 day	EXOTIC-6, -7, -8 [28]
TES	<u>1 day</u>	<u>Abdou <i>et al</i> [1, 4]</u>
	Negligible (on-line)	Demange <i>et al</i> [29]
CPS	1–5 days (batch-wise)	Riva <i>et al</i> [27]
	100 days	Abdou <i>et al</i> [1, 4]
	<u>10 days</u>	<u>Chosen for analysis</u>
FW	<u>1000 s</u>	<u>Riva <i>et al</i> [27]</u>
Divertor	1000 s	Riva <i>et al</i> [27]
Steam generator	1000 s	<u>Chosen for analysis</u>

IFC. Note that the CPS processing time is chosen to be 10 days arbitrarily to account for the slow recovery process expected in coolant systems, given the early stage of this technology, and to be conservative. However, as shown in [27] the CPS line is expected to have minimum impact on start-up inventory and fuel self-sufficiency because of the much smaller magnitude of tritium permeation to coolants in PFCs compared to the fueling rate to plasma and generation rate in blankets.

4. Tritium inventories and tritium self-sufficiency analysis

Tritium inventories and flow rates dynamics, and hence self-sufficiency, are complex functions of plasma physics, technology choices, fuel cycle design, and operating parameters. Dynamic modeling analyses show that the key parameters affecting tritium inventories, tritium start-up inventory, and required TBR are those summarized in table 4. Therefore, results selected for presentation in the rest of sections 4 and 5 will focus on these parameters.

4.1. Calculation of tritium inventory in various systems as function of key physics and technology parameters

The time evolution of tritium inventories in various components of the fuel cycle are presented in figure 3. These inventories refer to a reactor producing 3 GW of fusion power and are calculated for steady-state reactor operation, i.e. in this analysis we do not consider shut-down periods due to random failures or ordinary maintenance. In particular, we evaluate inventories for different values of TBF and fueling efficiency product, i.e. $f_b = 0.36\%$ and $\eta_f = 25\%$ (black lines), $\eta_f f_b = 1\%$ (blue lines), and $\eta_f f_b = 5\%$ (magenta lines).

As noted in the figure, the ISS is the most demanding component in terms of inventory build-up. The equilibrium value of tritium inventory in ISS is found after ~ 1 day of operation. The storage inventory decreases from its initial value to a minimum as tritium inventory builds up in the other components, and then, it starts to rapidly increase as inventory build-up in components has reached saturation. In particular, the minimum inventory in the storage system is found after ~ 6 –8 days.

Table 4. Key parameters affecting tritium inventories, and hence, required TBR.

1. Tritium burn fraction in the plasma (f_b)
2. Fueling efficiency (η_f)
3. Time(s) required for tritium processing of various tritium-containing streams, e.g. plasma exhaust, tritium-extraction fluids from the blanket (t_p)
4. Availability factor (AF)
5. ‘Reserve time’ (t_r), i.e. period of tritium supply kept in ‘reserve’ inventory in the storage system to keep plasma and plant operational in case of any malfunction in a part (q) of any tritium processing system
6. Parameters and conditions that lead to significant ‘trapped’ inventories in reactor components (e.g. in divertor, FW); and blanket inventory caused by bred tritium released at a rate much slower than the T processing time
7. Inefficiencies (fraction of T not usefully recoverable) in various tritium processing schemes (ε)
8. Doubling time (t_d) for fusion power plants (time to accumulate surplus tritium inventory sufficient to start another power plant)

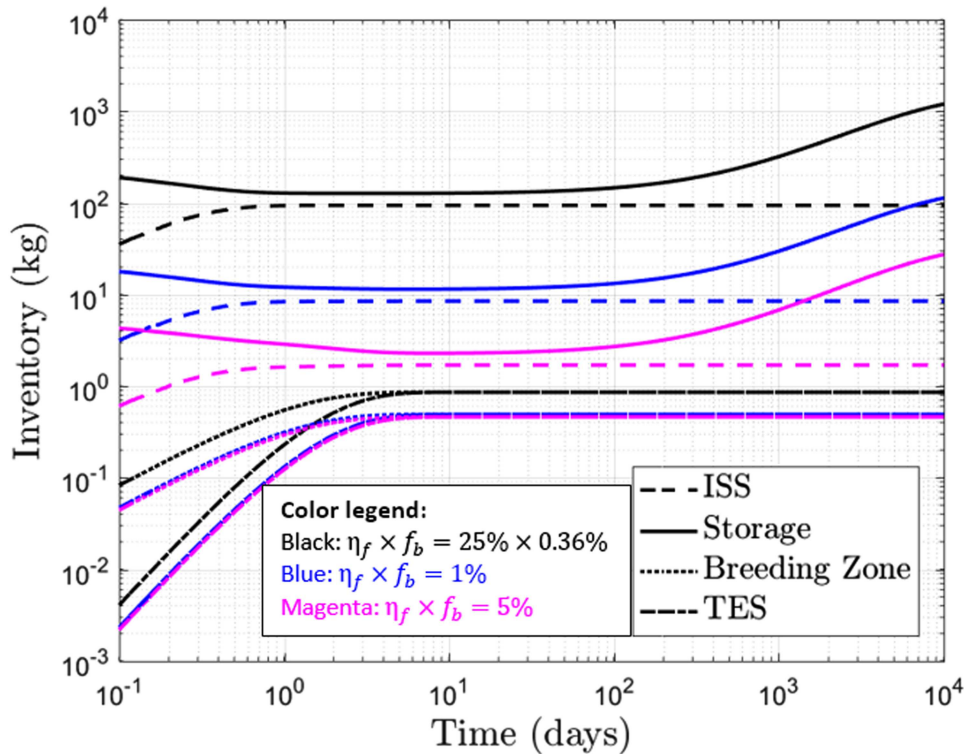


Figure 3. Tritium inventory evolution in various systems. The black lines represent $f_b = 0.36\%$ and $\eta_f = 25\%$, the blue lines show $\eta_f f_b = 1\%$, and the magenta lines show $\eta_f f_b = 5\%$. Parameters used in the analysis: processing time in the plasma exhaust (IFC) = 4 h; BZ residence time = 1 day; TES processing time = 1 day; availability factor = 100%; fusion power = 3 GW; reserve time = 24 h; fraction failing = 25%; doubling time = 5 years.

Note that the ISS inventory and the storage inventory are very sensitive to the burn fraction and fueling efficiency product, which determine the amount of tritium exhausted to the IFC line. In contrast, the BZ and its TES do not directly depend on the burn fraction and fueling efficiency; however, slight differences in the inventories in the BZ and TES are seen for different values of $\eta_f f_b$ due to the different required TBR obtained for each $\eta_f f_b$ considered. In particular, a required TBR of 1.82, which is impossible to achieve in practice, is found when ITER burn fraction obtained for maximum fueling capacity with 50-50 DT mix in the fuel is used in the analysis whilst values of $\eta_f f_b$ of 1% and 5% require a TBR of 1.08 and 1.02, respectively. As discussed in section 6, ITER operation will show if it is possible to improve these value because of specific plasma physics processes in fusion reactors.

In the following subsections, we perform tritium self-sufficiency analysis to explore the performance of the fuel cycle under a wide range of parameters and define high priority R & D. The tritium start-up inventory assessment is presented in section 5.

4.2. Physics and technology parameters window for tritium self-sufficiency

Tritium self-sufficiency is attained, according to equation (3.2), if $TBR_A \geq TBR_R$. The achievable TBR discussion was provided in section 3.3. In particular, it was found that the estimated achievable TBR is ~ 1.05 – 1.15 . Note that, as explained in section 3, the required TBR is a function of several plasma physics and technological parameters, e.g.

Table 5. Calculated values of required TBR using ITER burn fraction at maximum fueling capacity with 50-50 DT mix in the fuel $f_b = 0.36\%$ and fueling efficiency $\eta_f = 25\%$. Availability factors of 10%, 30%, 50%, 70%, 90%, and 100% are considered. Parameters used in the analysis: processing time in the plasma exhaust (IFC) = 4 h, BZ residence time = 1 day, TES processing time = 1 day, fusion power = 3 GW, reserve time = 24 h, fraction failing = 25%, doubling time = 5 years.

$f_b = 0.36\%, \eta_f = 25\%$						
AF	10%	30%	50%	70%	90%	100%
TBR _R	5.05	2.67	2.16	1.94	1.85	1.82

burn fraction (f_b), fueling efficiency (η_f), processing time, etc.

In this section, we explore the effect of various parameters on the required TBR in order to define the phase space of plasma physics and technology parameters in which tritium self-sufficiency can be attained. In order to account for uncertainties in predicting the achievable TBR, we attribute different levels of confidence in attaining tritium self-sufficiency to different values of required TBR. In particular, we consider attaining self-sufficiency:

- Unlikely: if $TBR_R > 1.15$ (where 1.15 corresponds to the maximum achievable TBR)
- Possible: if $1.05 < TBR_R \leq 1.15$ (area shown in light green in the plots presented in the following subsections)
- Attained with high confidence: if $TBR_R \leq 1.05$ (area shown in dark green in the plots presented in the following subsections)

An important finding is the strong dependence of the required TBR on the availability factor discussed earlier in section 3, particularly at low values of the burn fraction. Table 5 shows the calculated values of the required TBR using burn fraction $f_b = 0.36\%$ and fueling efficiency $\eta_f = 25\%$ for various values of the availability factor. The results show that the required TBR for these parameters is very high. Even with 100% availability factor, the required TBR is 1.82, which far exceeds the maximum achievable TBR in any fusion system. This leads to a very serious conclusion that self-sufficiency cannot be attained if future fusion reactors would have the burn fraction predicted for ITER when using the maximum capacity for fueling and 50-50 DT mix in the fuel, unless specific plasma physics processes in fusion reactors allow improvements, as described in section 6. Moreover, the initial start-up tritium inventory would be >200 kg for a 3000 MW reactor, which is totally unacceptable for many fundamental reasons as will be discussed in section 5. Table 5 also shows a strong dependency of the required TBR on the reactor availability factor.

4.2.1. Effect of tritium burn fraction, fueling efficiency, and tritium processing time on tritium self-sufficiency. Figure 4 shows the required TBR variation as a function of the fueling efficiency and burn fraction product ($\eta_f f_b$) for various values of the tritium processing time in the IFC for the plasma exhaust (t_p) (which is largely determined by the ISS). Representative

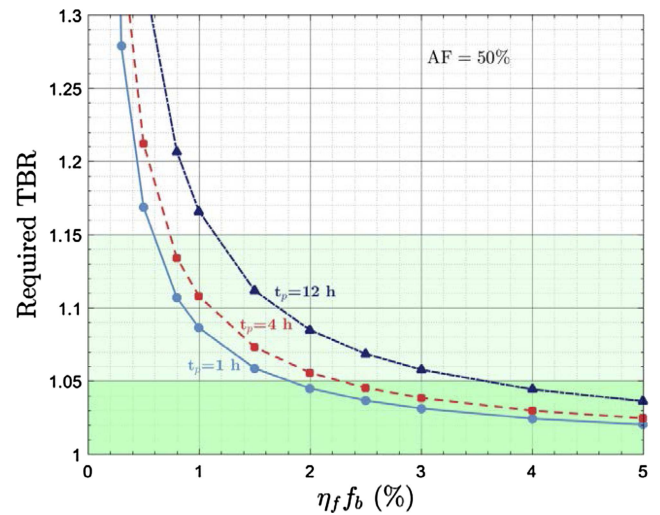


Figure 4. Required TBR as a function of the product of TBF and fueling efficiency for various tritium processing time in the plasma exhaust of the IFC (1, 4, and 12 h) and availability factor of 50%. Fixed parameters used in the analysis: BZ residence time = 1 day; TES processing time = 1 day; availability factor = 50%; fusion power = 3 GW; reserve time = 24 h; fraction failing = 25%; doubling time = 5 years.

values of 1, 4, and 12 h are used in the analysis. Reference parameters are shown in the caption for figure 4.

The results in figure 4 show that the TBR_R increases slightly if the product of TBF and fueling efficiency decreases from 5% to 3%, largely if $\eta_f f_b$ decreases from 3% to 1%, and dramatically if $\eta_f f_b$ is lower than 1%. Thus, burn fraction and fueling efficiency represent dominant parameters toward realizing tritium self-sufficiency. However, the results of figure 4 suggest that reducing the tritium processing time in the IFC (i.e. in the ISS in particular) has major impact on reducing the required TBR, especially at low $\eta_f f_b$. Conversely, if tritium processing time is long (>2 –4 h), self-sufficiency is impossible at $\eta_f f_b < 1\%$. Advances in fueling efficiency, e.g. via high field side (HFS) pellet injection which potentially provides $\eta_f \sim 25\%$ –50%, and innovative ideas to increase burn fraction to $\sim 2\%$, would improve the confidence in achieving tritium self-sufficiency by reducing the required TBR to ~ 1.15 (light green area in the plot of figure 4) for processing times shorter than 4 h. A wide region of the potential to attain self-sufficiency with high confidence is seen for $\eta_f f_b > 2\%$ at processing time of 1–4 h. Furthermore, required TBR in the 1.05–1.15 range is observed if $0.7\% < \eta_f f_b < 2\%$ and the processing time is less than 4 h. Hence, major effort should be paid to developing efficient processing units in the IFC to minimize the required processing time. Major improvements are needed for attaining tritium self-sufficiency with higher confidence level. The goal for R&D should be to achieve the product of fueling efficiency and TBF greater than 5% (or, at least not lower than 2%) and tritium processing time shorter than 4 h. Sections 6 and 7 discuss the plasma physics and fueling technology considerations in ITER and beyond, and present innovative ideas to improve the burn fraction and fueling efficiency.

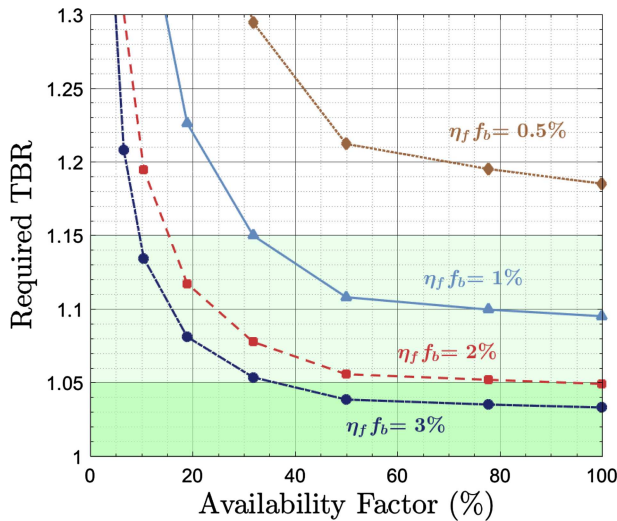


Figure 5. Required TBR as a function of reactor availability factor for various TBF and fueling efficiency product. Parameters used in the analysis: processing time in the plasma exhaust (IFC) = 4 h, BZ residence time = 1 day, TES processing time = 1 day, fusion power = 3 GW, reserve time = 24 h, fraction failing = 25%, doubling time = 5 years.

4.2.2. Self-sufficiency analysis during different stages of nuclear fusion development: the effect of reactor availability factor. In this section, we explore the effect of the reactor availability factors on tritium self-sufficiency. In particular, as we explained in section 3.6, low reactor availability factor is expected in the early stage of fusion technology development, e.g. for experimental facilities and possibly in DEMO(s) reactors, due to frequent random failures (short MTBF) and long times needed to repair/replace components (long MTTR).

Figure 5 shows that the TBR_R is strongly affected by the availability factor. In detail, the required TBR increases slightly when AF is reduced from 80% to 60%, significantly when AF is reduced from 60% to 30%, largely when AF is reduced from 30% to 10%, and dramatically when AF is less than 10%. On the one hand, these results imply that attaining tritium self-sufficiency in near-term fusion experimental facilities (e.g. FNSF, VNS, CTF, etc) could be impossible in light of the predicted low availability factor [4, 16]. On the other hand, we found that there only is a marginal change in the TBR_R if $AF > 60\%$ for specific values of $\eta_f f_b$. Thus, attaining tritium self-sufficiency in power reactors, which need to have $AF > 80\%$, will be less challenging provided that the burn fraction and fueling efficiency are high and the tritium processing time is short. To summarize, tritium self-sufficiency is:

- Impossible if $AF < 10\%$ for any $\eta_f f_b$
- Impossible if $\eta_f f_b < 0.5\%$ for any availability factor
- Possible if $AF = 15\%–30\%$ and $\eta_f f_b > 2\%$
- Possible if $AF > 30\%$ and $1\% \leq \eta_f f_b \leq 2\%$
- Possible with high confidence if $AF > 50\%$ and $\eta_f f_b > 2\%$

These results that show strong dependence of the potential to attain self-sufficiency in fusion devices on the availability

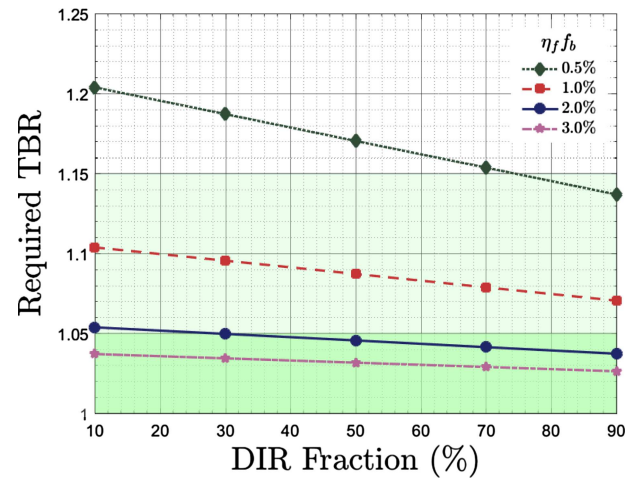


Figure 6. Required TBR as a function of DIR fraction for TBF and fueling efficiency products of 0.5%, 1.0%, 2.0%, and 3%. Parameters used in the analysis: processing time in the plasma exhaust (IFC) = 4 h, BZ residence time = 1 day, TES processing time = 1 day, fusion power = 3 GW, availability factor = 50%, reserve time = 24 h, fraction failing = 25%, doubling time = 5 years.

factor when AF is lower than $\sim 30\%$ are illuminating. Near term devices such as FNSF, VNS, CTF, and CFETR which are needed to test and develop fusion nuclear technology will have low availability. An essential element of the mission of these devices is RAMI, i.e. reliability growth and major improvements in maintainability. Experience from aerospace and fission industries show that RAMI programs take a long time. Therefore, these devices must have small fusion power in order to enable mitigation for shortfall in tritium breeding. Another element of the mission is improving the fuel cycle technology to shorten tritium processing times and reduce tritium inventories.

4.2.3. Mitigation of TBR requirements via direct internal recycling. The DIR technology was proposed by the EU-DEMO team as a smart architecture of the fuel cycle, useful to minimize the tritium inventory in the components of the IFC, and therefore reduce the required start-up inventory and improve safety [6]. The DIR loop carries a fraction of the fuel directly from the exhaust gas to the storage and management system and therefore bypassing the ISS which is the main component responsible for the long tritium processing time in the plasma exhaust of the IFC. A reduction of inventories in components of the IFC obtained through a successful implementation of the DIR technology has a direct effect on tritium self-sufficiency as well. In this section, we evaluate the required TBR for different fractions of tritium flow rates treated by the DIR (i.e. from 10% to 90%) whilst the remaining fraction of the plasma exhaust is processed in the IFC with an assumed processing time of 4 h.

Figure 6 shows a linear proportionality between the required TBR and DIR fraction. It is seen that the required TBR decreases as the fraction of fuel processed by the DIR increases. This effect is particularly noticeable at low TBF and fueling efficiency product, e.g. $\eta_f f_b$ of 0.5%, and 1%. For

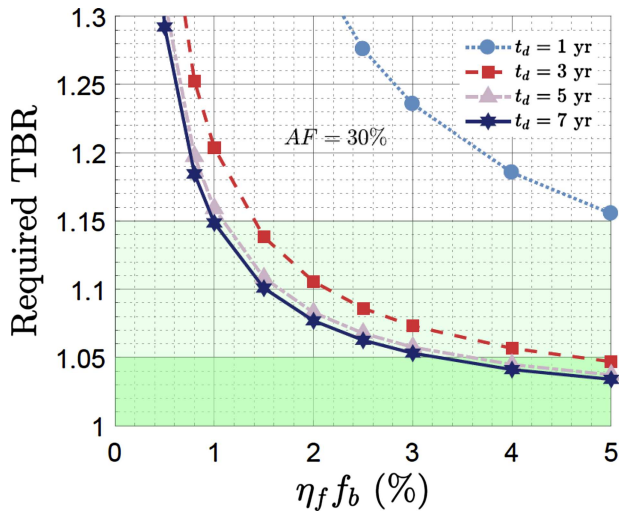


Figure 7. Required TBR as a function of the product of TBF and fueling efficiency for various doubling time (1, 3, 5, and 7 years) for availability factor of 30%. Parameters used in the analysis: processing time in the plasma exhaust (IFC) = 4 h, BZ residence time = 1 day, TES processing time = 1 day, fusion power = 3 GW, reserve time = 24 h, fraction failing = 25%, availability factor = 30%.

instance, for $\eta_f f_b$ of 1%, the required TBR is 1.120 when DIR is not performed, and it reduces to 1.075 if 80% of the plasma exhaust is fed to the DIR. This is a major reduction which helps increase the likelihood of achieving tritium self-sufficiency, especially if substantial improvements in the plasma physics areas are not obtained in the near term.

At higher $\eta_f f_b$, a lower flow rate is treated in the IFC as the tritium fueling rate considerably decreases. In this case, the DIR effect is less pronounced but still beneficial, as the required TBR can be reduced of a few percent when DIR is included, e.g. for $\eta_f f_b = 3\%$, the TBR_R ranges from 1.037 to 1.026 for DIR fraction in the range of 10%–90%. Thus, the analysis suggests that the DIR can significantly help to increase the likelihood of attaining tritium self-sufficiency, particularly if only moderate advancements are achieved in plasma physics and fueling technology and the increase of the $\eta_f f_b$ product is limited.

4.2.4. Penetration of fusion energy into power market. In this section, we analyze the effect of different doubling time (1, 3, 5, and 7 years) on the required TBR for a fusion near-term facility with a modest availability factor of 30% (figure 7) and for mature power reactors with a high availability factor of 80% (figure 8).

Due to the scarcity of tritium resources, the penetration of fusion technology into the energy market will be strongly affected by the capability of the first generation of fusion reactors to generate appropriate start-up inventory to start operation of new reactors in the shortest possible time, i.e. short doubling time. Note that the doubling time is 5–7 years in mature power industry, e.g. conventional power plants, fission reactors, etc. However, due to the scarcity of tritium resources and the inadequacy of non-fusion facilities to provide the required amount of tritium, the doubling time for fusion technology should be shorter, for instance ~ 1 –3 years, in order

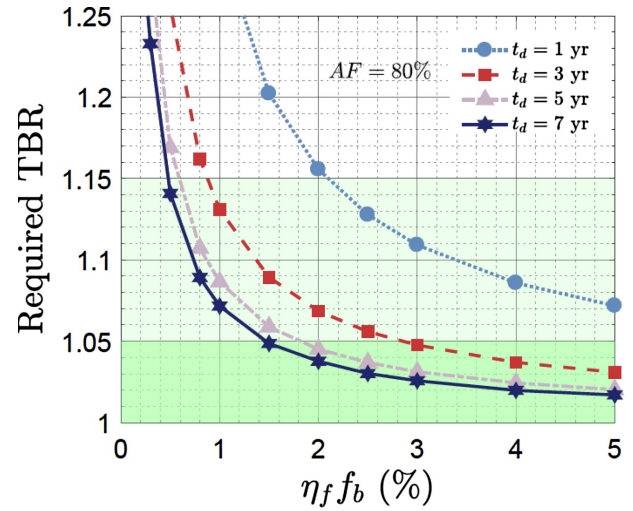


Figure 8. Required TBR as a function of the product of TBF and fueling efficiency for various doubling time (1, 3, 5, and 7 years) for availability factor of 80%. Parameters used in the analysis: processing time in the plasma exhaust (IFC) = 4 h, BZ residence time = 1 day, TES processing time = 1 day, fusion power = 3 GW, reserve time = 24 h, fraction failing = 25%, availability factor = 80%.

to provide the necessary tritium start-up inventory to every DEMO and early power reactors. Such a demanding requirement on doubling-time has implications on attaining tritium self-sufficiency.

Figures 7 and 8 show the required TBR as a function of the product of TBF and fueling efficiency for various doubling time (1, 3, 5, and 7 years) with the availability factor 30% in figure 7 but 80% in figure 8. As shown in figure 7 the required TBR falls in the possible self-sufficiency window for $\eta_f f_b > 1\%$ for doubling time of ~ 5 –7 years. Self-sufficiency is possible for a shorter doubling time, i.e. $t_d = 3$ years and $\eta_f f_b = 1.5\%$, while it is impossible to obtain for a very short doubling time of 1 year. Obtaining self-sufficiency with high confidence in near-term experimental facilities is more challenging due to the low availability and burn fraction and fueling efficiency product, and thus a longer doubling time could be needed. In figure 8, we notice that achieving self-sufficiency is less challenging in power reactors, due to an increase of the availability factor and the fact that mature power industry is characterized by longer doubling times.

5. Calculation of the required tritium start-up inventory and assessment of the availability of external tritium supply for start-up of near- and long-term fusion facilities

A special issue in fusion development is the ‘start-up tritium inventory’, also called ‘initial inventory’, which is the inventory that must be supplied to a fusion plant at the beginning of its operation. The start-up inventory is necessary because of the time lag between tritium production and use and the initial build-up of tritium inventories in various components. However, a large ‘start-up inventory’ represents a problem since there is no practical external source of tritium, and

the cost of producing it in fission reactors or accelerators is prohibitive.

With many independent countries currently designing their own DEMO reactors, e.g. EU-DEMO [31], K-DEMO [32], and planning operation to begin after 2050, it is necessary to accurately evaluate the tritium start-up inventory necessary to start DEMO(s), since external tritium resources may not be sufficient. Also, start-up inventory required for the early generation of power reactors is critical because it affects the required TBR and self-sufficiency as well as the ability to have a short doubling time for fast penetration of the power market. Minimizing the tritium start-up inventory is critical for successful fusion development. In this section, we calculate the tritium start-up inventory for different reactors, power levels, and technology performance to identify the most critical parameters affecting the tritium start-up inventory.

5.1. Availability of external tritium supply

The issue of external tritium supply from non-fusion sources is serious and has major implications on fusion development pathway. Tritium consumption in fusion reactors is unprecedented: a fusion reactor consumes ~ 55.8 kg of tritium per 1000 MW of fusion power per year. Tritium production rate in fission reactors is much smaller than the tritium consumption rate in fusion reactors: tritium production in light water reactors (LWR) is limited to $\sim 0.5\text{--}1$ kg year $^{-1}$ whilst CANDU reactors produce ~ 130 g per GWe per full power-year from n-D reaction. Future supply from CANDU depends on whether current reactors can be licensed to extend life by 20 years after refurbishment, which depends on political, national policy, and practical issues. Furthermore, tritium generation in fission reactors requires special tritium breeding systems and is very expensive ($\sim \$80\text{M--}\130M/kg , see for example references [33] and [7]). Other non-fission sources, e.g. proton accelerator (APT), were proved to be uneconomical. Because of the relatively short life of tritium, which decays at a rate of $\sim 5.5\%$ per year (12.32 years half-life), and the issues and limitations of tritium production in fission systems, tritium resources available now from non-fusion sources are irrelevant to evaluating availability of tritium for start-up of DEMO or other fusion devices which will be constructed 20 years from now or beyond.

The time evolution of tritium inventory available from CANDU to provide start-up for fusion reactors is presented in figure 9. With production and decay over 40 years of operation of CANDU reactors, tritium supply peaks at 27 kg in 2027. A successful ITER DT campaign to achieve the project neutron fluence goals starting in ~ 2036 will leave only < 4 kg at the end of its operation in ~ 2052 . Recent studies regarding commercially available tritium can be found in references [15, 192].

5.2. Dependence of tritium startup inventory on burn fraction, fueling efficiency and processing time

Figure 10 shows the calculated start-up inventory as a function of TBF and fueling efficiency product for tritium processing time in the plasma exhaust (IFC) of 1, 4, and 12 h for a reactor

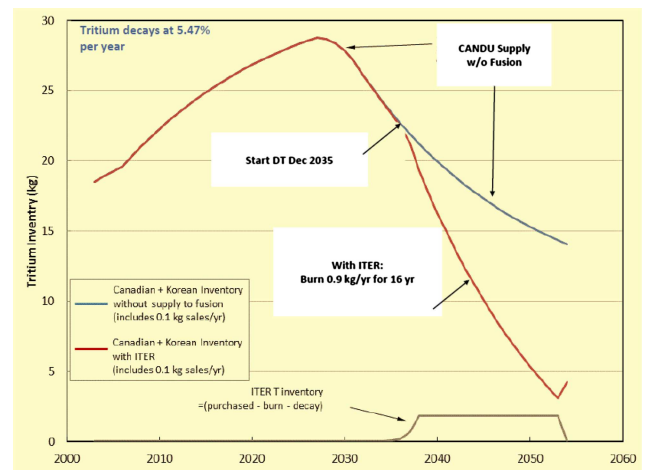


Figure 9. Tritium inventory available to provide start-up inventory in the temporal window 2000–2060.

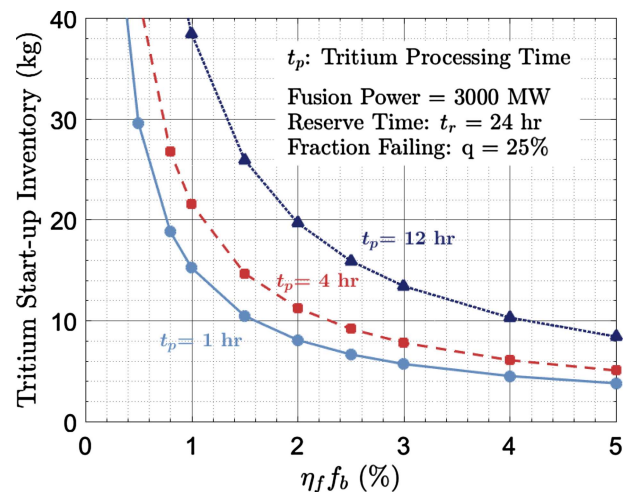


Figure 10. Start-up inventory as a function of TBF and fueling efficiency product for processing time in the plasma exhaust (IFC) of 1, 4, and 12 h. Parameters used in the analysis: BZ residence time = 1 day, TES processing time = 1 day, fusion power = 3 GW, reserve time = 24 h, fraction failing = 25%, doubling time = 5 years.

of 3000 MW fusion power. In the simulation, we account for a reserve time of 24 h and a fraction of the fuel cycle failing of 25%. The results show that the required tritium ‘start-up’ (initial) inventory depends strongly on the TBF, fueling efficiency, and tritium processing time in the plasma exhaust system (the time it takes to go through the vacuum pumping, impurity separation, ISS, fuel fabrication and injection). Low burn fraction, low fueling efficiency, and long processing time result in unacceptably large tritium start up inventory. The start-up inventory is > 20 kg for burn fraction and fueling efficiency product of $< 1\%$ and tritium processing time > 4 h. Such large required start-up inventory is not only difficult to supply, but also presents serious safety issues.

Figure 10 shows that a processing time reduction from 12 to 1 h corresponds to a start-up inventory decrease from ~ 39 kg to ~ 16 kg, i.e. difference of ~ 23 kg, when $\eta_f f_b = 1\%$, while a reduction from ~ 14 kg to ~ 6 kg, i.e. a difference of 8 kg,

is found when $\eta_f f_b = 3\%$. Thus, reducing the processing time is particularly useful at low to mid $\eta_f f_b$. For a 3 GW fusion power reactor, if the product of the TBF and fueling efficiency is $\sim 5\%$, or at least not smaller than 2% , the tritium initial start-up inventory is < 10 kg when $t_p \leq 4$ h. The required tritium start-up inventory can be smaller than 5 kg only for high burn fraction and fueling efficiency product ($\eta_f f_b > 4\%$) and short processing times (≤ 4 h) as well as small trapped inventory in all components such as PFCs and blanket.

Since most of the tritium in the plasma is exhausted to the IFC processing line due to low burn fraction, an efficient and fast tritium processing system must be designed in order to recover tritium and inject it into the plasma in the shortest possible time. In fact, if the time lag between tritium use and recovery increases, a larger start-up inventory will be necessary to compensate for delays in tritium availability. Thus, in order to reduce the start-up inventory, the tritium processing time must be minimized, e.g. by replacing batch technologies with continuous technology as explained in section 9. Moreover, a reduction of processing time implies lower inventory held in the various components of the fuel cycle, which is beneficial for safety. Obviously, as stated earlier, methods to attain high burn fraction as discussed in section 6 and to obtain high fueling efficiency as discussed in section 7 are necessary to keep the start-up inventory reasonably low.

5.3. Reduction of required tritium start-up inventory via direct internal recycling

As we discussed in section 4.2.3, the DIR concept represents an enhancement to the typical IFC scheme. In particular, the use of metal foil pumps and super-permeation technique allows the processing of some fraction of the exhaust gas in a continuous manner and to bypass the ISS, and thus reducing the processing time on plasma exhausts in the IFC loop and the associated inventories in the components of the loop. In this section, we explore the effect of the DIR system on the tritium start-up inventory.

Figure 11 shows the tritium start-up inventory obtained for DIR fractions in the range 10%–90% and for burn fraction and fueling efficiency products of 0.5%, 1%, 2%, and 3%. It is seen that increasing the fraction of fuel processed by the DIR has a remarkable impact on reducing the start-up inventory, particularly at a low burn fraction and fueling efficiency product. For $\eta_f f_b = 0.5\%$ the start-up inventory reduces from ~ 41 kg to ~ 26 kg when DIR fraction is increased from 10% to 90%. As $\eta_f f_b$ increases, the tritium flow rates in the IFC reduce; thus, the DIR effect is less dominant. Nonetheless, a considerable reduction of the start-up inventory is yet obtained, even for $\eta_f f_b = 3\%$, as the start-up inventory is reduced from ~ 7 kg to ~ 5 kg for DIR fraction from 10% to 90%. The results suggest that the DIR has major effects on reducing the start-up inventory, particularly in the case of low burn fraction and fueling efficiency product. Furthermore, the DIR provides a notable advantage even when major advances in plasma physics parameters are achieved, as we showed that the start-up inventory can be further reduced of ~ 1 – 2 kg for $\eta_f f_b > 3\%$.

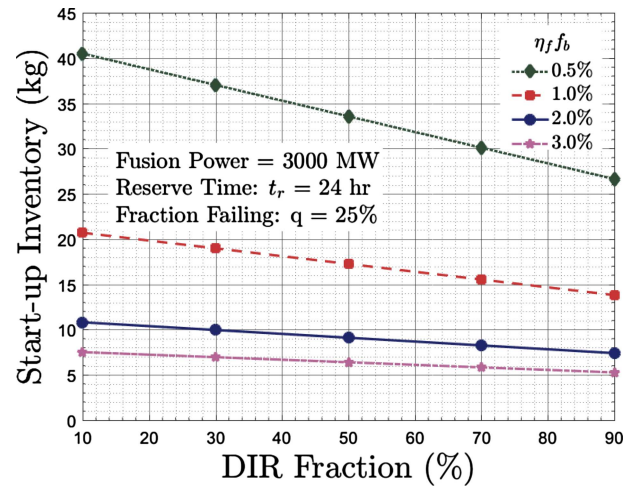


Figure 11. Start-up inventory as a function of DIR fraction for TBF and fueling efficiency products of 0.5%, 1.0%, 2.0%, and 3%.

Parameters used in the analysis: processing time in the plasma exhaust (IFC) = 4 h, BZ residence time = 1 day, TES processing time = 1 day, fusion power = 3 GW, reserve time = 24 h, fraction failing = 25%, doubling time = 5 years.

5.4. The necessity of high fuel cycle reliability to reduce the reserve inventory

As discussed earlier in section 3, a ‘reserve’ inventory is necessary for continued reactor operation under certain conditions such as a failure in a tritium processing system. In figures 12 and 13, we show the total start-up and reserve inventory, respectively as a function of reserve time 0–48 h and at various values of burn fraction and fueling efficiency product. Note that we use the fraction of the fuel cycle that has a failure as $q = 25\%$. The reserve inventory is proportional to the product of t_r and q . Therefore, the reserve inventory for other values of q can be deduced from the figures by using values of t_r that can keep the product $t_r q$ constant. Overall, the total start-up inventory can be < 10 kg if $t_r < 24$ h and $\eta_f f_b \geq 2\%$ and < 5 kg if $t_r < 6$ h and $\eta_f f_b \geq 3\%$ as seen in figure 12. Large amounts of tritium reserve inventory to compensate for some major malfunction in the tritium fuel cycle system may be not feasible at low $\eta_f f_b$. For example, ~ 9 – 10 kg of extra tritium are required if we increase the reserve time from 6 h to 24 h for $\eta_f f_b = 1\%$ (see figure 12) when the fraction of failure is $q = 25\%$. Thus, even though it is desirable to maintain the reactor in operation for as long as possible, when failures are not resolved in a few hours the reactor shutdown seems inevitable, since the reserve inventory magnitude may be too large. Moreover, in case of low availability factors in the early stages of fusion technology development, the reserve inventory is not as meaningful as it is for a mature technology since the reserve time ($t_r \sim$ hours) may be orders of magnitude lower than the MTTR (\sim days–months). For these situations, the fusion facility shutdown seems unavoidable and an extra amount of tritium should be obtained to overcome tritium radioactive decay during the repair time (this may be provided by the TBR without the need of purchasing extra tritium outside the reactor). If technology is more mature and reliable, and high $\eta_f f_b$ is reached, it is possible to increase the reserve time and, at the same time,

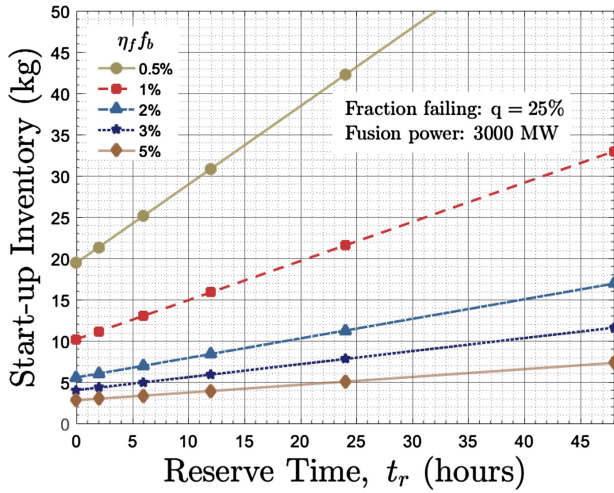


Figure 12. Start-up inventory as a function of the reserve time for various TBF and fueling efficiency products. Parameters used in the analysis: processing time in the plasma exhaust (IFC) = 4 h, BZ residence time = 1 day, TES processing time = 1 day, fusion power = 3 GW, fraction failing = 25%, doubling time = 5 years.

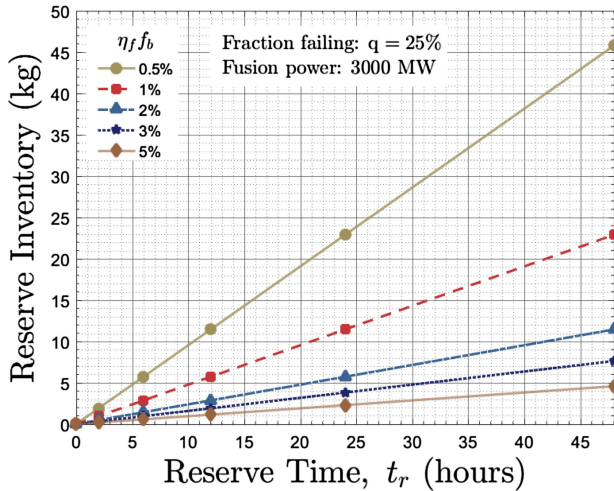


Figure 13. Reserve inventory as a function of the reserve time for various TBF and fueling efficiency products. Parameters used in the analysis: processing time in the plasma exhaust (IFC) = 4 h, BZ residence time = 1 day, TES processing time = 1 day, fusion power = 3 GW, fraction failing = 25%, doubling time = 5 years.

maintain acceptable values of reserve inventory. In figure 13, we see that the reserve inventory is always <5 kg if $\eta_f f_b > 2\%$ even for reserve time <24 h.

The analysis suggests that the tritium processing systems must be highly reliable in order to increase the overall reactor availability, since large reserve times seem not feasible in practice and lead to unacceptable reserve and start-up inventories requirements. A tritium reserve inventory should, however, be accumulated by using some of the TBR margin produced within the same reactor.

It is worth noticing that the reserve time also affects the required TBR. Figure 14 shows the effect of reserve time on required TBR. We note that the increase of the TBF narrows

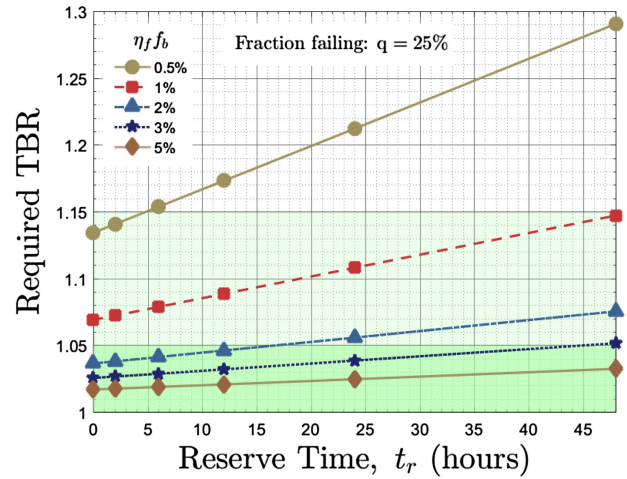


Figure 14. Required TBR as a function of the reserve time for various TBF and fueling efficiency products. Parameters used in the analysis: processing time in the plasma exhaust (IFC) = 4 h, BZ residence time = 1 day, TES processing time = 1 day, fusion power = 3 GW, fraction failing = 25%, doubling time = 5 years.

the difference in the required TBR. One day of reserve inventory with a failing fraction of 25% leads to $TBR_R \sim 1.15$ when the reactor has $\eta_f f_b \sim 1\%$. Higher burn fraction and fueling efficiency ($\eta_f f_b \geq 3\%$) allow a reserve time of 2 days and give $TBR_R \leq 1.05$, making self-sufficiency very likely. Even though the effect of longer reserve time on required TBR is noticeable, we can conclude that self-sufficiency is possible and/or possible with high confidence for a wide range of reserve times at mid-to-high burn fraction and fueling efficiency product.

5.5. Dependence of tritium start-up inventory on fusion power

Thus far, we calculated the start-up inventory for a fusion power of 3 GW. However, near-term fusion development facilities (e.g. FNSF, VNS, CTF, CFETR) are designed for lower fusion powers. In figure 15, we show the start-up inventory as a function of fusion power for TBF and fueling efficiency product of 0.5% and 5%, and reserve time of 6 and 24 h. The tritium processing time in the IFC is 4 h, and DIR is not considered. The lower value of the burn fraction and fueling efficiency product shown in red lines represents the state-of-the-art physics and technology parameters (2019). The higher value of the burn fraction and fueling efficiency product shown in blue lines assumes major advances in physics and technology. We found a linear dependency between the tritium start-up inventory and the fusion power. An important conclusion is that the required tritium start-up inventory for a fusion facility of 100 MW fusion power is as small as 1 kg at very low $\eta_f f_b \sim 0.5\%$ or a few hundreds of grams if $\eta_f f_b$ is higher. But the start-up inventory required for a large fusion power facility of 2–3 GW_f can be as high as ~30–40 kg at low $\eta_f f_b$. Advances in physics and technology to achieve $\eta_f f_b \sim 5\%$ will be required to obtain a start-up inventory <5 kg for large fusion power with a reserve time of 1 day.

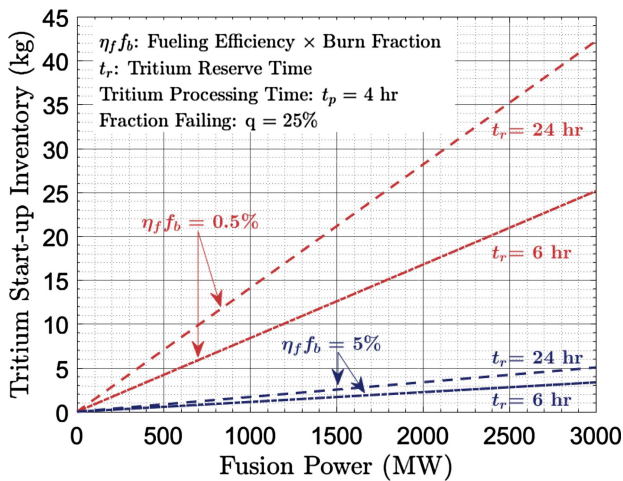


Figure 15. Start-up inventory as a function of fusion power for TBF and fueling efficiency product of 0.5% and 5%, and reserve time of 6 and 24 h. Parameters used in the analysis: processing time in the plasma exhaust (IFC) = 4 h, BZ residence time = 1 day, TES processing time = 1 day, fraction failing = 25%, doubling time = 5 years.

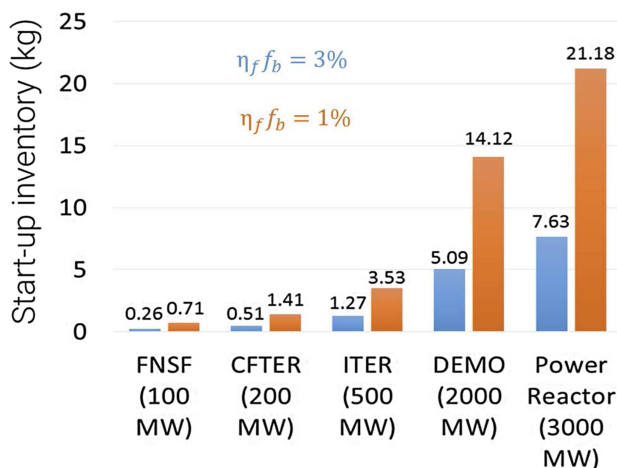


Figure 16. Start-up inventory for various fusion reactors (with different power level) and a TBF and fueling efficiency product of 1% and 3%. Parameters used in the analysis processing time in the plasma exhaust (IFC) = 4 h, BZ residence time = 1 day, TES processing time = 1 day, reserve time = 24 h, fraction failing = 25%, doubling time = 5 years.

We report in figure 16 the required start-up inventory for various fusion facilities at different power levels for the cases of $\eta_f f_b = 1\%$ and 3%. The start-up inventory is 710 g and 21.18 kg for 100 MW and 3000 MW, respectively, when $\eta_f f_b = 1\%$, and 260 g and 7.63 kg for 100 MW and 3000 MW, respectively, when $\eta_f f_b = 3\%$.

The results highlight that near-term fusion facilities should be designed for low fusion power (<150 MW) in order to keep the required start-up inventory relatively small and obtainable, i.e. less than a kilogram of tritium. Note that choosing a small fusion power level is also important to enable compensation of the shortfall in tritium breeding which the first near-term facilities will likely experience. Major advances in physics and

technology are necessary to reduce the start-up inventory in large fusion power facilities, e.g. DEMO and power reactors, which will have fusion power of 2–3 GW.

5.6. Other remarks on tritium start-up inventory

While we found that tritium self-sufficiency is strongly affected by the reactor availability factor, because of tritium loss due to radioactivity which is not compensated by tritium production during reactor downtime, the start-up inventory does not show a strong dependency on the reactor availability. In fact, the tritium start-up inventory mainly depends on the time lag between tritium production and usage: the longer the time needed to extract and process the tritium generated in the blanket and the tritium circulating in the IFC, the greater the tritium start-up inventory. Since the tritium inventory in the storage unit reaches a minimum in a few days (e.g. in ~ 6 –8 days as shown in figure 3) and then starts to increase, losses by radioactivity are modest in this ‘short-term’ and the effect of reactor availability is less pronounced. In case of forced reactor shut-down of several months, it will be necessary to reintroduce the amount of tritium that has decayed during maintenance period in order to restart operation at completion of maintenance period. Our analysis shows that the tritium start-up inventory depends mainly on the fusion power, the amount of reserve inventory which must be available in the storage system to overcome possible partial failure in the fuel cycle (see equation (3.3)), and the fuel cycle performance, i.e. on how efficient the fuel cycle is to extract tritium from blankets and process plasma exhausts in order to reduce the time lag between tritium production and use.

Note that some authors [12, 193, 194] have argued that a tritium start-up inventory is not required at the beginning of life (BOL) of fusion reactors. Instead, these authors propose to start operations under DD mode, and breed tritium by using the soft neutrons released in the $D(n, {}^3\text{He})D$ reaction and the tritium generated in the plasma via $D(p, T)D$ reaction. However, this is judged to be unattractive because this strategy presents substantial difficulties: (1) fusion in DD plasmas is more challenging to be achieved and knowledge of DD plasmas is limited (the proposed mode is much more demanding than current experiments with DD), (2) tritium production per neutron absorption is ~ 0.67 , which implies that long times could be needed to produce considerable amounts of tritium, and (3) examining the dynamics of the low source term and the saturation effects in all components of the fuel cycle show that >190 full operational days are needed to generate 1 kg of tritium. A DEMO will start at relatively low availability, typically $\sim 30\%$ as we discussed in other sections of the paper. So, 190 full operational days means >600 calendar days. Obviously, this is not an attractive way to start a machine like DEMO. This can also be translated to a severe economic penalty. Thus, the DD initial start option seems unpractical, would pose additional tokamak physics and technological problems, delay power production by years, and is not economically sensible [15].

We provide briefly explanation of why long time is needed to generate significant quantities of tritium in the DD start-up scenario. It is well known that every component in the

fuel cycle will, during commissioning with tritiated gases, first build up a residual tritium inventory until ‘saturation’ (dynamic equilibrium). This inventory is significant (kg scale). In practical terms, the achievement of saturation is often performed as part of commissioning of the facility and hence this effect does not play a role anymore when the actual operation is starting; but it is a tritium sink, which would have to be filled from the DD start-up.

In a pure DD start-up, the tritium produced in the BZ (from DD and, with increasing fraction, from DT) is extracted, but only a fraction of it will finally be re-injected, as some amounts are needed to saturate the blanket and tritium extraction components. T is removed from the plasma chamber via pumping, and then re-injected in the plasma chamber following the fuel cycle. Again, during a DD start-up, it is not in general possible to avoid that part of the exhaust T from the plasma is absorbed by the fuel cycle components until saturation is reached. So, only a fraction of exhaust T will be re-injected in the plasma. In this initial saturation phase, these two fractions will be very small. Once the saturation of the components is reached, they take the values of 100% (if we neglect delay times of the fuel cycle and second order effects).

Now, if we set up a mass balance, we see that the number of tritium particles in the plasma chamber is given by: (i) the losses for saturating the components, (ii) the T generation on different paths in the plasma and in the BZ, and (iii) the T generation by DT reactions in the plasma. If we solve the balance equations in the limit of small reinjection fractions, one can directly see that the DD reactions set the speed at which saturation is achieved. If we assume a DD reaction rate of the order of 10^{19} s^{-1} (this is the value provided by plasma simulation codes such as the PLASMOD module inside the EU systems code PROCESS for DEMO plasma profiles) we arrive at a T generation rate of $\sim 5 \times 10^{-5} \text{ g s}^{-1}$. This translates in the need of 194 full operational days to generate 1 kg of tritium.

It is important to note here that another method of providing the tritium start-up inventory for DEMO has been proposed which is consistent with a science-based framework for the development of blanket/FW, divertor and other components and materials for fusion nuclear technology [3, 4, 7, 21]. A fusion nuclear science facility (FNSF) is needed for the three stages of testing and development of FNT: scientific feasibility, engineering feasibility, and engineering development/reliability growth. FNSF is proposed to have relatively low fusion power to minimize the startup tritium inventory (see figure 16, for example). The tritium breeding ratio in FNSF can be increased beyond what FNSF needs for internal consumption so that a tritium inventory is accumulated sufficiently to provide the tritium startup inventory needed for DEMO. An example is shown in figure 17, which is reproduced from slide 24 of reference [7]. Note that the results in figure 17 were obtained several years ago assuming ITER start in 2018 and FNSF start in 2026. ITER construction and start date have been delayed considerably, and there is no firm date yet for construction and start of FNSF. Since schedule for fusion development continues to experience delays, we did not repeat the calculations with other start dates because the essence of the basic conclusions is the same.

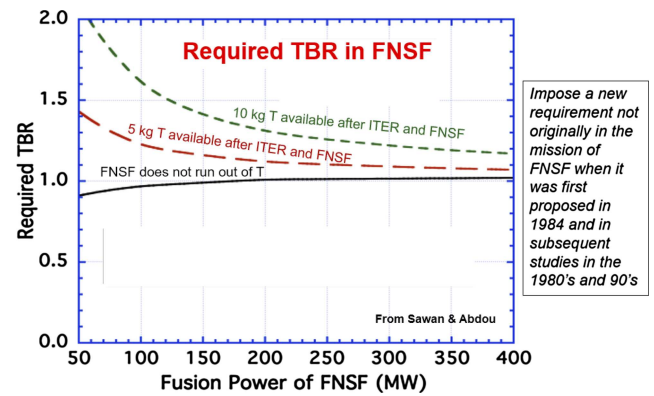


Figure 17. TBR required in FNSF for three scenarios: (1) FNSF does not run out of tritium, (2) 5 kg of tritium available after ITER and FNSF, and (3) 10 kg of tritium available after ITER and FNSF. The figure is reproduced from slide 24 of reference [7]. Note the results were obtained several years ago assuming earlier start dates for ITER and FNSF than the current schedule.

Figure 17 shows the required TBR as a function of fusion power in FNSF for three scenarios: (1) FNSF does not run out of tritium, (2) 5 kg of tritium available after ITER and FNSF, and (3) 10 kg of tritium available after ITER and FNSF. Some important observations can be drawn from the results. The smaller fusion power results in the required TBR being higher than can likely be achieved. But higher fusion power means that FNSF will need larger startup inventory. So, clearly there is a tradeoff. From earlier discussion in this paper, we recommend that (1) FNSF fusion power be $< 150 \text{ MW}$, and (2) the DEMO required startup inventory be minimized through the R & D we described. If the DEMO startup inventory is $\sim 5 \text{ kg}$ or less as shown in figure 16, then the required TBR in FNSF to accumulate this inventory is between 1.05 and 1.2 for fusion power in the range of 200 to 100 MW. These values of TBR can be achieved in FNSF through special designs of the blanket as discussed in the references we cited.

Note that R & D advances in physics and technology we discussed earlier can further lower tritium inventories and required TBR shown in figure 17. We conclude this section with a summary of key points that we discussed regarding tritium supply for fusion DEMO and reactors.

Confronting the consequences of fusion tritium consumption being large and the lack of adequate external non-fusion supply of T beyond ITER is critical for the development of fusion. The world fusion programs cannot depend on external non-fusion supply of T to: (1) provide startup T inventory for 2 or 3 DEMOs plus other facilities such as FNSF and CFETR, and (2) provide replacement for any shortfall in satisfying T self-sufficiency in large power fusion devices. Therefore, a credible fusion development pathway must develop a strategy that confronts this problem. Examples of some key elements of such a strategy are briefly stated below.

- Every effort must be done to minimize the required startup T inventory as discussed earlier in this paper (e.g. higher burn fraction, higher fueling efficiency, shorter T processing time, minimization of T inventory in all components)

- Minimize failures in tritium processing systems and required reserve time
- No DT fusion devices other than ITER can be operated without a full breeding blanket
- Development of breeding blanket technology must be done in low fusion power devices (e.g. low fusion power, small size FNSF)
- Find ways to use devices such as FNSF to accumulate excess tritium sufficient to provide the tritium inventory required for startup of DEMO as discussed above

6. Plasma physics aspects of the tritium burn fraction and predictions for ITER and beyond

6.1. Introduction and simple estimates of the tritium burn fraction in ITER

A simple determination of the TBF in ITER can be performed taking into account the T fueling needs to maintain high fusion gain (Q) plasmas and the associated fusion power production expected in such scenarios. We describe first a simple picture for the determination of the D and T fueling needs to maintain high Q plasmas in ITER. Throughout this section we will use the ITER baseline $Q = 10$ inductive scenario as the basis of our estimates. The same arguments apply to the two $Q = 5$ scenarios (1000 s long pulse and 3000 s steady-state burn) [49], which are probably more DEMO relevant regarding burn duration; the quantitative evaluations are similar but not the same given the different fusion power production and fueling rates foreseen for these $Q = 5$ scenarios compared to that for $Q = 10$.

ITER high Q plasmas will be fueled with D and T both by means of gas fueling and pellet injection [65]. The maximum D + T fueling rates for $Q = 10$ operation with up to 500 s burn in ITER is of $200 \text{ Pa m}^3 \text{ s}^{-1}$, with up to $400 \text{ Pa m}^3 \text{ s}^{-1}$ for shorter periods (typically of ~ 10 s duration), which may be required to control plasma density and power exhaust in confinement transients such as H–L transitions [42, 61]. Both the gas injection and pellet fueling systems can sustain the $200 \text{ Pa m}^3 \text{ s}^{-1}$ fueling rate for 500 s on their own providing a fueling DT mix of ~ 50 –50 at this maximum rate [65].

An evaluation of the minimum fueling rate of ITER $Q = 10$ plasmas can be determined on a simple basis including helium exhaust considerations, the DT plasma outflux to sustain the required pedestal density gradient of ITER $Q = 10$ H-mode plasmas and to ensure radiative divertor operation with acceptable divertor power fluxes [56, 74]. Regarding helium exhaust, the following considerations are made:

- He exhaust should match the alpha source corresponding to a fusion power production rate of 500 MW. This corresponds to $\Gamma_\alpha = 1.80 \times 10^{20}$ He-atoms/second, which is the same as the T-burn rate.
- He concentration in the core plasma should not exceed $C_{\text{He}} \leq 5\%$ to avoid reduction of fusion power by dilution. Assuming self-similar profiles for He and DT, as seen in experiments, the expected edge plasma He concentration is thus $n_{\text{edge-plasma}}^{\text{He}}/n_{\text{edge-plasma}}^{\text{DT}} = C_{\text{He}} \leq 5\%$.

- Helium de-enrichment at the edge of ITER plasmas is modeled to be $\eta_{\text{He}} \geq 0.1$ [54] which is well within the achieved values in present experiments; this means that the concentration of He at pump can be up to an order of magnitude lower than at the plasma edge ($n_{\text{neut-div}}^{\text{He}}/n_{\text{neut-div}}^{\text{DT}} \geq 0.1$ ($n_{\text{edge-plasma}}^{\text{He}}/n_{\text{neut-div}}^{\text{DT}}$)).

On this basis, the required pumped DT flux by the cryopumps together with He is:

$$\begin{aligned} \Gamma_{\text{DT}}^{\text{pumped}} &= \Gamma_\alpha / [C_{\text{He}} \cdot \eta_{\text{He}}] \geq 200 \times \Gamma_\alpha \\ &= 3.6 \times 10^{22} \text{ DT atoms/s} \sim 70 \text{ Pa m}^3 \text{ s}^{-1} \quad (6.1) \end{aligned}$$

This estimate needs to be compared with the evaluation of the source of particles in the confined plasma required to compensate the DT outflux from the plasma core and that required to provide the edge density required for radiative divertor operation.

The core source can be evaluated on the basis of the edge density profiles required to maintain core fusion performance and acceptable divertor heat exhaust in ITER $Q = 10$ plasmas [54, 73, 74], the extent of the region with reduced edge transport (so-called H-mode pedestal) and the level of the diffusion coefficient in the pedestal region:

$n_{\text{ped}} = 7\text{--}10 \times 10^{19} \text{ m}^{-3}$, required for $Q = 10$ operation depending on density peaking assumptions and fueling schemes [73, 76];

$n_{\text{sep}} \geq 5 \times 10^{19} \text{ m}^{-3}$, required for radiative divertor operation depending on edge plasma transport assumptions [54, 57, 58] for $Q = 10$ plasmas with acceptable power fluxes to the divertor;

$\langle \Delta_{\text{ped}} \rangle = 0.08 \text{ m}$, corresponding to $\sim 3\%$ of the average minor radius $\langle a \rangle$ as evaluated on the basis of existing experimental results and models for the pedestal plasma [74];

$D_{\text{ped}} = 0.03\text{--}0.1 \text{ m}^2 \text{ s}^{-1}$, which is comparable to neo-classical transport levels in the pedestal [51, 74];

This implies a core particle outflux of:

$$\begin{aligned} \Gamma_{\text{DT}}^{\text{core}} &= D_{\text{ped}} \times (n_{\text{ped}} - n_{\text{sep}}) / \Delta_{\text{ped}} \times S_{\text{plasma}} \\ &= 0.5\text{--}4.4 \times 10^{22} \text{ DT atoms/s} \sim 10\text{--}88 \text{ Pa m}^3 \text{ s}^{-1} \quad (6.2) \end{aligned}$$

where S_{plasma} is the plasma surface area ($S_{\text{plasma}} = 700 \text{ m}^2$). This core plasma particle outflux needs to be compensated by a corresponding particle source that is provided by the fueling systems.

Regarding the fueling requirements to achieve radiative divertor conditions, they have been extensively evaluated by edge plasma modeling. The precise fueling values depend on the level of impurity seeding, pumping speed applied by the cryopump and edge power flow levels but they are typically in the range of $\sim 100\text{--}200 \text{ Pa m}^3 \text{ s}^{-1}$ for $Q = 10$ operation [55, 56, 67, 74].

On the basis of the arguments above, a total fueling rate of up to $200 \text{ Pa m}^3 \text{ s}^{-1}$ may be required to operate $Q = 10$ ITER plasmas in order to provide the required core fueling, helium exhaust and radiative divertor plasma conditions for acceptable divertor power loads. If this fueling is performed with a 50–50 DT mix, the TBF in ITER would be $\sim 0.36\%$ at this maximum fueling rate level.

The simple approach above can also be applied to evaluate the TBF in fusion reactors such as DEMO. However, this can lead to a significant underestimate of the TBF in DEMO because the assumption that D and T should be provided 50–50 for the various fueling objectives above, which will also have to be met in DEMO, is not appropriate. In particular, specific features of edge neutral dynamics in ITER and fusion reactors, which are different from present experiments, open possibilities for optimization of tritium fueling and thus to improve the TBF beyond these simple estimates as will be described in detail in section 6.2.

6.2. Refinement of the tritium burn fraction in ITER by sophisticated edge plasma and edge-core plasma integrated modeling

The key physics differences between present experiments and ITER or DEMO that impact significantly the TBF are the inefficient penetration of edge recycled neutrals into the confined plasma and the need to sustain a relatively high separatrix density in burning plasma conditions to ensure acceptable power fluxes at the divertor through radiative divertor operation. The inefficient penetration of neutrals is caused by the large physical dimensions of ITER plasmas and the high temperatures in the SOL that ionize recycling neutrals before they can reach the confined plasma. This takes place for most H-mode plasma conditions in ITER with significant edge power flow levels, as shown in figure 18 [60] and has major implications for the fueling of ITER $Q = 10$ plasmas. In these plasmas, the ionization source for recycled neutrals in the plasma core is modeled to be negligible for the conditions in which acceptable divertor power loads ($\leq 10 \text{ MW m}^{-2}$) are achieved, as shown in figure 19 [58]. The core particle source from ionized recycling neutrals is evaluated to be in the range of $1\text{--}2 \text{ Pa m}^3 \text{ s}^{-1}$, which is more than an order of magnitude lower than the core plasma particle source required to sustain the core particle outflux as evaluated by equation (6.2).

This means that edge and core particle sources are decoupled in ITER (and DEMO) which allows for optimization of the TBF by differential fueling of D and T for the two separate missions of core plasma fueling and helium exhaust/divertor power flux control.

Fueling of the core plasma in ITER requires pellet injection. Due to the outwards drift of the high pressure plasmoid formed after pellet ablation, pellet injection from the HFS is required for deposition of particles beyond the pedestal plasma in ITER due to the high edge temperatures [69, 70]. Edge-core integrated simulations of ITER plasmas have been used to evaluate the required level of pellet injection to sustain $Q = 10$ operation for a range of core transport modeling and plasmoid drift assumptions [45, 74, 80] resulting in HFS pellet injection fueling rates of $\Gamma_{\text{DT}}^{\text{HFS}} \sim 20\text{--}40 \text{ Pa m}^3 \text{ s}^{-1}$ (an example is shown

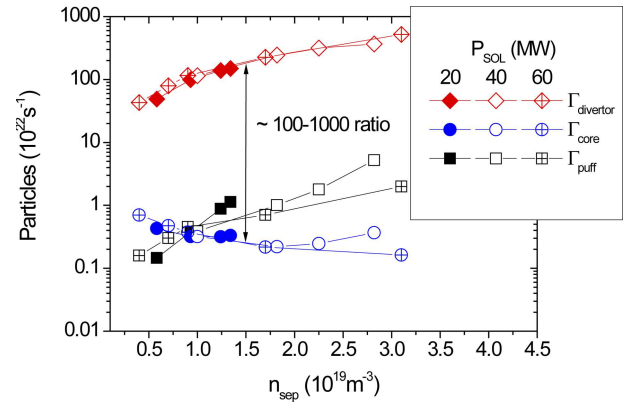


Figure 18. Total divertor particle flux determining the recycled neutral source (Γ_{div}), core plasma ionization source (Γ_{core}) and gas puffing flux (Γ_{puff}) versus separatrix density (n_{sep}) for a series of SOLPS simulations spanning the range $P_{\text{SOL}} = 20\text{--}60 \text{ MW}$. Reprinted from [60], Copyright © 2014 ITER Organization. Published by Elsevier B.V. All rights reserved.

in figure 20), similar to the simple estimates in section 6.1. This implies that the total T fueling source required to sustain a 50–50 concentration in the core plasma in ITER can be as low as $10\text{--}20 \text{ Pa m}^3 \text{ s}^{-1}$.

Concerning the fueling requirements to provide $Q = 10$ operation with acceptable divertor power loads, these are determined by the achievement of semi-detached divertor operation to dissipate the plasma power flux before it reaches the divertor target by radiative and atomic losses from hydrogenic isotopes and impurities. This is achieved by fueling of extrinsic impurities (neon typically in ITER) in the divertor plasma together with operation at high SOL plasma density to ensure low impurity concentrations in the core plasma, since a high core plasma impurity concentration can decrease fusion reactivity. The sustainment of such densities may require significant levels of gas fueling for $Q = 10$ operation. Typical gas fueling rates to provide radiative divertor operation in ITER $Q = 10$ plasmas and appropriate helium exhaust are typically in the range of $60\text{--}120 \text{ Pa m}^3 \text{ s}^{-1}$ [53, 68, 74]. Since gas fueling and recycling gas do not contribute significantly to core plasma fueling ($\leq 2 \text{ Pa m}^3 \text{ s}^{-1}$ as discussed above), the gas fueling isotope can be chosen to be D and in this way reduce significantly the T throughput required to sustain $Q = 10$ operation in ITER.

The result of the ITER studies with high fidelity edge plasma models and edge-core integrated models is that $Q = 10$ operation can be sustained with a T throughput of $10\text{--}20 \text{ Pa m}^3 \text{ s}^{-1}$ even when the total fueling rate of DT is $200 \text{ Pa m}^3 \text{ s}^{-1}$. This leads to a TBF of $1.8\text{--}3.6\%$ instead of the initially estimated 0.36% due to the inefficient fueling of the core plasma by gas puffing and recycling fluxes which are dominated by D. It should be noted, however, that this does not decrease the volume for DT fuel re-processing from the exhaust to recover T since the total fuel throughput remains the same. The difference is the T concentration in the exhausted fuel, which can be as low as $5\text{--}10\%$ of the total instead of 50% with the simple estimates in section 6.1.

It should be noted that, since ITER is an experimental reactor, the fueling system is designed to cover a wide range of

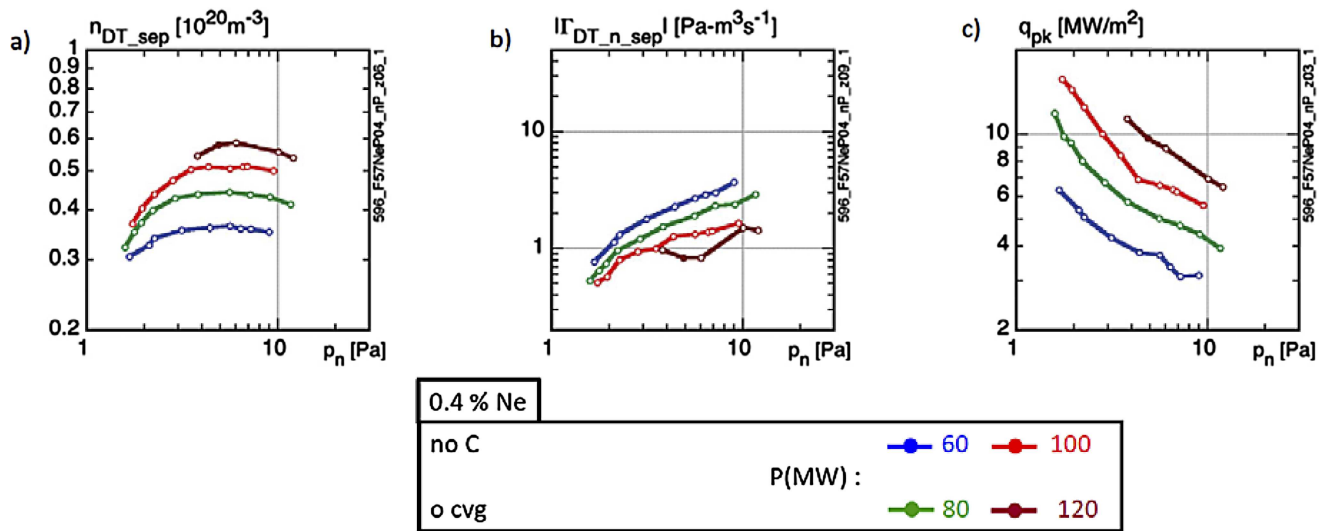


Figure 19. Variation of the separatrix plasma density (a), neutral influx to the plasma core (b) and peak power loading of the divertor target (c) with neutral pressure in the private flux region for a range of edge power flow values with 100–120 MW being typical for $Q = 10$ operation in ITER. Reproduced courtesy of IAEA. Figure from [58]. Copyright 2016 IAEA.

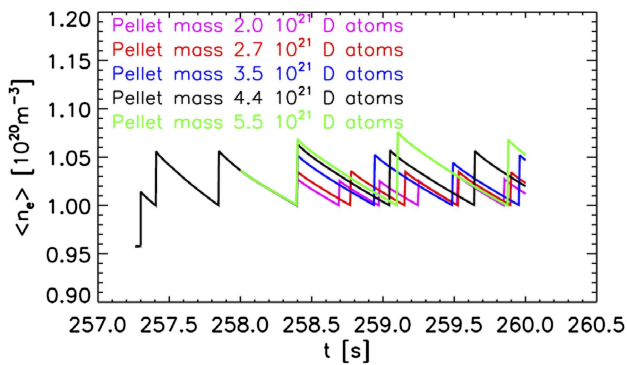


Figure 20. Evolution of the plasma volume-average density by means of pellet injection (4.4×10^{21} DT atoms per pellet) in a 15 MA/5.3 T ITER DT $Q = 10$ baseline plasma for different pellet injection frequencies corresponding to a fueling range $\Gamma_{DT}^{HFS} \sim 31\text{--}44$ Pa m^3 s^{-1} . Reproduced with permission from [45]. © 2018 Crown copyright. Reproduced with the permission of the Controller of Her Majesty's Stationery Office.

D/T fueling ratios both by pellet injection and by gas fueling independently [65] even if the expectations are that the T throughput can be kept at very moderate values compared to the maximum capabilities of the system. This is justified by the fact that the estimates above are performed with physics models whose results have been compared with experimental results but cannot be fully validated for ITER plasma conditions since these cannot be achieved in present tokamak experiments. Thus, several uncertainties remain regarding particle transport and scenario requirements in ITER, which can impact the results above regarding the TBF; the major open physics/scenario integration issues are described below.

6.2.1. Open physics/scenario integration issues impacting the prediction of the TBF in ITER. As mentioned above, there remain uncertainties regarding the physics processes determining particle transport as well as scenario integration aspects of $Q = 10$ plasmas that can affect the required fueling levels and

corresponding TBF from the estimates above. The main open issues for ITER in this area are described briefly below.

ELM control and associated fueling requirements Control of edge localized modes (ELMs) associated with H-mode operation in ITER is required to ensure acceptable power fluxes to PFCs during these short transients and to provide impurity exhaust from the main plasma [62, 75].

The integrated simulations for fueling of ITER $Q = 10$ plasmas described above are generally carried out in stationary conditions while in H-mode with ELMs particle outfluxes are usually dominated by the ELMs. Despite this, the stationary simulations provide an appropriate description of the ELM-averaged value of the particle outflux from the plasma that needs to be compensated by HFS pellet injection. For instance, for controlled ELMs in ITER $Q = 10$ plasmas with ELM energy loss $\Delta W_{ELM} = 0.6$ MJ and an average power flux carried by ELMs of $P_{ELM} = 18\text{--}36$ MW, the associated particle loss per ELM is:

$$\Delta N_{ELM} = \Delta W_{ELM} / 3T_{ped} = 2.5 \times 10^{20} \text{ DT ions} \quad (6.3)$$

assuming that these small ELMs are convective [59] and that the pedestal temperature is $T_{ped} \sim 5$ keV for $Q = 10$ plasmas, as predicted by MHD studies taking into account SOL plasma characteristics in ITER [74]. This corresponds to a total average particle outflux driven by ELMs:

$$\Gamma_{ELM} = 0.7 - 1.5 \times 10^{22} \text{ DT ion/s} = 15 - 30 \text{ Pa } m^3 \text{ s}^{-1} \quad (6.4)$$

which is similar to that evaluated with the integrated modeling codes described above.

What is not included in this estimate above and in many of the integrated modeling studies for $Q = 10$ operation are the impact on fueling requirements that the schemes to obtain the required level of ELM control have on fuel throughput and the TBF. This is dependent on the ELM control scheme applied and can have different impact on the TBF as discussed below.

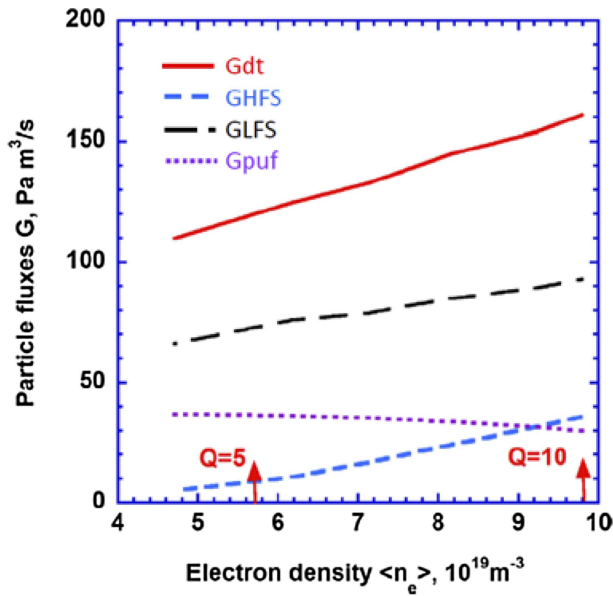


Figure 21. Integrated edge-core simulations for ITER 15 MA/5.3 T, $P_{\text{aux}} = 50$ MW H-mode plasmas covering a range of densities and resulting Q . The total DT fueling throughput (G_{DT}) required for core fueling ($G_{\text{HFS}} - 50-50$ DT), ELM control by pellet pacing ($G_{\text{LFS}} - 100\%$ D) and divertor power flux control ($G_{\text{puf}} - 100\%$ D) is modeled self-consistently. Reproduced courtesy of IAEA. Figure from [74]. © 2017 ITER.

In ITER, the baseline ELM control scheme relies on the application of 3D fields by a set of 27 in-vessel ELM control coils [62]. When 3D fields are applied for ELM control a significant particle outflux is observed in experiments leading to a so-called density pump-out (see e.g. [48]). Initial estimates of such effect on ITER $Q = 10$ plasmas indicate that ELM suppression by 3D fields can reduce the core plasma particle confinement by up to 35% [78], although this remains an open R & D topic. Such a decreased particle confinement would require a corresponding increase of pellet fueling to maintain the same core plasma density. Thus, for these ELM suppressed H-mode conditions $\Gamma_{\text{DT}}^{\text{HFS-ELM suppression}} \sim 27-54 \text{ Pa m}^3 \text{ s}^{-1}$ and, correspondingly, the TBF would drop to 1.3–2.6% for the maximum total fueling of $200 \text{ Pa m}^3 \text{ s}^{-1}$ in ELM suppressed $Q = 10$ plasma conditions.

The secondary ELM control scheme in ITER relies on the control of the ELM frequency by pellet injection [44, 62, 71]. This is expected to require up to 30–60% of the total throughput since the estimated pellet size for ELM triggering is $\sim 1-2 \times 10^{21}$ DT atoms/pellet [44] and the triggering of ELMs reduces the fueling efficiency of pellets [72]. Integrated edge-core plasma simulations including ELM control by pellet pacing have been carried out taking into account HFS pellet injection for core plasma fueling, LFS pellet injection for ELM control and gas and impurity fueling for divertor power load control [74]. These simulations find that, since fueling efficiency from LFS pellet injection is very low, the mission of ELM triggering can be performed by pure-D pellets. This, together with using D gas fueling for divertor plasma power flux control, allows maintaining a TBF of 1.8% even for fueling rates near $200 \text{ Pa m}^3 \text{ s}^{-1}$, when all these processes are modeled self-consistently, as shown in figure 21.

Pedestal particle transport An important basic assumption in the plasma fueling physics picture above, which impacts the TBF, is that fueling of the core plasma by recycling species is solely determined by ionization of recycled neutrals inside the separatrix and diffusive-like transport in the edge plasma region. It is known that the picture of diffusive-like transport does not always apply to plasma particle transport, in particular for impurities, but also for the main ions in the plasma core. Particle pinches can lead to significant particle fluxes for the main ions both because of neoclassical transport (i.e. the Ware pinch) and turbulent transport effects.

While the understanding of core particle and impurity transport is rather advanced (see e.g. [40]), the situation in the edge and pedestal region is much more uncertain, in particular for main DT ion transport, and remains an open R & D topic. Experimental evidence from present devices indicates that impurity transport in the pedestal region is compatible with neoclassical transport being dominant [77], while for main ion transport diffusive-like transport (without an inwards convective component or pinch) can describe adequately the observed behavior within experimental uncertainties. Dedicated experiments and modeling for ASDEX Upgrade has shown that the build-up of the density in the H-mode pedestal region can be described satisfactorily without the inclusion of a turbulent inwards pinch or with one but with a very low value of 0.5 m s^{-1} [82], as shown in figure 22. The lack of a significant inwards edge pinch for DT ions is in agreement with edge turbulent transport simulations for ITER $Q = 10$ plasma [41].

A neoclassical physics mechanism driving a convective inwards DT flux in the pedestal due to ambipolarity and force balance [46] has been identified, but this only leads to significant inwards DT ion flux for high impurity densities in the pedestal. However, these high impurity densities lead to significant core plasma radiation in ITER and this is not compatible with the required energy confinement necessary to achieve $Q = 10$. For DEMO, in which the edge power flow is much larger than the required power to access the high confinement H-mode, higher core plasma radiation and impurity levels may be compatible with high Q operation. This mechanism may be relevant for plasma DT fueling in DEMO and this is discussed in more detail in section 6.3.

To illustrate the consequences that the existence of an edge inwards pinch can have on the plasma fueling in ITER, we can evaluate the associated particle influx that an inwards pinch with a low value of $v_{\text{ped}} = 1 \text{ m s}^{-1}$ for D and T can cause in ITER:

$$\begin{aligned} \Gamma_{\text{DT}}^{\text{core}} &= (n_{\text{ped}} + n_{\text{sep}})/2 \times v_{\text{ped}} \times S_{\text{plasma}} \\ &= 4.6 \times 10^{22} \text{ atoms/s} \sim 90 \text{ Pa m}^3 \text{ s}^{-1} \quad (6.5) \end{aligned}$$

This corresponds to $\sim 50\%$ of the total fuel throughput in ITER. If this transport mechanism were to materialize in ITER, edge fueling would therefore contribute significantly to core plasma fueling. Such inwards convective DT influx at the plasma edge would decrease the need for core DT fueling by HFS pellet injection but would also link edge recycling with the core plasma. This decreases the margin to control independently the edge and core D/T concentrations compared to that

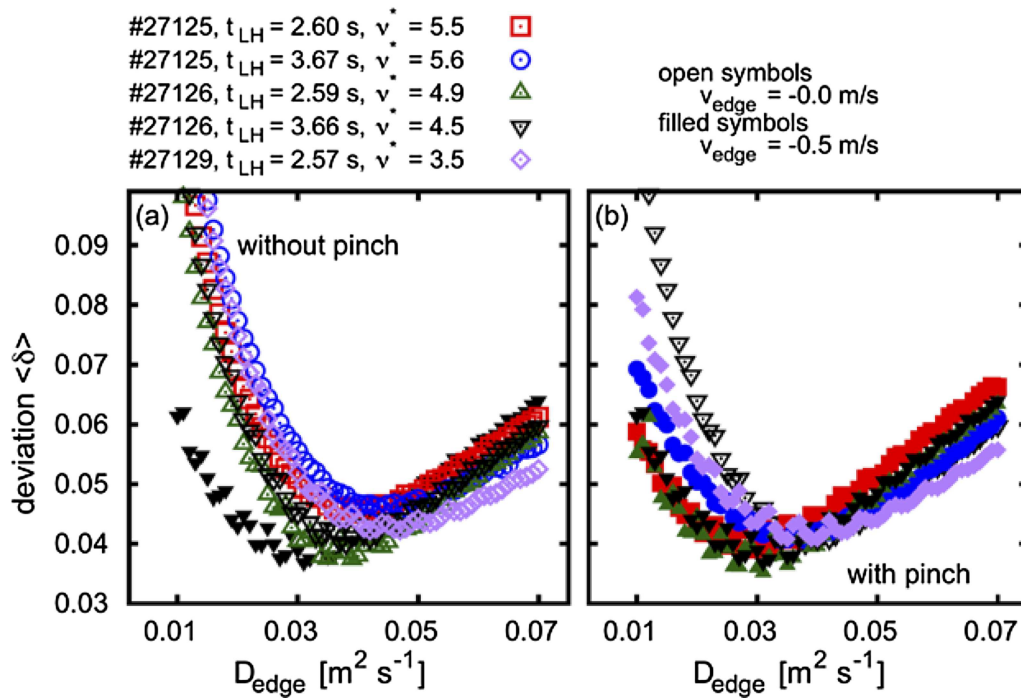


Figure 22. Deviation of the modeled density profile in the build-up after the transition to H-mode plasma in ASDEX Upgrade versus the value of the edge diffusion coefficient used in the modeling (D_{edge}) for a range of discharges with different collisionalities: (a) modeling of all H-mode phases without an edge pinch (open symbols) and for comparison one modeling with an inwards pinch $v_{\text{edge}} = -0.5$ m s⁻¹ (filled symbols) are shown. (b) Modeling of all H-mode phases with edge pinch and one modeling without pinch. A time span of 300 ms is analyzed. Reproduced courtesy of IAEA. Figure from [82]. Copyright 2013 IAEA.

when neutral ionization is the dominant source of particles in the core plasma. If a significant edge inwards DT pinch were at work in ITER $Q = 10$ plasmas, it would be thus required to fuel a similar amount of D and T both by gas fueling and pellet injection to achieve a 50–50 DT level in the core plasma. This has been found to be required in present experiments where edge recycling contributes significantly to core fueling [47] and would lead to low TBF of $\sim 0.36\%$ to be achievable in ITER.

DT core particle transport Regarding core DT fueling differences in D and T transport in the core plasma have been observed in modeling that can affect the ratio of T to D that needs to be provided by HFS pellets to achieve a 50–50 DT mix and thus the TBF. In the central part of the plasma, where transport is expected to have a low level of turbulence, simulations for ITER assuming that neoclassical transport dominates indicate that the T and D flows can have different directions due to the higher mass of T, with T flowing outwards while D flows inwards [63]. This implies that to get a 50–50 DT mix in the central part of the plasma the inwards anomalous particle flux should have a higher concentration of T to counteract this effect.

Integrated modeling of separate D and T core plasma turbulent particle transport has been performed including HFS pellet fueling for ITER [76]. In these simulations, it is found that the efficiency of T fueling, when 50–50 DT pellets are injected, is lower than that of D by $\sim 30\%$, as shown in figure 23. This trend for a faster inwards particle transport for the lighter isotopes in mixed-isotope hydrogenic plasmas has been confirmed in JET experiments [66] and thus seems a robust trend,

although its quantitative evaluation for ITER requires further studies. Interestingly, the studies in [76] also show that the resulting DT plasma mix by separate D and T pellet injection, while providing an average fueling 50–50 DT, depends on pellet size and injection sequence. These can be used to reduce the amount of T injected by HFS pellet fueling to get a 50–50 DT mix in the central part of the plasma where fusion reactions take place. While R & D in this area should continue to understand the separate transport of D and T in the core plasma and to optimize D/T ratio control, on the basis of existing results these effects are not likely to affect strongly the TBF estimated from integrated modeling predictions for ITER in section 6.2.

6.3. Possible differences between ITER and DEMO impacting the TBF

In most aspects of the DEMO particle transport and edge plasma behavior affecting the TBF no major differences are expected from ITER, since the DEMO plasma size and edge densities and temperatures will also make core plasma fueling by recycling DT fluxes very inefficient. Similarly, core plasma transport aspects in DEMO should be similar to those of ITER since both require high density low collisionality plasmas for optimum fusion power production. There will be quantitative differences between ITER and DEMO associated with the higher pedestal temperatures in DEMO which affect the efficiency of HFS pellet fueling, since this is strongly dependent on the value of the edge temperature [69, 70]. Similarly, the solution adopted for ELM control or avoidance in DEMO

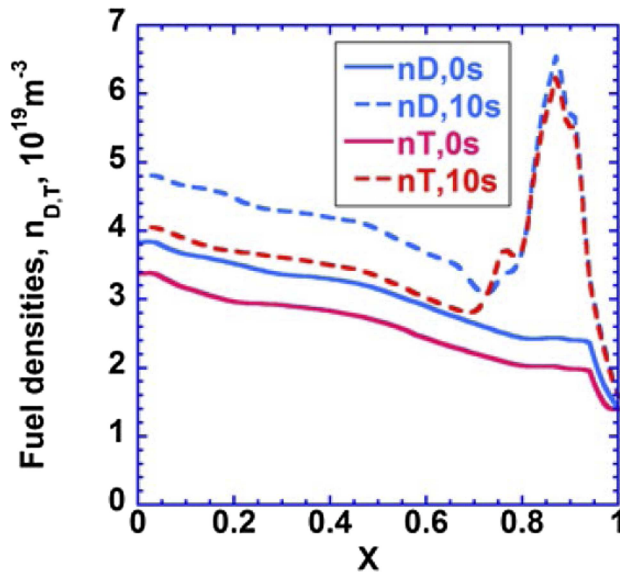


Figure 23. Density profiles at 10 s in the access to ITER $Q = 10$ plasma conditions following start of the injection of HFS pellets made of 50–50 DT showing a lower efficiency to increase the T density in the central plasma region compared to D. Reproduced from [76]. CC BY 3.0.

is likely to be different from ITER and, thus, this may have a different impact on the TBF in DEMO than in ITER.

One area where DEMO might deviate significantly from ITER regarding T fueling is in the role of edge inwards pinches in providing core plasma fueling from recycling DT fluxes. Whether this is an important effect or not depends on the specific power exhaust solution and the fusion power production level that are considered for DEMO. If a conventional exhaust solution is adopted for DEMO, and not an advanced divertor solution, this consists of an ITER-like radiative divertor solution combined with a significant level of core plasma radiation (or core radiative solution) as summarized in table 6 [64].

In this case, impurity levels at the edge of the plasma can be significant since impurities are well screened by neoclassical transport effects due to the large temperature gradients in the pedestal [43] and the high separatrix density required for divertor power exhaust. This efficient edge impurity screening allows large edge impurity densities while core impurity levels remain moderate and compatible with high fusion energy production. The high impurity densities at the plasma edge lead to an inwards DT pinch due to ambipolarity and force balance effects described by neoclassical transport [46]. As explained in section 6.2.1, a sizable inwards edge DT pinch (regardless if neoclassical or anomalous) provides a way for recycling fluxes to contribute to plasma core fueling which can have a significant impact on the TBF. The importance of this mechanism is strongly dependent on the specific DEMO operating scenario since this determines the level of impurities required to provide core radiative exhaust. In the case of the EU DEMO 1 design, integrated modeling studies have shown that an inwards DT pinch at the pedestal exists but it is not large, as shown in figure 24, and its impact on DT fueling is very moderate [79].

This type of core radiative plasma scenarios is not relevant for ITER high Q operation since in this case the margin of

the total plasma heating power (P_{tot}) above the power required to access high confinement ($P_{\text{L-H}}$) is much smaller than in DEMO, as shown in table 6. Thus, these high core plasma radiation regimes are not compatible with high confinement and high Q operation in ITER. Despite this, the physics of these radiative scenario regimes and their impact on DT fueling can be studied in ITER at moderate levels of plasma current and field. For instance, for 7.5 MA/2.65 T DT plasmas with $\langle n_e \rangle = 0.85n_{\text{GW}}$, where n_{GW} is the Greenwald density limit, $P_{\text{L-H}} = 25$ MW. If such a plasma is heated by the ITER baseline heating schemes at their maximum power of $P_{\text{tot}} = 73$ MW, the ratio of $P_{\text{tot}}/P_{\text{L-H}}$ in this plasma is similar to that in EU DEMO 1 and core radiative plasma scenarios with high plasma confinement can thus be accessed in ITER for these plasma conditions, albeit at a low $Q \sim 0.5$ –1.

Integrated plasma modeling studies have been carried out for these plasma conditions in which a radiative core plasma scenario is achieved by fueling of neon or argon (see figure 25). In these plasma conditions significant inwards pinches at the plasma edge are expected for DT in ITER $v_{\text{edge}} = -3$ to -5 m s $^{-1}$, which corresponds to a total influx 3.0 – 6.0×10^{22} DT ions/s or 60 – 120 Pa m 3 s $^{-1}$. In these conditions, the edge D/T level would be replicated in the core plasma thus removing the capability to control edge D/T and core D/T ratios independently, unlike in $Q = 10$ plasma conditions in ITER. If such high levels of edge inwards pinch would occur in DEMO, this might lead to a lower TBF being achievable in DEMO than in ITER. Therefore, this potential detrimental effect of neoclassical transport for high radiative core plasma scenarios should be taken into account in evaluating DEMO scenarios and eventually explored in ITER as part of the DEMO targeted experiments in the ITER research plan [49].

6.4. Summary and conclusions for plasma physics aspects of the tritium burn fraction

To provide an accurate evaluation of the TBF in ITER and DEMO detailed integrated modeling of the plasma should be applied going beyond the simple particle balance and core plasma transport studies usually utilized for this purpose. Such TBF evaluation has to include the integration of scenario requirements for the successful demonstration of fusion energy generation, such as of power and helium exhaust. This is necessary because the required plasma conditions to provide this exhaust can have a significant impact on the fueling of the plasma by recycling species as well as on edge particle transport. An evaluation of the TBF in ITER using integrated modeling including these integration aspects shows that a TBF = 1.8–3.6% may be achievable instead of the 0.36% derived from simple estimates. It should be noted that, while the TBF can be significantly higher than evaluated with the simpler approach, the total amount of recycled DT fuel that needs to be reprocessed is very similar for the integrated modeling predictions and those from simpler models. The estimates of the maximum achievable TBF in ITER, however, remain uncertain due to incomplete physics knowledge of core and edge DT transport in ITER plasmas and on the quantitative impact of ELM control on the TBF for ITER.

Table 6. Total heating power (P_{tot}), H-mode threshold power (P_{L-H}), minimum edge power flow compatible with high confinement assuming a margin of 25% above P_{L-H} ($P_{\text{sep}}^{\text{min}}$) and corresponding maximum radiated power in the plasma core ($P_{\text{rad}}^{\text{core,max}}$) for ITER [50] and the EU DEMO 1 design [81].

Device	P_{tot} (MW)	P_{L-H} (MW)	$P_{\text{sep}}^{\text{min}}$ (MW)	$P_{\text{rad}}^{\text{core,max}}$ (MW)	$P_{\text{rad}}^{\text{core,max}}/P_{\text{tot}}$ (%)
ITER ($Q = 10$)	150	70	88	62	41
DEMO	460	133	166	294	64

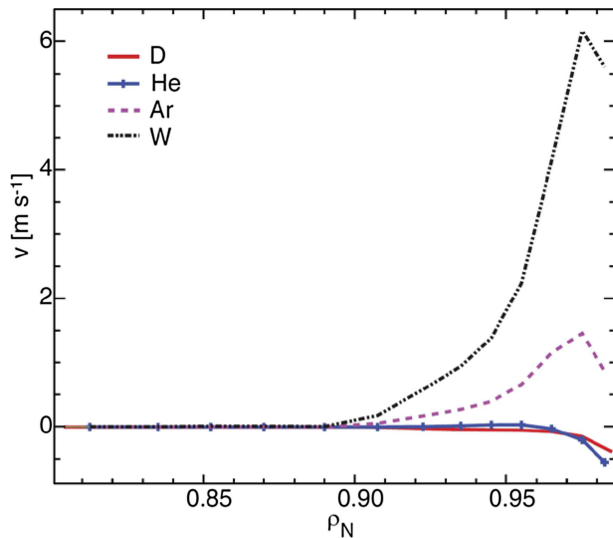


Figure 24. Edge profiles of neoclassical convective velocities for D (similar for T), helium, argon and tungsten for an EU DEMO 1 reference plasma. Reproduced courtesy of IAEA. Figure from [79]. © 2015 EURATOM.

The results obtained for ITER are expected to be similar to those for DEMO although quantitative differences regarding the efficiency of core plasma fueling by pellet injection may arise from the much higher edge temperatures expected in DEMO compared to ITER and the different level of core confinement. In addition, there may be qualitative differences for particular power exhaust scenarios, namely those requiring significant radiation and impurity densities at the edge of the core plasma. These can potentially lead to a significant fueling of the core plasma by recycled DT fluxes due to changes in edge DT transport and could be detrimental to optimize the TBF in DEMO. Whether such effects are sizable or not depends strongly on the DEMO operating scenario and fusion power production assumptions and needs to be analyzed in detail together with the power exhaust scenario considered.

7. Plasma fueling technology and predictions of fueling efficiency for ITER and DEMO based on experiments and modeling

7.1. Fueling technology background

The technology for fueling fusion plasmas has progressed significantly over the past three decades of research and development in this field. Fueling by pellet injection has evolved into the preferred method to fuel a burning plasma due to

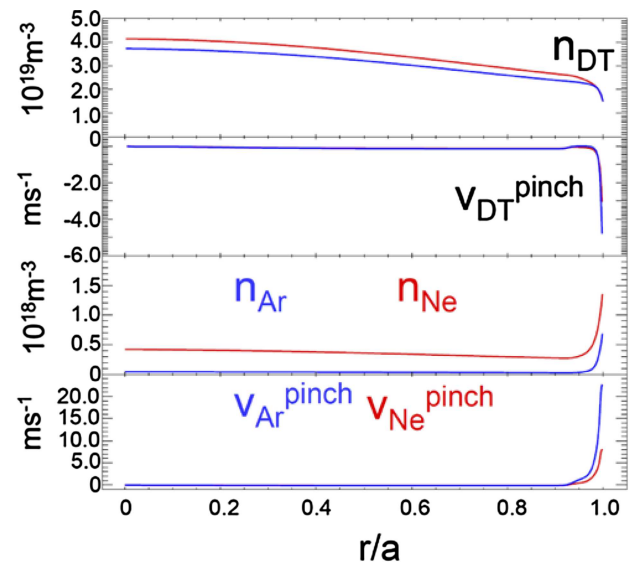


Figure 25. Core DT density, DT pinch, neon and argon densities and pinch velocities for two 7.5 MA/2.65 T plasmas in ITER with $P_{\text{tot}} = 73$ MW and radiative power fractions of $\sim 60\%$ obtained by either neon or argon puffing [52].

its technology maturity and improved efficiency compared to other schemes such as gas fueling and neutral beam fueling. A recent review paper [83] has been published that describes many of the improvements in pellet injector technology such as continuous extrusions for steady-state operation, HFS injection for tokamaks, and high-speed pellet injection for deeper fuel penetration. The fueling of plasmas with gas is much simpler technology than that of pellets, but it suffers from poor time response due to the slow flows through long capillary tubes both inside a machine and external to it. But more of an issue for gas fueling is the poor penetration of neutral atoms through the SOL of the plasma that we describe in more detail in the next section. Neutral beams are also capable of fueling the plasma and are found to inject non-negligible amounts of fuel in present day smaller experiments. However, in a large burning plasma device, the beams will have to operate at high energies approaching or exceeding 1 MeV in order to penetrate deep into a large high-density plasma. This of course is also beneficial for depositing the beam neutrals (i.e. fuel) where it is needed, but the currents of the beams will be very modest compared to the volume and particle content of the plasma and will thus result in very little plasma core fueling, significantly less than what is needed to maintain high density and replace burned D and T ions.

The technology for pellet injection is described in detail in previous review articles [83, 84] and so we just briefly review

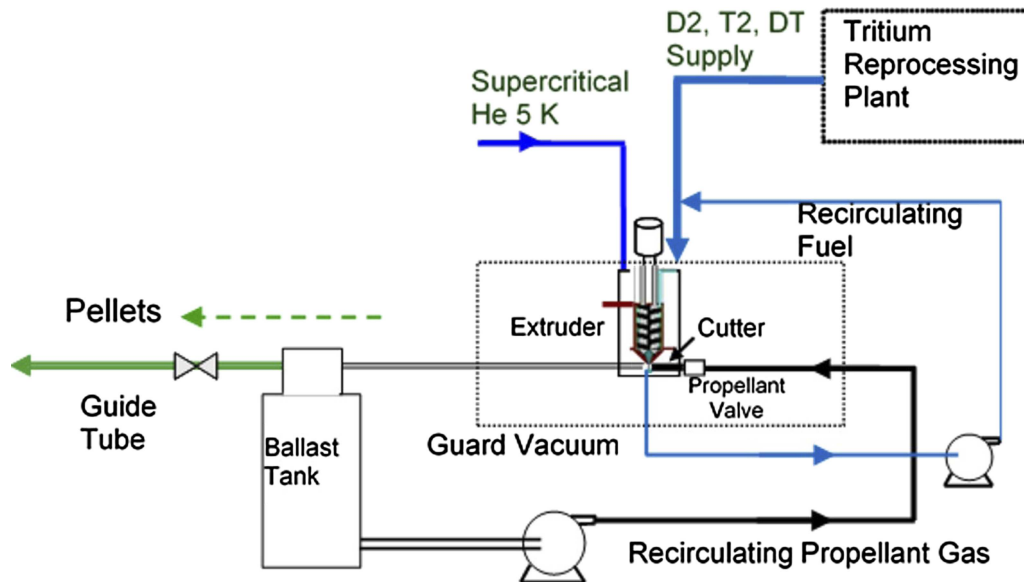


Figure 26. A block diagram of a gas gun based pellet injection system.

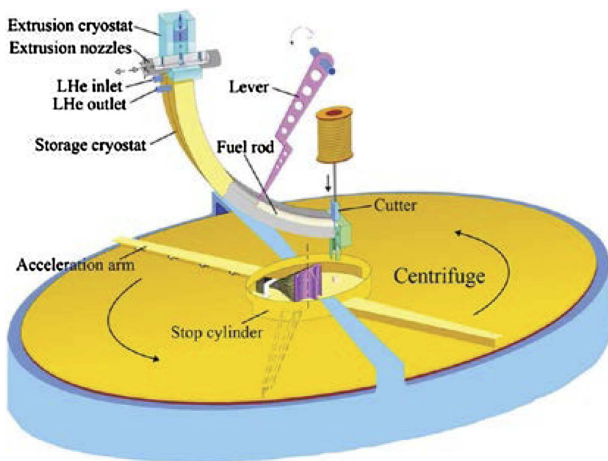


Figure 27. Centrifuge pellet injector used on ASDEX Upgrade from reference. [83] 2018, reprinted by permission of the publisher (Taylor & Francis Ltd, <http://www.tandfonline.com>.)

here the options for this technology in a burning plasma device. The pellets would be fabricated by using a continuous extruder to produce steady state flowing solid ribbons of DT fuel that can be cut into pellets and accelerated into the plasma. The two most developed pellet acceleration schemes are the repeating gas gun and the centrifuge. Gas guns are used effectively in several present-day experiments [83] and have the ability to fire pellets on demand as long as the extrusion is available for cutting and chambering a pellet. They do require propellant gas to accelerate the pellets at levels on the order of 10 mbar l per pellet for the ITER design [84]. This gas must be recovered by vacuum pumps before entering the torus and recirculated to avoid reprocessing large amounts of gas by the tritium exhaust processing plant. A diagram of a gas gun based pellet injection system similar to what is being developed for ITER is shown in figure 26. A centrifuge pellet injector on the other hand as shown in figure 27 does not require propellant gas and can therefore operate without the additional

complication of a gas recirculation loop. Centrifuges have been used successfully in present day experiments [85] however one has not been used with a steady-state capable pellet feed system and so that capability needs to be developed and demonstrated.

7.2. Fueling efficiency data from tokamaks

Fueling efficiency has been studied in a number of tokamak and stellarator experiments in the past couple decades [86–88]. The fueling efficiency has generally been defined as the fraction of injected fuel that remains in the plasma after the injection event has ended. (Note that the fueling efficiency mentioned here does not include the losses during pellet acceleration and transport through the tubes that guide the pellet from the outlet of the injector to the position where the pellet enters the plasma chamber.) In practice this is defined as the total increase in number of plasma electrons ΔN_{e-pl} divided by the number of injected electrons from the fuel atoms N_{e-inj} and is determined by measurements of plasma electron density profiles before and just after a fueling event.

$$\eta_{eff} = \Delta N_{e-pl} / N_{e-inj} \quad (7.1)$$

For pellet fueling this is fairly straight forward as the pellet ablation event from an injected pellet is generally completed in a millisecond or less and is easily detected in the plasma.

There are aspects of the pellet injection event that can affect the fueling efficiency and make it less than the ideal 100% that one might expect. For one, the pellet can be ablated by fast ions or energetic alpha particles in the SOL before it reaches the plasma confinement region, thus losing atoms on the way into the plasma that end up being ionized and swept into the divertor where they may not result in net fuel to the plasma. Also, pellets have been found to trigger ELMs when injected in H-mode plasmas that can result in a significant fraction of the pellet mass being ejected from the ELM perturbation

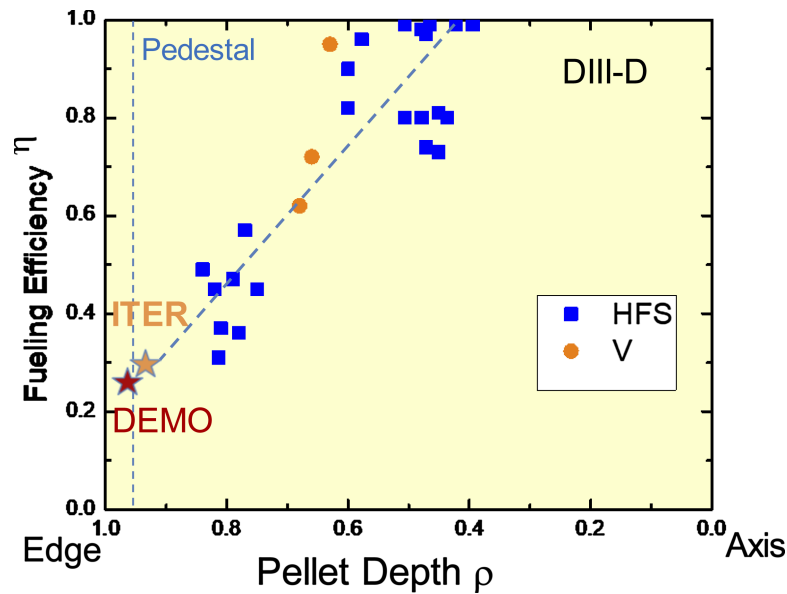


Figure 28. Fueling efficiency from deuterium pellets injected from the HFS inner wall and vertical V + 1 port as a function of their penetration depth to normalized minor radius (normalized toroidal flux) in DIII-D H-mode plasmas without ELM mitigation being applied. The dashed line is a fit to the data with extrapolation to ITER and DEMO.

to the plasma edge as the pellet is still entering the plasma. Such events on DIII-D were found to eject in some cases more than 50% of the pellet mass when large ELMs were triggered [86]. For this reason, it is critical to avoid plasmas with large ELMs that result in poor fueling efficiency. Not only do large ELMs present a problem for erosion of PFCs that has resulted in extensive research into ELM mitigation [89], but they also inhibit any chance to efficiently fuel the plasma with pellets. A third aspect of pellet injection that can lead to less than ideal fueling efficiency is the polarization cross field drift during the pellet deposition process that can eject a significant fraction of the pellet mass into the scrape of layer on the low field side (LFS) of the plasma [90]. This effect, which is believed to be driven by ∇B and curvature drifts in the pellet cloud as it expands along field lines, is particularly problematic for pellets injected on the LFS of a tokamak and is the reason that fueling from the inner wall (HFS) of tokamaks has been planned for use on ITER. This effect has not been found to be very strong in stellarator plasmas [91], which have much weaker ∇B than a similar size tokamak.

The fueling efficiency from gas fueling is more difficult to quantify since the gas flows into the plasma over much longer periods of time than single pellet injection events. One attempt to quantify this was in a study comparing gas and pellet fueling on DIII-D [86] where the gas was injected at a steady flow rate over a 3 s long period of time and compared to the resulting plasma density increase at the end of that period. Using this method, the analysis of the data found that less than 1% of the injected gas could explain the modest density increase in the plasma.

The location of the gas injection from the inner wall had some modest improvement on the efficiency versus from the LFS, but not nearly the same level of improvement as seen

with pellets injected from the inner wall versus the outside midplane. In a burning plasma device such as ITER that will operate at high plasma density, the opacity of neutrals injected from the wall is much worse than in a smaller lower magnetic field machine such as DIII-D as calculations have shown [84, 92]. One would therefore expect the fueling efficiency of gas in a more reactor relevant regime to be extremely poor and not very useful for getting tritium into the core plasma efficiently. Gas fueling will nonetheless be useful for feedback control of the divertor operating parameters where efficient fueling and fast time response is not required.

The most extensive pellet fueling efficiency studies that have been published were on the DIII-D tokamak and so we summarize those here for extrapolation to larger burning plasma devices. In these studies [90], performed in H-mode plasmas without ELM mitigation being applied, it was found that HFS pellet injection (from the tokamak inner wall) was much more efficient than LFS (outer midplane) injection because of the polarization drift and ELM triggering issues mentioned above. More recent data has been added to the database and shown in figure 28 where smaller 1.8 mm pellets that contain 3×10^{19} atoms are included to show how the fueling efficiency changes with more shallow penetrating pellets. These smaller pellets are the ones in the plot with penetration outside of $\rho = 0.7$. In these pellet events there was no ELM mitigation technique being applied and so each pellet was found to trigger a large type I ELM. The penetration of all these pellets was well beyond the top of the edge H-mode pressure pedestal. With this level of penetration, the fueling efficiency was found to be well less than 50%. The remainder of the pellet mass ended up being deposited in the SOL and largely flowing to the divertor where it can produce some level of neutral fueling over longer periods of time.

7.3. Fueling of ITER and DEMO burning plasmas

In ITER and even more so in a DEMO tokamak as envisioned by the EU, the fueling pellet penetration in burning plasmas is expected to be significantly shallower than in the results above from DIII-D. The pedestal temperature of these plasmas is expected to be on order of 5 keV or more, which will lead to very high pellet ablation rates that scale as $T_e^{11/6}$ from the well known neutral gas shielding pellet ablation model [93] whose scaling has been extensively verified in a multimachine pellet ablation database [94].

The plan for ITER is to use HFS pellet injection for the primary fueling source [84] with cylindrical pellets up to 5.3 mm in size that can be DT mixtures up to 90% tritium, limited by the purity of tritium separation available in the tritium plant. The speed of the pellets for intact injection will be limited due to the complicated path that they must take in a guide tube starting at ports near the bottom of the machine that are routed under the divertor and behind inner wall blanket modules. The curves in this guide tube geometry were tested and found to deliver intact pellets only if they were $<300 \text{ m s}^{-1}$ [95]. The design for DEMO must take the routing of pellets for optimal fueling into the design from the initial concept to final design in order to make sure that higher speed pellets can be routed into the plasma intact and with minimal erosion. The use of curved guide tubes will have some limitation but hopefully can be optimized to much higher speeds than 300 m s^{-1} [96]. A straight trajectory from above the machine through a vertical port that reaches the HFS of the plasma is also an option that could be compatible with very high speed pellets from a repeating two-stage gas injector [97, 98].

In a DT pellet injection system, there will be losses of the solid DT fuel in cutting and firing the pellets. These losses will not affect the overall tritium fueling efficiency because any excess extrusion material can be collected with pumps and recirculated directly back in the extruder input without needing to be processed for isotope separation in the tritium plant. In fact, the ITER pellet injection system is being designed to operate this way to minimize the size of the tritium processing plant [99].

7.4. Anticipated fueling efficiency and implications

We expect shallow penetration of pellets in ITER and a DEMO plasma, even for a pellet with a content of 10% of the plasma content, which is believed to be the limit of density perturbation that can be tolerated without adversely affecting the plasma. Therefore, the question remains what the resulting fueling efficiency will be in such shallow penetration high performance H-mode plasmas. Existing pellet systems on today's experiments have difficulty producing and injecting pellets small enough to achieve shallow penetration just to the pressure pedestal in H-mode plasmas as expected in these burning plasmas. This makes extrapolation from today's deeper penetrating pellets and performance predictions extremely difficult. Points on the figure 28 plot indicate some extrapolation from the DIII-D penetration scaling but are highly uncertain and may be overly optimistic depending on how much of the pellet mass is immediately ejected by a triggered ELM. If ELM

mitigation is successful at greatly reducing the ELM magnitude or eliminating ELMs altogether, then we may find much higher fueling efficiency at these shallow penetration levels than this linear extrapolation shows. It is fair to say that it will be a necessity to eliminate large type I ELMs being triggered by the fueling pellets to have any chance for a high fueling efficiency.

Interaction of fueling pellets with detached divertor operation is another unknown in the burning plasma regime that could have implications on how well divertor operation can be controlled. If the pellet fueling is inefficient for the reasons mentioned above, then the impulses of gas or plasma in the SOL that reach the divertor could result in local radiation imbalances and lead to confinement degradation as has been seen in MARFEs on existing tokamaks. Pellet fueling research in this area has begun [100, 101] and should be examined in as close to ITER conditions as possible.

If DEMO is a stellarator and not a tokamak, then we can expect that there will not be a helpful ExB polarization drift effect to help with fueling efficiency. On the other hand, there may also not be strong type I ELMs to contend with. The same issue with neutral opacity would be expected since the device would operate at high density and thus pellet fueling will still be preferred over gas fueling. Since outside midplane injection would be the most practical for a stellarator device without a strong ExB drift, it is possible to envision a high-speed injection technique that could be applied instead of a single stage light gas gun or centrifuge. In particular, a two-stage gas gun approach is possible to achieve 2.5 km s^{-1} or higher pellet speeds and thus deeper penetration as required in a burning plasma [87]. The challenge will be to further develop high-speed pellet technology to make it practical and reliable enough for a reactor application. Thus far it has only been demonstrated at a 1 Hz short pulse capability [102].

8. Tritium safety

To ensure the safety and licensing of future fusion reactors, designs must minimize inventories and limit the release of hazardous materials under all operational conditions. Hazardous materials in fusion reactors include beryllium and radioactive species such as tritium and the products of neutron activation. Tritium is a primary safety concern as it is unavoidably present as the fuel for the fusion reaction and it is continuously transported throughout the plant. General safety approaches include minimizing tritium inventories, reducing tritium permeation through materials, and decontaminating material for waste disposal. Minimization of tritium inventories is the focus of several technologies including efficient extraction from breeding materials and coolant streams as well as fuel cycle components. This section will provide a summary of tritium safety in two parts: tritium hazards and regulations, and tritium permeation and management.

8.1. Tritium hazards and regulations

Extensive discussion on tritium physical properties, chemistry, and biological effects can be found in the US DOE-STD-1129-

Table 7. DOE fusion safety standard requirements for protection of the public from exposure to radiation. Reproduced (adapted) with permission from [104].

	US DOE Fusion requirement	US DOE Regulatory limit
Normal and anticipated operational occurrences	0.1 mSv/y (10 mrem/y)	1 mSv/y (100 mrem/y)
Off-normal conditions (per event)	10 mSv (1 rem)	250 mSv (25 rem)

2015 tritium handling and safe storage [103]. This section provides a brief summary.

Tritium is a radioactive isotope of hydrogen containing two neutrons and a proton which decays with a half-life of 12.32 years as



The emitted β particle has a range in air of roughly 5 mm, an average energy of 5.7 keV, and a maximum energy of 18.6 keV. Therefore, tritium does not produce penetrating radiation and cannot pass through the dead layer of skin cells. Tritium is only hazardous when it enters the body by skin absorption, ingestion, or inhalation of tritiated gas, vapor, or solid particulates. The dose received by tritium exposure depends on the chemical form. Solid tritide dust (MQ_x) remains in the body the longest and is the most hazardous. Tritiated water (Q_2O) has a biological half-life of 10 days. Molecular gaseous tritium (Q_2) is least hazardous as only small quantities are absorbed by the human body. Here, Q represents the hydrogen isotopes tritium (T), deuterium (D), and protium (H), and any combination of these.

The majority of tritium chemistry is similar to that of hydrogen which allows it to combine with other elements to form a variety of compounds. Tritium is a gas at room temperature in its pure molecular form (Q_2) and can react with other elements to form gaseous species such as methane (CQ_4), and liquid or vapor species such as water (Q_2O) and ammonia (NQ_3). Tritium can also be substituted for hydrogen and deuterium in oils or lubricants. When absorbed into metals to form metallic tritides, tritium can exist in the solid phase at room temperature. Measurement of tritium concentration is difficult in bulk solids with non-destructive methods, whereas ion chambers can be used to measure concentration in gas-phase, scintillation counting in the liquid phase, and swipes/scintillation counting for surfaces. The radioactivity of tritium produces chemistry differing from protium and deuterium. As tritium decays, the energy released can desorb gases yielding an increase in pressure. The decay energy can also break chemical bonds, for example during the radiolysis of tritiated water or catalysis of reforming and exchange reactions.

Due to the variety of tritium chemistry, containment is challenging. Tritium rapidly disperses in the gas-phase, diffuses through solids such as polymers and metals, and exchanges with hydrogen to form mobile carriers such as water, oils, and particles. Controls for other forms of radiation such as shielding and air filtration are not suitable for tritium. The only suitable objective is to minimize or eliminate direct personal contact by limiting tritium inventory and containing tritium

with impermeable barriers. Further information on tritium hazards can be found in the US DOE guidance on tritium handling and storage [103].

For tritium use in fusion reactors, the main safety concern is the exposure of personnel and the public both in normal operation and in accident scenarios. The US DOE fusion safety standard (FSS) [104] safety policy requires that:

- The public shall be protected such that no individual bears significant additional risk to health and safety from the operation of those facilities above the risks to which members of the general population are normally exposed.
- Fusion facility workers shall be protected such that the risks to which they are exposed at a fusion facility are no greater than those to which they would be exposed at a comparable industrial facility.
- Risks both to the public and to workers shall be maintained as low as reasonably achievable (ALARA).
- The need for an off-site evacuation plan shall be avoided.
- Wastes, especially high-level radioactive wastes, shall be minimized.

The FSS [104] identifies two sets of radiological criteria to be used for evaluating tritium (and other radioactive) releases: regulatory limits and fusion requirements. Regulatory limits come from title 10 of the Code of Federal Regulations, and apply to the maximally exposed individual off-site, using conservative assumptions. Fusion requirements set more stringent limits, but can be evaluated using best-estimate techniques. The fusion requirements are designed to (1) limit risks from exposure during normal operation to 0.1% of the cancer fatality risks from all other sources, and (2) avoid the need for public evacuation under any circumstances, according to EPA protective action guidelines. The rationale behind these values is described in more detail in [105]; the corresponding limits on radiation dose are summarized in table 7.

The physical releases of tritium (e.g. in grams, or grams/y) that would lead to such doses depend on the characteristics of a particular site, including its size (distance to site boundary), weather characteristics, etc. DOE places no specific limits on the physical releases, only on the dose a member of the public could receive from these. A dose conversion factor of 0.35 mSv/g tritium, obtained for a generic site as described in [106], has been used in recent studies (e.g. [107]); this leads to a fusion requirement of ≤ 0.286 g/y from normal operations. ITER, under construction in France, complies with International Commission on Radiation Protection (ICRP), International Atomic Energy Agency (IAEA), and French regulations. The Institute for Radiological Protection and Nuclear Safety (IRSN) published a reference document that outlines

the safety and radiation protection considerations for fusion reactors [108]. Tritium release from ITER is conservatively assumed to be solely tritiated water and is not to exceed 2.5 g/y in years of heavy maintenance and 0.6 g/y under normal operation. The tritium site limit in the whole facility is 4 kg and limit in the vacuum vessel is 1 kg.

While there is no US regulatory limit on tritium inventory for future fusion reactors, large inventories increase the likelihood of releases in excess of regulatory limits during normal and off-normal events. As a result, larger inventories could necessitate larger reactor sites, off-site evacuation plans, or both, thereby reducing the attractiveness of the plant. Minimizing the overall tritium inventory of a plant is therefore an important safety objective in its design.

8.2. Tritium permeation and management

High temperature operation is inherent to a fusion power plant; however, tritium is very mobile in the metal alloys used as structural materials at these temperatures. In fact, tritium uptake and permeation through structural materials is the primary method for tritium losses under normal operating conditions [107, 109]. These permeation losses challenge the safety of the plant as tritium can permeate to undesirable areas resulting in unintended environmental release or exposure to personnel.

Tritium permeation through metals is described by three consecutive processes (figure 29): (1) surface dissociative-adsorption, (2) bulk diffusion, and (3) recombinative-desorption. The first process of permeation is the incoming flux of dissociative-adsorbing tritium molecules given by

$$J_d = K_d P \quad (8.2)$$

At the same interface the adsorbed atoms can also recombinative-desorb resulting in a flux leaving the surface described by

$$J_r = K_r C^2 \quad (8.3)$$

The rate constants K_d and K_r are for dissociative-adsorption and recombinative-desorption, respectively, of tritium molecules on the surface. C is the concentration of adsorbed tritium at the gas-phase tritium partial pressure of P . If dissociation and recombination are in equilibrium, the relation between pressure and concentration at each surface interface follows Sieverts' law:

$$C = K_S \sqrt{P} \quad (8.4)$$

where K_S is the Sieverts' constant, also referred to as the solubility constant, defined by

$$K_S = \sqrt{K_d/K_r} \quad (8.5)$$

When surface processes are fast and in equilibrium, hydrogen transport is in the diffusion-limited regime where the concentration gradient across the metal defines the permeating flux. Here, the flux (J) is dependent on the difference in the square roots of hydrogen partial pressure on the high-pressure (P_h) and low-pressure (P_l) sides, hydrogen permeability (Φ),

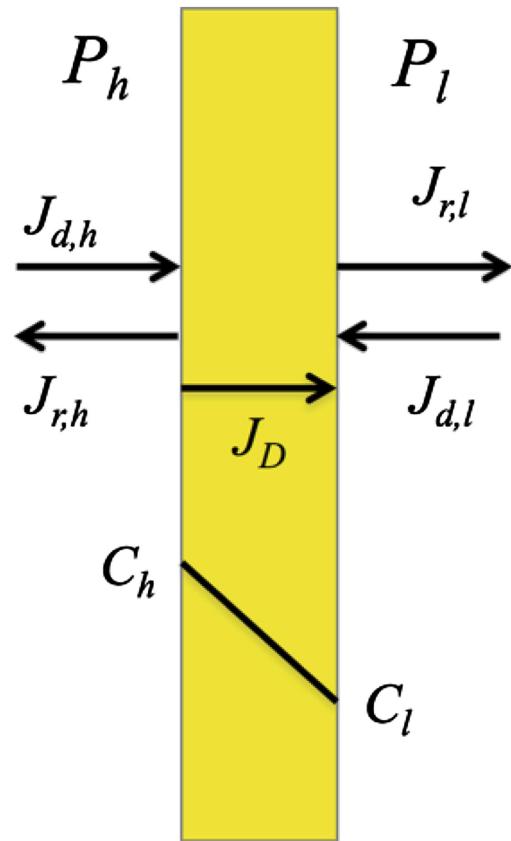


Figure 29. Surface and bulk transport processes involved in tritium permeation through metals.

and wall thickness (l). Permeability is the constant of proportionality and is defined by the product of hydrogen diffusivity (D) and solubility (K_s). Herein, the equation defining flux is also referred to as the Richardson equation:

$$J = \frac{\Phi}{l} (\sqrt{P_h} - \sqrt{P_l}) \quad (8.6)$$

Permeability (Φ) is described by an Arrhenius function and commonly increases with temperature. However, being the product of solubility and diffusivity, it can decline with temperature for certain exothermic hydrogen occluders. So far, this discussion has assumed isothermal conditions, however, in fusion relevant environments, such as in the divertor, first wall, and blanket systems, large temperature gradients exist. In this case, it may be important to consider the thermomigration component to diffusive flux (Soret diffusion) and include the heat of transport Q^* :

$$J = -D \left(\frac{\partial C}{\partial x} + \frac{Q^* C}{RT^2} \frac{\partial T}{\partial x} \right) \quad (8.7)$$

Recent work at CIEMAT demonstrated the importance of Soret diffusion in hydrogen permeation, however, also expressed the difficulty in accurate experimental measurements [110].

The diffusion-limited regime is only applicable for clean surfaces and high partial pressures. This model does not apply in the surface-limited or intermediate transport regimes. In

the surface-limited regime the flux scales with $\sim P$ instead of $\sim\sqrt{P}$, the concentration profile across the metal is nominally flat and permeation rates are generally significantly less than those in the diffusion-limit regime. Surface-limitations are beneficial for reducing tritium permeation in structural materials, but detrimental to extraction technologies using high permeability materials. The transition between diffusion-limited and surface-limited is described by a dimensionless number (W') [111]:

$$W' = \frac{K_d P^{0.5} l}{DK_S} \quad (8.8)$$

When $W' \gg 1$; permeation is in the diffusion-limited regime, characteristic of large dissociation rate constant, high pressure, thick materials, and low permeability. When $W' \ll 1$ permeation is in the surface-limited regime, characteristic of low dissociation rate constant, low pressure, thin materials, and high permeability.

In the surface-limited regime, the permeating flux is commonly described by equation (8.2) and the dissociation constant can be defined as

$$K_d = \frac{\alpha}{\sqrt{2\pi mkT}} \quad (8.9)$$

The denominator is the kinetic theory coefficient with the particle mass (m), particle temperature (T), and Boltzmann constant (k). The sticking coefficient (α) represents the fraction of the impinging particle flux that permeates through the membrane. The sticking coefficient is generally assumed to be thermally activated and dependent on the thermodynamic and kinetic properties of the incident surface. Clean metal surfaces are expected to have values of $\alpha = 1$ resulting in the diffusion-limited transport regime, whereas oxidized or ‘poisoned’ surfaces have values of α approaching zero, resulting in the surface-limited regime.

To accurately predict the permeation of tritium through materials, one needs values for diffusivity, solubility, dissociative-adsorption rate constant, and recombination-desorption rate constant for the temperature range of interest. Diffusivity and solubility are relatively straightforward to measure, and large databases [112–117] exist for materials of interest such as pure metals, RAFM steels, austenitic stainless steels, Ni–Cr-based superalloys, and V–Cr–Ti alloys.

Techniques to measure hydrogen diffusion in metals include equilibrium and nonequilibrium methods and are discussed in detail by Völkl and Alefeld [118]. Equilibrium methods consist of nuclear magnetic resonance and quasi-elastic neutron scattering. The most common nonequilibrium methods consist of permeation, electrochemical, mechanical relaxation, and resistivity. To gain accurate data from permeation and electrochemical methods, conditions must be such that $W' \gg 1$. Mechanical methods circumvent surface related issues by introducing hydrogen into the metal and measuring diffusion by the Gorsky effect under a dilation gradient. Solubility is typically measured by applying a known quantity of hydrogen to a sample and the uptake is measured either by the pressure difference in volumetric methods such as a Sieverts’ type apparatus or gravimetrically with

microbalances. The ‘theoretical’ hydrogen isotope permeability reported in reviews [112, 113] are the product of independent measurements of solubility and diffusivity using the methods described above.

Carefully executed measurements of surface rate constants on clean surfaces agree well with theory [119], but these data can be difficult to obtain, and results can vary widely for differing surface conditions. A few research groups have conducted campaigns on measuring surface constants. Perujo, Serra, and colleagues used the method of ‘reverse permeation’ to obtain values for RAFM steels [120–122], austenitic steels [123], Inconel 625 [123], and Incoloy 800 alloys [124]. Grant and colleagues developed a method of pressure modulation and applied it to pure Ni and Ni–Th alloys [125] and stainless steel 304 [126]. Hatano and colleagues [127, 128] used an UHV chamber with O₂ dosing capabilities to measure surface constants at low pressure for V and Nb.

Another challenge in the accurate modeling of tritium transport is the effect of trapping sites. Serra *et al* [114] provides a review of tritium transport parameters including discussion on trapping effects for a variety of materials. For example, in RAFM steels, trapping at defect sites reduces the apparent diffusivity at temperatures <523 K, whereas the diffusion through tungsten is nominally completely controlled by trapping effects [129].

Various codes such as TMAP, FUS-TPC, EcosimPro, and TAS model multicomponent tritium transport in fusion systems. The tritium migration analysis program (TMAP) was developed by the fusion safety program at INL, United States, in the 1980s for safety analysis of systems handling tritium [130]. TMAP models the permeation through materials with incorporated surface rates, diffusion and solubility limits, multiple trapping sites, heat transfer, flows between enclosures, and chemical reactions within enclosures [131, 132]. FUS-TPC, developed by Franza *et al* at ENEA, Italy in 2011 is a fusion version of the tritium permeation code for sodium-cooled fast reactors (SFR-TPC) [133]. CIEMAT has led the development of a tritium transport toolkit for EcosimPro, and applied to several of the EU candidate DEMO blanket concepts [134]. The fusion reactor tritium analysis system (TAS) was developed in the 2000s by the team for Frontier Development of Science (FDS) team at the Institute of Nuclear Energy Safety Technology, China [135]. These codes have been employed to model tritium phenomena such as retention in PFCs [136, 137], permeation through blanket components [138–141], and environmental and biological impacts from release events [142].

Permeation barriers are studied with an aim to inhibit the transport of tritium through structural materials. Several reviews on permeation barrier technology have been conducted in the past 25+ years [115, 116, 140, 143–146]. Permeation barriers are low permeability layers such as oxides, carbides, and nitrides applied onto surfaces to reduce permeation rates. Layers are applied either by oxidizing metal alloy surfaces creating a ‘natural’ barrier or by coating metal surfaces with an external material. The effectiveness of permeation barriers is described by the permeation reduction factor

(PRF) which is the ratio of native material permeability to that of the barrier covered material.

PRFs in controlled laboratory settings are measured up to 10^5 . However, these coatings rely on defect-free layers and any pores or cracks are essentially short-circuit paths for hydrogen transport. For example, the permeability of SiC varies 5–6 orders of magnitude [147], and the PRF of Er_2O_3 coatings was found to be inversely proportional to grain boundary density [148]. This relates to the degradation of permeation barriers in radiation environments where defects are formed. Many high PRF barriers result in PRFs < 100 once neutron irradiated [149–153]. However, only a limited set of neutron irradiation experiments have tested permeation barriers and the mechanism of degradation is still not fully understood. Hollenberg *et al* [143] proposed three basic models of transport through permeation barrier systems: the composite diffusion model, the area defect model, and the surface desorption model. Causey *et al* [115] concluded that the most likely form of transport model is a combination of the area defect model and the surface desorption model due to the fact that barriers do not change the permeation activation energy and the transition to the surface-limited regime occurs at higher than anticipated pressures. Both these models are dependent on the defect area and the effective distance hydrogen must traverse to reach the metal. Radiation generally increases the area of defects giving rise to higher permeation rates.

The need for extremely high PRF permeation barriers will be dictated by blanket type, structural materials, process design features, and tritium extraction efficiencies. For example, the main loss paths in the FNSF with a DCLL blanket concept are through primary PbLi pipes, primary He pipes, and vacuum vessel walls. Though the FNSF analysis assumed that high ($\sim 90\%$) extraction efficiencies could be achieved in PbLi. DOE FSS targets could be met in this design with the application of permeation barriers with a PRF ~ 100 and no additional mitigations [107]. Similar results were also suggested for an analysis of DEMO [109]. It is important to note that these analyses are critically dependent on tritium solubility in Pb–17Li, an uncertain value that spans two orders of magnitude. Alternatively, Tanabe suggests much higher PRFs of 10^5 – 10^6 are required for ferrite materials in similar system designs [154]. Undoubtedly, tritium permeation barriers in some form will be required to meet the radioactive release requirements, and barrier coatings are likely part of a ‘defense in depth’ approach. Other strategies such as double jacketed pipes provide a less sophisticated but practical method of tritium management. Here, heated components at risk of tritium permeation losses are surrounded by an external jacket where purging and pumping recovers the permeated tritium [155].

Aside from limiting tritium permeation losses, other management activities such as outgassing and detritiation also factor into the safety of a plant. Tritium can accumulate in surface contaminants such as oils, water, and lubricants as well as on high surface area materials such as catalysts and adsorbents. Prior to breaching tritium confinement barriers for maintenance operations, tritium should be recovered to the highest

extent possible. This involves at least a single evacuation or potentially more aggressive measures such as repeated back-filling and evacuation with heating. Detritiation must occur in order to safely dispose of materials that have an affinity for uptake such as structural materials and metal hydrides. Detritiation consists of vacuum heating with repeated exposure to protium to facilitate exchange reactions [156].

9. Options for tritium fuel cycle technology for DEMO and required R & D

The sections above have identified fuel cycle parameters of central importance on start-up inventory, doubling time and tritium inventories associated with self-sufficiency of a fusion reactor. Section 4 elaborates the strong influence of the product of TBF and fueling efficiency, and approaches to increase them are developed further above. This parameter reflects improvement potentials on the plasma physics side. For the fuel cycle the product of TBF and fueling efficiency defines the load, so higher values of the product result in lower throughputs at given fusion power. The throughputs are then translated into inventory numbers based on the basis of the reference set of parameters and processing times listed in tables 1–3.

On the other side, the architecture of the fuel cycle itself can also help to reduce inventories at given product of TBF and fueling efficiency. The introduction of DIR is an example of that. A smart fuel cycle architecture should hence consider inventory minimization as one design driver. Ideally, the final configuration of the fuel cycle combines moderate improvements of the product of TBF and fueling efficiency with the DIR ratio. The latter reflects the improvement potential on the fuel cycle engineering side, and avoids the need for excessive improvement on physics.

Finally, the fuel cycle can only perform as good as the individual technologies allow for. We have therefore conducted a rigorous system engineering approach, where technology surveys were evaluated and ranked according to weighted requirement tables [157–160]. In the following we will discuss the best performing technology options behind all fuel cycle system blocks and identify which space for improvement there is to come up with reduced processing times. As outlined in section 4 above, the impact of processing time can be quite substantial, in particular for values of fueling efficiency times burn fraction of $< 1\%$. The most obvious way to speed up processing is in replacing batch technologies by continuous technologies wherever possible. Some system blocks in the fuel cycle build on the same technology as in ITER, some others involve novel technology which requires additional R & D to develop it to a similar technology readiness. We will go through all sub-systems as laid out in figure A.1 in the appendix A and also in figure 1.

9.1. Vacuum pumping

In almost all larger tokamaks, also in ITER, cryogenic pumping is used for particle exhaust from the plasma chamber. This comes from the fact that cryogenic vacuum pumping can be designed to be perfectly tritium-compatible. Furthermore, with strong active cooling of the cryosurfaces it can process the

typical very high surface related throughputs that appear as direct consequence of the limited achievable numbers of the product of TBF and fueling efficiency. However, due to the batch operation principle and the accumulation of the pumped gas associated with that, operation of these pumps gets complicated in particular for longer pulse times. Depending on the chosen staggering interval between the pumps, typical pumping times for a reactor scale device are in the order of 20–30 min, as are the regeneration times. This time interval is included in the integral 4 h that have been assumed as processing time for the fuel clean-up and ISS. After this time, the total pump ensemble behaves quasi-continuous, i.e. there is no further increase in inventory. A steady-state inventory will be built up that, for a 3 GW machine will be in the order of 700 g. This inventory is a significant contribution to the fuel cycle operational inventory. To eliminate this, continuous pumping systems are being developed, which would make the processing time and resulting inventories negligible. As turbomolecular pumps would not survive the exposure to tritiated gases at such pressures over a sufficiently long time, EU has started a development program of mercury based continuous vacuum pumping, using mercury vapor diffusion pumps backed by liquid ring pumps with mercury as working fluid [161], as mercury has practically zero solubility for tritium.

Triggered from the 20 years' development of the cryopumps for ITER, there are design software tools available for flow simulations and cryogenic design considerations that have been validated in representative scale experiments. So that no near-term actions are needed. Whereas the active design development of diffusion pumps has practically stopped 50 years ago, when the turbomolecular pump technology came up. The application of diffusion pumps for fusion requires a pump design which is easily scalable, better than the existing circular designs. As mercury diffusion pumps have only been researched about 100 years ago, modern design tools will now be employed (such as novel hybrid multi species codes for particle tracking over a wide range of gas rarefaction) to understand and predict the multitude of complex flow phenomena appearing in these pumps such as backstreaming, shockwave formation and nozzle jet and wall interaction. First demonstration experiments have already been performed; figure 30 is illustrating a recently built purely mercury based pump train that confirmed first designs of both pump types. It is intended in EU to build a representative scale infrastructure for mercury pumping.

9.1.1. Fuel separation. As discussed in section 4.2.3, the introduction of a DIR loop that carries pure fuel directly from the exhaust gas to the fueling systems can help a lot to reduce inventories. It also helps to reduce the overall processing time, in particular if the largest fraction of the fuel would go the quick and short DIR way whilst only a small remainder would go the slow and long way all through the tritium plant. The DIR concept requires a new functionality being installed in the fuel cycle, namely a technology to extract the fuel at the low densities close to the divertor. There are three driving requirements for any appropriate technology, namely (i) be able to extract a significant fraction of the arriving exhaust gas stream, (ii)



Figure 30. Photo of the integrated mercury driven diffusion pump/ring pump test train.

extract the hydrogens with high selectivity (negligible amount of non-hydrogenic species), and (iii) be sufficiently quick so as to not introduce additional processing times.

The classical way to do this is the use of permeable membranes, however at the low densities in the divertor ports, which do not provide sufficient driving force, they do not work efficiently. There are currently two technology variants under further R & D. One is exploiting the phenomenon of superpermeation which allows suprathreshold hydrogen particles to permeate through a metal foil with surface barrier whereas all other species do practically not permeate through the foil [162]. One essential feature of the metal foil pump (MFP) is an ideal sharpness of the fuel separation. The superpermeation principle is being studied intensely in EU to be integrated in the so-called MFP [163, 164]. The energization of the hydrogen shall be achieved by a cold plasma source, see figure 31, which promises to come with improved lifetime characteristics, compared with the hot filament that was suggested earlier. Although the degree of ionization in the cold plasma is moderate, operation in the fusion environment at high external fields is non-trivial. While seeding gases in the tokamak exhaust gas being pumped are becoming a larger fraction along the MFP, there might be parasitic effects to the generation of suprathreshold hydrogen as the noble gases lead to a stronger depopulation of high energy electrons which would otherwise produce the suprathreshold hydrogen. A comprehensive experimental program is ongoing [165].

Alternatively, one could use a distributed cryogenic pumping with separate stages for heavy gas condensation (80 K), condensation of the lighter PEG (25–30 K), hydrogen pumping by cryosorption at activated charcoal of ~ 15 K, and finally a helium cryosorption stage [166]. A separation can be achieved by combining the different temperature dependencies for condensation/adsorption of the different gas species together with a separate regeneration of the individual stages, if there are valves which can close the stage compartments during regeneration. It has been found that high DIR fractions can be achieved, but that it is challenging to reduce the part of non-hydrogenic species to the small amounts required.



Figure 31. Candidate cold plasma source for the MFP under laboratory testing.

From principle considerations, it is obvious that there exists an optimum recycle ratio, coming from the fact that the processes in the tritium plant require certain minimum tritium contents to work properly. As the ISS in the OFC is not only fed from the hydrogen of the unrecycled exhaust gas, but also taking the hydrogens from CPS and TES, a practical upper limit value is reached when the latter two streams become the dominant load. This is illustrated in figure 32, which shows for two TBR ratios how the estimated tritium inventory in the DEMO fuel cycle depends on the chosen DIR fraction for an assumed integral plant availability of 30% with statistical outages [167, 168]. From this sensitivity analysis, a design value of 80% for the DIR-fraction is derived.

9.2. Fuel clean-up

The main function of the fuel clean-up sub-system is to separate the arriving gas into three streams, namely (i) the fuel stream for re-use, (ii) the PEG stream for re-use (if not the decision is taken to skip any re-processing) via appropriately sized decay tanks for the activated species, and (iii) the remaining detritiated impurity stream. Please note that, additional to the tokamak exhaust, impurities from the blanket TESs might also be in the scope of the exhaust processing system, a requirement which has, however, not yet been included in the current architecture. The fuel clean-up system will be the first part of

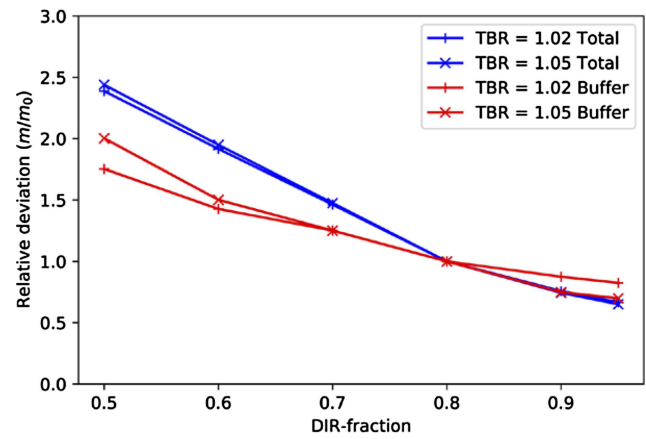


Figure 32. Sensitivity of tritium inventory on DIR fraction at an $\eta_{rfb} = 1\%$.

the tritium plant in line to receive gas from the tokamak downstream the pumping systems, as such the design of the systems will look differently depending on if a DIR loop is included or not.

For inventory and continuity reasons classical permeation membrane technology with a number of suitably sized palladium-silver permeators will be employed for bulk hydrogen separation, rather than cryogenic adsorption on molecular sieve or getter bed technology, as the latter do neither match the expected low tritium inventory of a permeator based system nor the negligible processing times. Permeator-based fuel recovery can be scaled from ITER [169], where the same technology is utilized for the same task, up to DEMO sizing requirements without any issue, although in case of a DIR architecture the high PEG content of the exhaust would reduce the hydrogen partial pressure differential across the membrane, which is the driving factor for permeation. It should be possible to overcome this by increasing overall process pressure whilst maintaining a high vacuum on the permeate side. This defines an upper limit on a feasible DIR ratio which is in good agreement with the 80% number discussed in figure 32 above.

Also for tritium recovery from tritiated impurities, ITER technologies may well serve as a good candidate. It consists of a catalyst bed and permeator loop for the first stage impurity processing, followed by a palladium membrane reactor for final detritiation. The proposed set up includes cracking and recovery of hydrogen isotopes, followed by an oxidation final clean-up sub system which ensures effective second stage tritium recovery. In case of a DEMO fuel cycle with DIR, the main difference is the quantity of PEGs relative to the amount of impurities requiring detritiation. The system would have to be sized to take account of this, both in terms of increased gas flow and the reduction of efficiency due to any blanketing effect of the PEGs.

For PEG separation there exist several technologies and the choice not only depends on scoring well against the key design criteria, but on the specific application (particularly the number and type of different PEGs: Ar, Xe, Ne, Ar, N₂) which is unclear currently. In particular, if nitrogen is involved and

then ammonia has to be treated with the impurities, the PEG separation would become significantly larger. Options include pressure swing absorption, cryogenic trapping, and molecular sieving by porous membranes. R & D of different membrane types [170, 171] has started to get quantitative numbers on separation efficiencies and hence allow for a sizing of this sub-system. As there will most probably be more than one PEG species, a range of technologies in combination, put into the most efficient and appropriate sequence, may be the best solution.

9.3. Isotope separation system (ISS)

The ISS uses cryogenic distillation to separate the incoming hydrogenic gas stream into the different pure hydrogen isotopes. Cryogenic distillation suffers from the inventory issue that there is a significant amount of hydrogen isotopes being liquefied, and is responsible for the long processing times assumed for this system block. At ITER, a total of four distillation columns and several equilibrium reactors (equilibrator) are installed. A large number of stages (of the order of 100) is needed for the columns, which makes operation complex and costly. Furthermore, the design of such cryodistillation columns is tailored to a pre-defined performance, which does not leave flexibility. ITER is posing the requirement to provide the different isotopes in pure form, mainly for experimental flexibility of the ITER campaigns. This is not required at DEMO, where one and the same plasma discharge will 'only' be repeated. It is therefore sufficient to mainly provide D_2 and T_2 at the requested composition, rather than separating and then combining the gases again. This situation brings back a number of technologies which have been discarded at ITER, because they do not achieve the purity requirements as cryogenic distillation does, but have the advantage of shorter times.

9.3.1. Isotope rebalancing and protium removal (IRPR). This leads to adding one additional system block upfront the classical ISS, for isotope rebalancing (IR) and protium removal (PR), which is only treating the fuel stream coming from the permeator stage of fuel clean-up [160]. The task of IR is to re-establish the required fuel mixture composition before reinjection to the torus. The PR is needed to process and separate protium, which inevitably enters the system via out-gassing or replacement reactions. The produced fuel stream with adjusted mixture composition is directly feeding the storage and management sub-system, as is the permeated stream from the MFPs. In IRPR the protium content is reduced to the requested level (below 1%) and the deuterium and tritium ratios are reduced in a way which results in a ratio of 50:50 in combination with the flow from the MFP. This may require that not all the flow from fuel clean-up will be treated but bypasses the columns and gets mixed back.

The operation principle of IRPR is based on an absorption based process. The unit consists of two columns. In the first, a flow enriched in tritium will be sent to the gas management system. In the second column all the protium plus a certain amount of deuterium are separated and sent to ISS.

This results into a flow with less than 1% of protium content. One advantage of the absorption based technology is that it provides some flexibility to work at different target points so that the composition of the fuel injected into the tokamak could be adjusted—however slowly. This is contrary to a classical distillation column which has to be designed to one point only. In this concept using a separate IRPR system, the objective of the remaining cryogenic distillation based ISS shifts to detritiate gaseous streams containing trace amounts of tritium received from other systems internal or external to the tritium plant. Streams with trace tritium compositions include not only the two streams from IRPR (deuterium-rich stream removed as excess from IR, and protium-rich stream recovered from the PR), but also partial streams from the TES or the CPS.

Two quasi continuous absorption based technologies are under research for DEMO at the moment. One is based on temperature swing absorption [172], eventually in conjunction with a membrane stage [173]. The alternative technology is based on pressure swing absorption. The performance and sizing in both cases depends strongly on the absorption materials used. R & D efforts are under way to identify and characterize suitable materials.

9.4. Exhaust detritiation (EDS) and water detritiation system (WDS)

The discharge of tritium must be minimized in accordance with the ALARA principle and must as a minimum be below the regulatory discharge limits. The EDS system is a key part of ensuring this objective is met. The purpose of an EDS is to capture any tritium, from waste process gas or potentially contaminated air, in both gas and water vapor form. This includes input streams coming from HVAC systems, glove box vent systems and air from other rooms with tritiated components. The tritium is prevented from leaving the facility into the environment and instead will then be made available for reuse. The ITER detritiation system provides the most relevant template on which to develop DEMO requirements. At ITER, the system is split down into several sub-systems which handle various input gas streams, under different operational conditions and with differing detritiation requirements. It is expected that the DEMO EDS will operate on the principle of converting tritium to tritiated water, which is considered the only viable method to reliably and efficiently remove tritium from a large throughput of air. Consequentially, this is the main feed of water into the WDS.

The lead choice of technology for water detritiation is combined electrolysis and catalytic exchange (CECE), which is an industrialized process well developed for heavy water detritiation of CANDU reactors [174]. A liquid phase catalytic exchange (LPCE) column is used to move tritium from gas phase into water, with clean hydrogen out of the top and concentrated tritiated water out of the bottom. Optimized schemes are available that closely integrate WDS and ISS [175]. The very high decontamination factors that can be achieved in CECE results in a large reduction in volume of water to be treated by the ISS.

It is believed that the design for DEMO can be derived from the existing one for ITER, for both EDS [176] and WDS [177], however at a clearly larger size. To end up with efficient and economical water detritiation is very challenging for large quantities of tritium-contaminated water. Firstly, it works better with high tritium concentrations in the water, and secondly, due to the direct electrolysis, the CECE process is very energy intensive, as are alternative technologies at similar readiness level (such as water distillation which requires hundreds of theoretical plates with high reflux and reboiler duties). A more efficient technology is highly desired and R & D is ongoing in this area, although being fully fundamental for the time being, e.g. based on electrochemical pumping [178].

It would not be sensible to size WDS to handle all possible sources of water simultaneously, therefore the design must include some large buffer tanks available for temporary storage of tritiated water prior to feeding into WDS. The processing times of WDS are therefore linked to large variations, which explains the large spread assumed in table 2 from hour scale (for a configuration with IRPR) to day scale (for a configuration without IRPR).

Permeation of tritium into cooling water loops will necessitate cleaning up of cooling water. The breeder blanket coolant will have a CPS, which will pass some inventory to WDS assuming the coolant is water.

9.5. Coolant purification system (CPS)

The CPS treats the coolant streams from blanket, divertor and first wall. This can be helium or water which contains tritium (Q_2 in general) that permeates into the coolant. Obviously, this system will be first-of-its kind at DEMO scale. The main duties of the CPS are (i) extraction of tritium from the coolant to below specified levels, (ii) removal of solid, liquid and gaseous impurities, and (iii) control of the coolant chemistry (by adjusting the oxidation-reduction potential of the coolant).

At the moment, several blanket concepts [179] are under investigation which involve either water (at 15 MPa corresponding to $\sim 300^\circ\text{C}$ for WCLL) or helium (at $300\text{--}500^\circ\text{C}$ at 8 MPa for HCPB) or even lithium lead in the case of the dual coolant blanket. This also holds for the cooling of the first wall and the divertor.

The largest challenge comes from the huge coolant flowrate (several 1000 kg s^{-1} of water or helium). The general strategy is therefore that only a fraction of the coolant flow is processed by the CPS, given by the assumed CPS efficiency (above 90%), the total coolant flow rate, the tritium permeation rate from the blanket to the coolant loop, and the allowable tritium concentration inside the coolant [180]. In such a design exercise, it is quickly found that the tritium permeation rate in WCLL is much higher than in HCPB, which asks for significantly larger fractions of the water coolant flow that need to be purified than in case of helium (order of magnitude of 100 kg s^{-1} water compared to 1 kg s^{-1} helium).

For identification of a promising helium CPS technology one can start from the CPS of the helium-cooled TBMs of ITER in which the tritium removal foresees the

transformation of HT into HTO, by the use of high temperature oxidizing beds, and the following adsorption of the generated tritiated water in molecular sieve beds, at room temperature. The process proposed for the ITER CPS uses mature and consolidate technologies (that are also being used in fission applications). In principle such a process can be scaled up to fulfill DEMO requirements but it comes with some drawbacks. Thus, 100% regeneration of the metal oxide bed and reducing bed is difficult to achieve and includes oxy-hydrogen explosion hazards due to the use of oxygen (in the metal oxide bed) and hydrogen (in the reducing bed) together with the possible presence of hydrogen (in the metal oxide bed) and oxygen (in the reducing bed). On the other side, if this risk is avoided, one would have to size the components such that they do need a regeneration not before the next planned maintenance period (ITER approach). Obviously, this results in very big components and produces large amounts of tritiated waste. In this regard, an alternative solution is under exploration in EU based on new high capacity non-evaporable getter (NEG) materials [181] which avoids the Q_2 oxidation step to form Q_2O .

For detritiation of the water coolant two principal technology options exist, namely water distillation on one side, and electrolysis or CECE as discussed above on the other side. However, a review of existing facilities from CANDU reactors easily shows that a scale-up from the existing size of a coolant water detritiation facility (in kg h^{-1} range) to the requested size will not deliver a feasible solution. The water CPS is only manageable if a suitable strategy for reducing T permeation from blanket into coolant is applied; initial estimations ask for required PRFs between 100 and 1000. In the latter case, an ITER-sized WDS system would be sufficient to keep the tritium inventory in the coolant loop in the some 10 g level. In spite of decades of research, tritium permeation barriers that would work reliably under the neutron and gamma radiation conditions of DEMO are still not available [182]. Given the importance of permeation barriers, a strong R & D program is currently ongoing world-wide including demonstration at reactor conditions [183]. The alternative approach for the water CPS is based on an off-line plant, assuming that the water coolant in the primary cooling system is replaced with fresh water after one year of DEMO operation [184]. The discharged water coolant is then processed off-line in an external facility. It has been found that there is potential to reduce the permeation barrier performance requirement and still have a water CPS with the same features of ITER WDS and maintain the tritium concentration in the water coolant below the limits.

9.6. Tritium extraction system (TES)

A TES is providing the tritium generated by the blankets to the fuel cycle. The chemical form in which the tritium comes depends on the blanket concept and the chosen tritium extraction technology. There are two breeder options, namely solid vs liquid breeder [185]. In the liquid design, lithium lead is used as the breeding material as well as the neutron multiplier and tritium carrier.

The reference technology being studied to recover tritium from liquid lithium lead breeder blankets at DEMO scale is

permeation against vacuum (PAV) [186]. This is a novel and continuous technology with an efficiency clearly higher than what is achievable with the gas liquid contactor approach chosen for ITER. PAV holds for any coolant option that may be combined with the lithium lead (WCLL, HCLL, DCLL). By extracting tritium using PAV, an almost pure stream of tritium can be expected to be received by the tritium plant, together with trace amounts of hydrogen isotopes and water, largely dependent on the permeation membrane surface chemistry, which is yet to be determined. R & D is ongoing to demonstrate the feasibility of this concept [187] and depending on the results, the gas stream from TES has to enter the IFC either at ISS/IRPR (if only hydrogenic) or fuel clean-up (if containing other impurities as well). As a fall-back solution, the vacuum sieve tray technology is also under study, however, scale-up to DEMO scale has been found to be complex [188].

A pebble bed breeder blanket contains the lithium in the form of lithium ceramic pebbles and beryllium as a neutron multiplier. In order to extract the tritium, the blanket is purged with helium (in a closed loop). The current reference technology chosen to do this is cryogenic trapping. This involves a purge of helium, doped with small amounts of hydrogen. The purge gas flow will then be treated in TES which contains a reactive and a cryogenic molecular sieve bed (RMSB and CMSB respectively), with two of each as one will be absorbing while the other is regenerated and vice versa to maintain an almost continuous flow. The proposed TES design results in multiple streams being sent to the tritium plant. It will produce Q_2 with He from the regeneration of the CMSB to be sent to fuel clean-up, Q_2O from the regeneration of the RSMB to be sent to the WDS, and Q_2 to be sent to the ISS.

9.7. Fueling system

The tritium plant, via a storage and management system that takes the product streams of ISS and combines it with the recycle flows coming from the vacuum pumping and the IRPR, if there are, will finally supply the fueling systems. As outlined in section 6, the main function of the core fueling system is to compensate burn-out, to keep the plasma density constant and to control the helium concentration. The chosen technology for core fueling is pellet injection, which needs to be done at the inboard side of the machine. As already explained in section 7, depending on the injection location, different technologies for acceleration can be used. The plasma zones which are reachable by direct line of sight injection are less efficient than the ones reachable by using curved guide tubes. This means that for the former solution, the pellets have to arrive at higher velocities (above 1 km s^{-1}), which can be performed by gas guns [189], whilst curved guide tubes can work with centrifuges at limited speeds (below 1 km s^{-1}) [97]. The core radiator PEG species may be introduced into the core as admixed component to the pellets. The largest challenge for pellet fueling on DEMO comes from the fact that such a system (highly repetitive, continuous, tritium-compatible) has not yet been demonstrated for the DT gas mixture that shall be processed. For making a design of a pellet injection system,

the transmission performance of the injection line has to be properly understood.

Gas injection (mainly to the divertor) does also involve gases that have to be provided from the fuel cycle. Puffing is implemented by conventional pipes with valves connected to higher pressure gas reservoirs, the same technology as used in ITER is foreseen [190].

10. Summary

The tritium aspects of the DT fuel cycle embody some of the most challenging feasibility and attractiveness issues in the development of fusion systems. The review and analyses in this paper provided important information to understand and quantify these challenges and to define the phase space of plasma physics and fusion technology parameters and features that must guide a serious R & D in the world fusion program. We focused in particular on components, issues and R & D necessary to satisfy three ‘principal requirements’ that are critical for the successful development and safe operation of fusion facilities: (1) achieving tritium self-sufficiency within the fusion system, (2) providing a tritium inventory for the initial start-up of a fusion facility, and (3) managing the safety and biological hazards of tritium. A primary conclusion of this paper is that the physics and technology state of the art will not enable DEMO and future power plants to satisfy these principal requirements. We have defined specific areas, ideas, and goals for physics and technology R & D to meet these requirements. However, our analysis shows that a successful outcome of this R & D cannot be assured. We hope that the careful, relatively detailed analysis presented in this paper can stimulate new ideas and approaches toward achieving the feasibility of the DT fuel cycle.

Tritium consumption in fusion reactors is 55.8 kg per 1000 MW fusion power per year, which is huge and unprecedented. Tritium production rate in fission reactors is much smaller: $\sim 0.5\text{--}1 \text{ kg year}^{-1}$ in an especially designed light water reactor and $\sim 130 \text{ g}$ per GW year in CANDU reactors. The world supply of tritium from CANDU reactors will be practically exhausted by a successful ITER DT campaign to achieve the project neutron fluence goals by 2052. Therefore, DEMO and other DT fusion facilities cannot rely on external tritium sources.

While deuterium is abundant in nature and stable, tritium is rare and has short half-life of 12.32 years. Therefore, tritium inventories are continuously lost by radioactive decay. In a fusion facility, this loss must be compensated by increasing the TBR and the start-up inventory. Physics and technology conditions that result in large tritium inventories can lead to large increase in required tritium breeding beyond what is achievable, and increasing the start-up inventory beyond what is obtainable, in addition to increasing safety risks.

The tritium fuel cycle consists of: (1) an IFC, which is the inner loop that includes plasma fueling system, plasma exhaust (vacuum pump), fuel clean-up, isotope separation, exhaust and water detritiation, and storage and management, and (2) an OFC that includes breeding blanket, bred tritium extraction

and processing, tritium trapped in plasma-facing components (first wall, divertor, etc), and coolant processing.

A powerful fuel cycle dynamics model was developed to calculate time-dependent tritium inventories and flow rates in all parts and components of the fuel cycle for different ranges of parameters and physics and technology conditions. The model accounts for tritium production, extraction, trapping, loss by radioactive decay, and all processes in the fuel cycle. The model also computes the required TBR and the required initial start-up tritium inventory. Dynamics modeling analyses show that the key parameters affecting tritium inventories, tritium start-up inventory, and required TBR are the TBF in the plasma (f_b), fueling efficiency (η_f), processing time of plasma exhaust in the IFC (t_p), reactor availability factor (AF), reserve time (t_r) which determines the reserve tritium inventory needed in the storage system in order to keep the plant operational for time t_r in case of any malfunction of any part of the tritium processing system, and the doubling time (t_d).

Tritium self-sufficiency is realized if the achievable TBR is \geq the required TBR. The best estimate of the achievable TBR for the most detailed blanket system designs available is ≤ 1.15 . But there is uncertainty of $\sim 10\%$ due to differences between integral experiments and calculations that cannot be resolved until we build and operate a practical blanket system in a DT fusion facility. Another way to state this is that there is a high confidence that an achievable TBR of 1.05 can be obtained, but there is less confidence that an achievable TBR of 1.15 can be realized. The 10% margin we use here does not account for uncertainties due to major changes in design definition, which can be large. The required TBR, TBR_R , was calculated using the dynamics modeling and it is a very strong function of many physics and technology parameters. In order to account for uncertainties in predicting the achievable TBR, we attribute different levels of confidence in attaining tritium self-sufficiency to different values of the required TBR. In particular, we consider attaining self-sufficiency: (1) unlikely: if $TBR_R > 1.15$, (2) possible: if $1.05 < TBR_R < 1.15$, and (3) attainable with high confidence: if $TBR_R < 1.05$.

Results show that major advances beyond the state-of-the-art of plasma physics and fusion technology (represented by ITER where relevant) are necessary to realize a successful DT fusion cycle in DEMO and power plants. The main reason is that current predictions of low burn fraction ($f_b = 0.36\%$), low fueling efficiency ($\eta_f < 25\%$), and long time (several hours) required for processing of tritium in the plasma exhaust in the IFC result in very large tritium inventories and flow rates. These lead to unacceptable values of very high required TBR (attaining tritium self-sufficiency is unlikely) and very large tritium start-up and operational inventory.

Our studies show that self-sufficiency is possible (i.e. the required TBR is in the 1.05–1.15 range) if the product of burn fraction and fueling efficiency ($\eta_f f_b$) is $> 0.7\%$ and the processing time is less than 4 h (assuming BZ residence time = 1 day, TES processing time in the OFC = 1 day, fusion power = 3 GW, reserve time = 24 h, fraction failing = 25%, doubling time = 5 years). However, $\eta_f f_b > 2\%$ and processing time of 1–4 h are required to achieve tritium self-sufficiency with high confidence (i.e. required TBR < 1.05). Note that if

$\eta_f f_b = 2\%$ and the processing time is 4 h, the tritium start-up inventory for a 3 GW fusion reactor is ~ 11 kg, while it is < 5 kg only if $\eta_f f_b = 5\%$ and the processing time is 1 h. To achieve these stringent requirements a serious R & D program in physics and technology is necessary.

In the last decade, the EU-DEMO team introduced the DIR concept. In this concept, a DIR loop carries fuel directly from the exhaust gas to the fueling systems without going through the ISS. This helps to reduce the overall processing time and tritium inventories. This technology has positive effects on the required TBR as well. For instance, for $\eta_f f_b$ of 1% and tritium processing time of 4 h, the required TBR is 1.12 when DIR is not performed, and it reduces to 1.075 if 80% of the plasma exhaust is fed to the DIR. For the same parameters the start-up inventory reduces from 21 kg to 15 kg (for 3 GW of fusion power). These major reductions help increase the likelihood of achieving tritium self-sufficiency, and partially alleviate the stringent requirements on burn fraction and fueling efficiency. The DIR concept requires a new functionality being installed in the fuel cycle, namely a technology to extract the fuel at the low densities close to the divertor. One option is exploiting the phenomenon of superpermeation which allows suprathreshold hydrogen particles to permeate through a metal foil with surface barrier whereas all other species do practically not permeate through the foil. The superpermeation principle is being studied intensely in EU to be integrated in the so-called MFP.

A significant finding is the strong dependence of the required TBR on the reactor availability factor (AF). The fundamental reason of this dependency is that during the reactor downtime tritium production in blankets is interrupted whereas tritium loss by radioactive decay continues, inexorably. Thus, the required TBR increases in case of low availability factor, since much more tritium must be produced when the reactor operates to compensate for the losses of the downtime. Simulations show that tritium self-sufficiency is: impossible if $AF < 10\%$ for any $\eta_f f_b$, possible if $AF > 30\%$ and $1\% \leq \eta_f f_b \leq 2\%$, and possible with high confidence if $AF > 50\%$ and $\eta_f f_b > 2\%$. These results are of particular concern in light of the low availability factor predicted for the near-term plasma-based experimental facilities (e.g. FNSF, VNS, CTF, etc), and can have repercussions on tritium economy in DEMO reactors as well, unless significant advancement in RAMI is obtained.

We found a linear dependency between the tritium start-up inventory and the fusion power. An important conclusion is that the required tritium start-up inventory for a fusion facility of 100 MW fusion power is as small as 1 kg at very low $\eta_f f_b \sim 0.5\%$ or a few hundreds of grams if $\eta_f f_b$ is higher. The results highlight that near-term fusion facilities should be designed for low fusion power (< 150 MW) in order to keep the required start-up inventory relatively small and obtainable, i.e. less than a kilogram of tritium.

Since fusion power plants will have large powers for better economics, it is important to maintain a ‘reserve’ tritium inventory in the tritium storage system to continue to fuel the plasma and avoid plant shutdown in case of malfunctions of some parts of the tritium processing lines. But our results show that a reserve time as short as 24 h leads to unacceptable reserve and

start-up inventory requirements. For example, ~ 10 kg of extra tritium are required if we increase the reserve time from 6h to 24h for $\eta_f f_b = 1\%$. Overall, the total start-up inventory can be < 10 kg if $t_r < 24$ h and $\eta_f f_b \geq 2\%$ and < 5 kg if $t_r < 6$ h and $\eta_f f_b \geq 3\%$. Thus, high reliability and fast maintainability of all components in the fuel cycle are necessary in order to avoid the need for storing reserve tritium inventory sufficient for continued fusion facility operation for more than a few hours.

To accelerate the penetration of fusion technology into the energy market short doubling times are required so that a DEMO or early-generation fusion reactor would be able to provide tritium inventory for start-up of other reactors in a reasonable time of ~ 1 – 3 years. Our results show that this is not achievable with state-of-the-art physics and technology parameters and conditions. R & D required to overcome this serious difficulty has been defined. For mature fusion power economy, doubling times of > 7 years are typical and do not pose a problem.

The physics aspects of plasma fueling, TBF, and particle and power exhaust are highly interrelated and complex, and predictions for DEMO and power reactors are highly uncertain because of lack of experiments with burning plasmas. Extensive modeling has been carried out to predict burn fraction, fueling requirements, and fueling efficiency for ITER, DEMO, and beyond. The fueling rate required to operate $Q = 10$ ITER plasmas in order to provide the required core fueling, helium exhaust and radiative divertor plasma conditions for acceptable divertor power loads was calculated and the ITER fueling systems designed to provide it with some flexibility. If this fueling is performed with a 50–50 DT mix, the TBF in ITER would be $\sim 0.36\%$, which is too low to satisfy the self-sufficiency conditions derived from the dynamics modeling discussed above. Extrapolation to DEMO using this approach would also yield similarly low TBF. Extensive analysis presented in section 6 shows that specific features of edge neutral dynamics in ITER and fusion reactors, which are different from present experiments, open possibilities for optimization of tritium fueling and thus to improve the TBF.

The key physics differences between present experiments and ITER or DEMO that impact significantly the TBF are the inefficient penetration of edge recycled neutrals into the confined plasma and the need to sustain a relatively high separatrix density in burning plasma conditions to ensure acceptable power fluxes at the divertor through radiative divertor operation. The inefficient penetration of neutrals is caused by the large physical dimensions of ITER plasmas and the high temperatures in the SOL that ionize recycling neutrals before they can reach the confined plasma. The ionization source for recycled neutrals in the plasma core is modeled to be negligible for the conditions in which acceptable divertor power loads (≤ 10 MW m^{-2}) are achieved. This means that edge and core particle sources are decoupled in ITER (and DEMO) which allows for optimization of the TBF by differential fueling of D and T for the two separate missions of core plasma fueling and helium exhaust/divertor power flux control.

Fueling of the core plasma in ITER (and DEMO) requires pellet injection. Due to the outwards drift of the high

pressure plasmoid formed after pellet ablation, pellet injection from the HFS is required for deposition of particles beyond the pedestal plasma in ITER due to the high edge temperatures. Concerning the fueling requirements to provide $Q = 10$ operation with acceptable divertor power loads, these are determined by the achievement of semi-detached divertor operation to dissipate the plasma power flux before it reaches the divertor target by radiative and atomic losses from hydrogenic isotopes and impurities. This is achieved by fueling of extrinsic impurities in the divertor plasma together with operation at high SOL plasma density to ensure low impurity concentrations in the core plasma. The sustainment of such densities may require significant levels of gas fueling. Since gas fueling and recycling gas do not contribute significantly to core plasma fueling, the gas fueling isotope can be chosen to be D and in this way reduce significantly the T throughput required to sustain $Q = 10$ operation.

The result of the ITER studies with high fidelity edge plasma models and edge-core integrated models is that $Q = 10$ operation can be sustained with a T throughput of 10 – 20 Pa m^3 s^{-1} even when the total fueling rate of DT is 200 Pa m^3 s^{-1} . This leads to a TBF of 1.8 – 3.6% instead of the initially estimated 0.36% due to the inefficient fueling of the core plasma by gas puffing and recycling fluxes which are dominated by D. It should be noted, however, that this does not decrease the volume for DT fuel re-processing from the exhaust to recover T since the total fuel throughput remains the same. The difference is the T concentration in the exhausted fuel, which can be as low as 5 – 10% of the total instead of 50% with the all 50 – 50 DT fueling.

The estimates above are performed with physics models whose results have been compared with experimental results but cannot be fully validated for ITER plasma conditions since these cannot be achieved in present tokamak experiments. Thus, several uncertainties remain regarding particle transport and scenario requirements in ITER (and DEMO), which can impact the results above regarding the TBF. The major open physics/scenario integration issues, discussed in section 6, are: (1) ELM control and associated fueling requirements, (2) pedestal particle transport, and (3) DT core particle transport.

In most aspects of the DEMO particle transport and edge plasma behavior affecting the TBF no major differences are expected from ITER, since the DEMO plasma size and edge densities and temperatures will also make core plasma fueling by recycling DT fluxes very inefficient. Similarly, core plasma transport aspects in DEMO should be similar to those of ITER since both require high density low collisionality plasmas for optimum fusion power production. There will be quantitative differences between ITER and DEMO associated with the higher pedestal temperatures in DEMO which affect the efficiency of HFS pellet fueling, since this is strongly dependent on the value of the edge temperature. Similarly, the solution adopted for ELM control or avoidance in DEMO is likely to be different from ITER and, thus, this may have a different impact on the TBF in DEMO than in ITER.

The technology for fueling fusion plasmas has progressed significantly over the past three decades. Fueling by pellet

injection has evolved into the preferred method to fuel a burning plasma due to its technology maturity and improved efficiency compared to other schemes such as gas fueling and neutral beam fueling. The polarization cross field drift during the pellet deposition process has shown that HFS injection is advantageous for achieving efficient fueling and thus will be used on ITER. Potential issues of pellet ablation in the SOL from energetic particles and triggering of ELMs leading to the ejection of fuel can lead to less efficient fueling and remain as active areas of research.

The fueling efficiency of gas in a reactor relevant regime is expected to be extremely poor and not very useful for getting DT fuel into the core plasma efficiently. Gas fueling will nonetheless be useful for feedback control of the divertor operating parameters where efficient fueling and fast time response is not required. The pellet fueling efficiency studies that have been performed on existing experiments point to reduced efficiency with shallow penetration as expected in a burning plasma. It is difficult in present experiments to mimic the shallow penetration expected and thus extrapolation from today's deeper penetrating pellets is extremely difficult. From the existing DIII-D penetration scaling fueling efficiency is expected in DEMO to be <25%, but such extrapolations could be overly optimistic depending on how much of the pellet mass is immediately ejected by a triggered ELM. The ITER high pedestal temperatures and large size will be critical to understanding how efficient the expected shallow pellet fueling will be in a future DEMO device.

To ensure the safety and licensing of future fusion reactors, designs must minimize inventories and limit the release of hazardous materials under all operational conditions. Tritium is a primary safety concern as it is unavoidably present as the fuel for the fusion reaction and it is continuously transported throughout the plant. General safety approaches include minimizing tritium inventories, reducing tritium permeation through materials, and decontaminating material for waste disposal. The safety standard requirements for protection of the public and release guidelines for tritium have been reviewed in section 8. Approaches to minimizing tritium inventories and flow rates were identified above through the use of dynamics modeling to understand the controlling physics and technology parameters. Tritium permeation is a particularly challenging problem for reasons that include: (1) most fusion blankets have high tritium partial pressure, (2) the temperature of the blanket is high (500 °C–700 °C), (3) the surface area of heat exchanger is large, with thin walls, and (4) tritium in parts of the system is in elementary forms. These are perfect conditions for tritium permeation. In the meantime, the allowable tritium loss rate is very low (~10 Ci/day), which is many orders of magnitude below that in most blanket designs. Therefore, a tritium permeation barrier is necessary with a PRF estimated to be 10^5 – 10^6 . Given that typical permeation barriers have PRF of only ~100, developing strategies for minimizing tritium permeation requires aggressive R & D.

Tritium control and management will be one of the most difficult issues for fusion energy development because of the many issues addressed in this paper, and also because of the very large scale-up from the state of the art. The quantity of

tritium to be managed in the ITER fuel cycle is much larger than the quantities typically managed in CANDU and light water fission reactors (which represent the present-day state of practical knowledge). The amount of tritium to be managed in a DEMO blanket (production rate ~400 g/day) is several orders of magnitude larger than that expected in ITER, while the allowable T-releases could be comparable.

In conclusion, successful development of the DT fuel cycle for DEMO and future fusion reactors requires an intensive R & D program in key areas of plasma physics and fusion technologies. This program requires strong interactions among scientists from the plasma physics and fusion technology fields as well as effective international collaboration.

Acknowledgments

The authors wish to acknowledge the collaborations and efforts of many colleagues in their organizations and the broader world fusion community on many aspects of this paper. Section 6 summarizes modeling results obtained thanks to the extensive efforts of members of the ITER Organization and collaborators. Special thanks are due to A. Polevoi, X. Bonnin, A.S. Kukushkin, R.A. Pitts, H.D. Pacher, E. Militello-Asp, V. Parail, F. Köchl, L. Garzotti, S. Wiesen for their contributions to the studies summarized in the section. Some of this work was supported by the task agreement between UCLA-NFRI for Cooperation on R & D for Fusion Nuclear Science to Expedite the Realization of Magnetic Fusion Energy. Part of this work was supported by the US DOE under contracts DE-AC05-00OR22725 and DE-FC02-04ER54698. Part of this work was carried out within the framework of the EUROfusion Consortium and has received funding from the EURATOM research and training program 2014–2018 and 2019–2020 under Grant Agreement No. 633053. The views and opinions expressed herein do not necessarily reflect those of the European Commission.

Disclaimer

ITER is the Nuclear Facility INB No. 174. The views and opinions expressed herein do not necessarily reflect those of the ITER Organization. This publication is provided for scientific purposes only. Its contents should not be considered as commitments from the ITER Organization as a nuclear operator in the frame of the licensing process.

Acronyms

ALARA: As low as reasonably achievable

APT: Accelerator production of tritium

BOL: Beginning of life

CANDU: Canada deuterium uranium

CECE: Combined electrolysis and catalytic exchange

CFETR: China fusion engineering test reactor

CIEMAT: Centro de Investigaciones Energéticas, Medioambientales y Tecnológicas (Center for Energy, Environment and Technology)	MFP: Metal foil pump
CMSB: Cryogenic molecular sieve bed	MHD: Magneto hydro dynamic
CPS: Coolant purification system	MQx: Solid tritide dust
CTF: Component test facility	MTBF: Mean time between failures
CXN: Charge exchange neutrals	MTTR: Mean time to repair
D: Deuterium	NEG: Non-evaporable getter
DCLL: Dual coolant lead lithium	ODE: Ordinary differential equation
DIR: Direct internal recycling	OFC: Outer fuel cycle
DOE: Department of Energy	PAV: Permeation against vacuum
DT: Deuterium–tritium	PFC: Plasma facing component
EDS: Exhaust detritiation system	PEG: Plasma enhancement gas
ELM: Edge localized mode	PR: Protium removal
ENEA: National Agency for New Technologies, Energy and Sustainable Economic Development	PRF: Permeation reduction factor
EPA: Environmental protection agency	RAFM: Reduced activation ferritic martensitic
FDS: Frontier development of science	RAMI: Reliability availability maintainability inspectability
FNSF: Fusion nuclear science facility	R & D: Research and Development
FSS: Fusion safety standard	RMSB: Reactive molecular sieve bed
FUS-TPC: Fusion-devoted tritium permeation code	SLS: System-level simulation
FW: First wall	SOL: Scrape-off layer
HCCR-TBM: Helium coolant ceramic reflector test blanket module	T: Tritium
HCLL: Helium cooled lithium lead	TAS: Tritium analysis system
HCPB: Helium cooled pebble bed	TBF: Tritium burn fraction
HFS: High field side	TBR: Tritium breeding ratio
HVAC: Heating ventilation and air conditioning	TES: Tritium extraction system
IAEA: International atomic energy agency	TMAP: Tritium migration analysis program
ICRP: International commission on radiation protection	VNS: Volumetric neutron source
IFC: Inner fuel cycle	WDS: Water detritiation system
IR: Isotope rebalancing	WCLL: Water cooled lithium lead
IRPR: Isotope rebalancing and protium removal	
ISS: Isotope separation system	
ITER: International thermonuclear experimental reactor	
JET: Joint European Torus	
K-DEMO: Korean DEMO reactor	
LFS: Low field side	
LPCE: Liquid phase catalytic exchange	
MARFE: Multifaceted asymmetric radiation from the edge	

Symbols (in order of appearance by section)

Sections 1-5

f_b : Tritium burn fraction in the plasma

η_f : Fueling efficiency

t_p : Processing time of plasma exhaust in the inner fuel cycle (s)

t_r : Reserve time (s)

t_d : Doubling time (s)

TBR_A : Achievable tritium breeding ratio

TBR_R : Required tritium breeding ratio

AF: Availability factor	$n_{\text{edge-plasma}}^{\text{DT}}$: Edge plasma DT density (m^{-3})
τ_i : Tritium residence time in the i th component of the fuel cycle (s)	η_{He} : Helium (de-)enrichment at the plasma edge
I_i : Tritium inventory of the i th component of the fuel cycle (kg)	$n_{\text{neut-div}}^{\text{He}}$: He neutral density at divertor pump (m^{-3})
$(I_j/\tau_j)_i$: Tritium flow rate from the j th component to the i th component of the fuel cycle (kg s^{-1})	$n_{\text{neut-div}}^{\text{DT}}$: DT neutral density at divertor pump (m^{-3})
I_i/τ_i : Tritium flow rate out of the i th component of the fuel cycle (kg s^{-1})	$\Gamma_{\text{DT}}^{\text{pumped}}$: Pumped DT flux by the divertor pump (DT atoms s^{-1} or $\text{Pa m}^3 \text{s}^{-1}$)
S_i : Tritium source term in the i th component of the fuel cycle (kg s^{-1})	n_{ped} : Pedestal top density (m^{-3})
ε_i : Non-radioactive tritium losses from the i th component of the fuel cycle	n_{sep} : Electron separatrix density (m^{-3})
λ : Tritium decay rate (s^{-1})	$\langle \Delta_{\text{ped}} \rangle$: Pedestal width (i.e. width of the edge transport barrier) (m)
S : Point neutron source (neutrons s^{-1})	$\langle a \rangle$: Average plasma minor radius (m)
\dot{N}^- : Tritium burning rate (kg s^{-1})	D_{ped} : Diffusion coefficient in the pedestal region ($\text{m}^2 \text{s}^{-1}$)
\dot{T}_f : Tritium fueling rate (kg s^{-1})	$\Gamma_{\text{DT}}^{\text{core}}$: Core DT flux (DT atoms s^{-1} or $\text{Pa m}^3 \text{s}^{-1}$)
\dot{T}_i : Tritium injection rate (kg s^{-1})	S_{plasma} : Plasma surface area (m^2)
n_{T} : Tritium plasma density (m^{-3})	Γ_{div} : Total divertor particle flux determining the recycled neutral source (DT atoms s^{-1} or $\text{Pa m}^3 \text{s}^{-1}$)
n_{D} : Deuterium plasma density (m^{-3})	Γ_{core} : Core plasma ionization source (DT atoms s^{-1} or $\text{Pa m}^3 \text{s}^{-1}$)
n : Generic species plasma density, i.e. tritium or deuterium (m^{-3})	Γ_{puff} : Gas puffing flux (DT atoms s^{-1} or $\text{Pa m}^3 \text{s}^{-1}$)
σ : Energy-dependent cross section for the DT reaction (m^2)	P_{SOL} : Scrape-off layer power (MW)
v : Particle velocity (m s^{-1})	$\Gamma_{\text{DT}}^{\text{HFS}}$: High field side pellet injection fueling rate (DT atoms s^{-1} or $\text{Pa m}^3 \text{s}^{-1}$)
$\langle \sigma v \rangle$: Averaged product of energy-dependent cross section and particle velocity ($\text{m}^3 \text{s}^{-1}$)	ΔW_{ELM} : ELM energy loss (MJ)
τ^* : Effective confinement time (s)	P_{ELM} : Average power flux carried by ELMs (MW)
τ : Confinement time (s)	ΔN_{ELM} : Particle loss per ELM (DT ions)
R : Recycling coefficient	T_{ped} : Pedestal top temperature (keV)
I_{S}^0 : Tritium start-up inventory in storage unit (kg)	Γ_{ELM} : Total average particle outflux driven by ELMs (DT atoms s^{-1} or $\text{Pa m}^3 \text{s}^{-1}$)
I_{S} : Time-dependent tritium inventory in storage unit (kg)	$\Gamma_{\text{DT}}^{\text{HFS-ELM suppression}}$: DT flux for high field side pellet injection with ELM suppressed H-mode conditions (DT atoms s^{-1} or $\text{Pa m}^3 \text{s}^{-1}$)
I_{r} : Tritium reserve inventory in storage unit (kg)	v_{ped} : Pedestal plasma pinch velocity (m s^{-1})
$I_{\text{S}}^{\text{min}}$: Minimum tritium inventory in storage unit (kg)	v_{edge} : Edge plasma velocity (m s^{-1})
q : Fraction of the fuel cycle failing	P_{tot} : Total heating power (MW)
f_{DIR} : Direct internal recycling fraction	$P_{\text{L-H}}$: H-mode threshold power (MW)
	$P_{\text{sep}}^{\text{min}}$: Minimum edge power flow compatible with high confinement (MW)
Section 6	$P_{\text{rad}}^{\text{core,max}}$: Maximum radiated power in the plasma core (MW)
Q : Fusion gain	$\langle n_e \rangle$: Average electron density (m^{-3})
Γ_{α} : Alpha source corresponding to a certain fusion power (He-atoms s^{-1} or $\text{Pa m}^3 \text{s}^{-1}$)	n_{GW} : Greenwald density limit (m^{-3})
C_{He} : Helium concentration in the plasma	
$n_{\text{edge-plasma}}^{\text{He}}$: Edge plasma He density (m^{-3})	

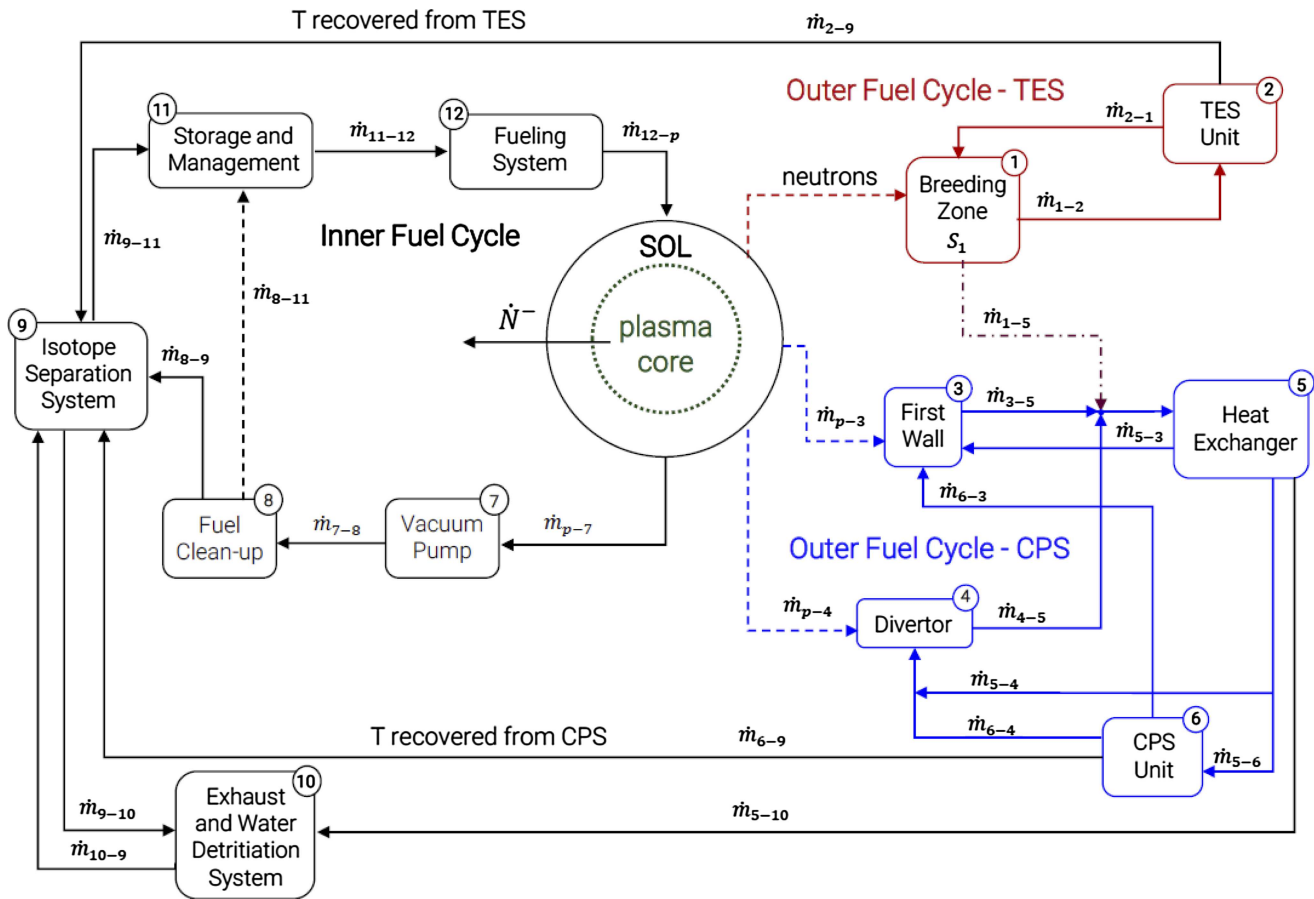


Figure A.1. Schematic of the fuel cycle with tritium flow rates into and out of components used to build the tritium dynamics mathematical model. The flow rates are defined as $\dot{m}_{j-i} = \left(\frac{\dot{m}}{r_j}\right)_i$ as expressed in equation (3.1).

Section 7

ΔN_{e-pl} : Total increase in number of plasma electrons

N_{e-inj} : Number of injected electrons from the fuel atoms

η_{eff} : Fueling efficiency

ρ : Normalized pellet penetration depth

T_e : Plasma pedestal temperature (keV)

Section 8

J_d : Dissociative-adsorbing tritium molar flux ($\text{mol m}^{-2} \text{s}^{-1}$)

J_r : Recombinative-desorbing tritium molar flux ($\text{mol m}^{-2} \text{s}^{-1}$)

K_d : Dissociative-adsorption rate constant ($\text{mol m}^{-2} \text{s}^{-1} \text{Pa}^{-1}$)

K_r : Recombinative-desorption rate constant ($\text{mol}^{-1} \text{m}^4 \text{s}^{-1}$)

P : Gas-phase tritium partial pressure (Pa)

C : Concentration of adsorbed tritium (mol m^{-3})

K_S : Sieverts' constant (solubility) ($\text{mol m}^{-3} \text{Pa}^{-0.5}$)

P_h : Partial pressure on the high-pressure side (Pa)

P_l : Partial pressure on the low-pressure side (Pa)

Φ : Permeability ($\text{mol m}^{-1} \text{s}^{-1} \text{Pa}^{-0.5}$)

Q^* : Heat of transport (J)

R : Ideal gas constant ($\text{J mol}^{-1} \text{K}^{-1}$)

T : Temperature (K)

W' : Permeation number

α : Sticking coefficient

m : Particle mass (kg)

k : Boltzmann constant (J K^{-1})

Appendix A. Mathematical formulation of the tritium fuel cycle dynamics model

See figure A.1 and tables A.1 and A.2.

Derived ODEs

$$\frac{dI_1}{dt} = \Lambda \dot{N}^- + (1 - \eta_2) \frac{I_2}{\tau_2} - \frac{I_1}{T_1} \quad (\text{A.1})$$

$$\frac{dI_2}{dt} = (1 - f_{1-5}) \frac{I_1}{\tau_1} - \frac{I_2}{T_2} \quad (\text{A.2})$$

Table A.1. Tritium flow rates in the OFC of figure A.1.

Component	Flow rate
1	$S_1 = \Lambda \dot{N}^-$ $\dot{m}_{2-1} = (1 - \eta_2) \frac{I_2}{\tau_2}$ $\dot{m}_{1-2} = -(1 - f_{1-5}) \frac{I_1}{\tau_1}$ $\dot{m}_{1-5} = -f_{1-5} \frac{I_1}{\tau_1}$ Losses = $-\varepsilon_1 \frac{I_1}{\tau_1} - \lambda I_1$
2	$\dot{m}_{1-2} = (1 - f_{1-5}) \frac{I_1}{\tau_1}$ $\dot{m}_{2-12} = -\eta_2 \frac{I_2}{\tau_2}$ $\dot{m}_{2-1} = -(1 - \eta_2) \frac{I_2}{\tau_2}$ Losses = $-\varepsilon_2 \frac{I_2}{\tau_2} - \lambda I_2$
3	$\dot{m}_{p-3} = f_{p-3} \frac{\dot{N}^-}{\eta_f f_b}$ $\dot{m}_{5-3} = f_{5-3} (1 - f_{5-6}) (1 - f_{5-10}) \frac{I_5}{\tau_5}$ $\dot{m}_{6-3} = f_{6-3} (1 - \eta_6) \frac{I_6}{\tau_6}$ $\dot{m}_{3-5} = -\frac{I_3}{\tau_3}$ Losses = $-\varepsilon_3 \frac{I_3}{\tau_3} - \lambda I_3$
4	$\dot{m}_{p-4} = f_{p-4} \frac{\dot{N}^-}{\eta_f f_b}$ $\dot{m}_{5-4} = (1 - f_{5-3}) (1 - f_{5-6}) (1 - f_{5-10}) \frac{I_5}{\tau_5}$ $\dot{m}_{6-4} = (1 - f_{6-3}) (1 - \eta_6) \frac{I_6}{\tau_6}$ $\dot{m}_{4-5} = -\frac{I_4}{\tau_4}$ Losses = $-\varepsilon_4 \frac{I_4}{\tau_4} - \lambda I_4$
5	$\dot{m}_{1-5} = f_{1-5} \frac{I_1}{\tau_1}$ $\dot{m}_{3-5} = \frac{I_3}{\tau_3}$ $\dot{m}_{4-5} = \frac{I_4}{\tau_4}$ $\dot{m}_{5-3} = -f_{5-3} (1 - f_{5-6}) (1 - f_{5-10}) \frac{I_5}{\tau_5}$ $\dot{m}_{5-4} = -(1 - f_{5-3}) (1 - f_{5-6}) (1 - f_{5-10}) \frac{I_5}{\tau_5}$ $\dot{m}_{5-6} = -f_{5-6} (1 - f_{5-10}) \frac{I_5}{\tau_5}$ $\dot{m}_{5-10} = -f_{5-10} \frac{I_5}{\tau_5}$ Losses = $-\varepsilon_5 \frac{I_5}{\tau_5} - \lambda I_5$
6	$\dot{m}_{5-6} = f_{5-6} (1 - f_{5-10}) \frac{I_5}{\tau_5}$ $\dot{m}_{6-3} = -f_{6-3} (1 - \eta_6) \frac{I_6}{\tau_6}$ $\dot{m}_{6-4} = -(1 - f_{6-3}) (1 - \eta_6) \frac{I_6}{\tau_6}$ $\dot{m}_{6-12} = -\eta_6 \frac{I_6}{\tau_6}$ Losses = $-\varepsilon_6 \frac{I_6}{\tau_6} - \lambda I_6$

$$\frac{dI_3}{dt} = f_{p-3} \frac{\dot{N}^-}{\eta_f f_b} + f_{5-3} (1 - f_{5-6}) (1 - f_{5-10}) \frac{I_5}{\tau_5} + f_{6-3} (1 - \eta_6) \frac{I_6}{\tau_6} - \frac{I_3}{T_3} \quad (\text{A.3})$$

$$\frac{dI_4}{dt} = f_{p-4} \frac{\dot{N}^-}{\eta_f f_b} + (1 - f_{5-3}) (1 - f_{5-6}) (1 - f_{5-10}) \frac{I_5}{\tau_5} + (1 - f_{6-3}) (1 - \eta_6) \frac{I_6}{\tau_6} - \frac{I_4}{T_4} \quad (\text{A.4})$$

$$\frac{dI_5}{dt} = f_{1-5} \frac{I_1}{\tau_1} + \frac{I_3}{\tau_3} + \frac{I_4}{\tau_4} - \frac{I_5}{T_5} \quad (\text{A.5})$$

$$\frac{dI_6}{dt} = f_{5-6} (1 - f_{5-10}) \frac{I_5}{\tau_5} - \frac{I_6}{T_6} \quad (\text{A.6})$$

Table A.2. Tritium flow rates in the IFC of figure A.1.

Component	Flow rate
7	$\dot{m}_{p-7} = (1 - \eta_f f_b - f_{p-3} - f_{p-4}) \frac{\dot{N}^-}{\eta_f f_b}$ $\dot{m}_{7-8} = -\frac{I_7}{\tau_7}$ Losses = $-\varepsilon_7 \frac{I_7}{\tau_7} - \lambda I_7$
8	$\dot{m}_{7-8} = \frac{I_7}{\tau_7}$ $\dot{m}_{8-9} = -(1 - f_{8-11}) \frac{I_8}{\tau_8}$ $\dot{m}_{8-11} = -f_{8-11} \frac{I_8}{\tau_8}$ Losses = $-\varepsilon_8 \frac{I_8}{\tau_8} - \lambda I_8$
9	$\dot{m}_{2-9} = \eta_2 \frac{I_2}{\tau_2}$ $\dot{m}_{6-9} = \eta_6 \frac{I_6}{\tau_6}$ $\dot{m}_{8-9} = (1 - f_{8-11}) \frac{I_8}{\tau_8}$ $\dot{m}_{10-9} = \frac{I_{10}}{\tau_{10}}$ $\dot{m}_{9-10} = -f_{9-10} \frac{I_9}{\tau_9}$ $\dot{m}_{9-11} = -(1 - f_{9-10}) \frac{I_9}{\tau_9}$ Losses = $-\varepsilon_9 \frac{I_9}{\tau_9} - \lambda I_9$
10	$\dot{m}_{5-10} = f_{5-10} \frac{I_5}{\tau_5}$ $\dot{m}_{9-10} = f_{9-10} \frac{I_9}{\tau_9}$ $\dot{m}_{10-9} = -\frac{I_{10}}{\tau_{10}}$ Losses = $-\varepsilon_{10} \frac{I_{10}}{\tau_{10}} - \lambda I_{10}$
11	$\dot{m}_{8-11} = f_{8-11} \frac{I_8}{\tau_8}$ $\dot{m}_{9-11} = (1 - f_{9-10}) \frac{I_9}{\tau_9}$ $\dot{m}_{11-12} = -\frac{\dot{N}^-}{\eta_f f_b}$ Losses = $-\lambda I_{11}$
12	$\dot{m}_{11-12} = \frac{\dot{N}^-}{\eta_f f_b}$ $\dot{m}_{12-p} = -\frac{\dot{N}^-}{\eta_f f_b}$

Table A.3. Flow rates fractions and component efficiencies assumed for the reference case.

Flow rate fraction	Value
f_{1-5}	10^{-2}
f_{p-3}	10^{-4}
f_{p-4}	10^{-4}
f_{5-3}	0.6
f_{5-6}	10^{-2}
f_{5-10}	10^{-4}
f_{6-3}	0.6
f_{8-11}	0
f_{9-10}	10^{-1}
η_2	0.95
η_6	0.95

$$\frac{dI_7}{dt} = (1 - \eta_f f_b - f_{p-3} - f_{p-4}) \frac{\dot{N}^-}{\eta_f f_b} - \frac{I_7}{T_7} \quad (\text{A.7})$$

$$\frac{dI_8}{dt} = \frac{I_7}{\tau_7} - \frac{I_8}{T_8} \quad (\text{A.8})$$

$$\frac{dI_9}{dt} = (1 - f_{8-11}) \frac{I_8}{\tau_8} + \frac{I_{10}}{\tau_{10}} + \eta_2 \frac{I_2}{\tau_2} + \eta_6 \frac{I_6}{\tau_6} - \frac{I_9}{T_9} \quad (\text{A.9})$$

$$\frac{dI_{10}}{dt} = f_{5-10} \frac{I_5}{\tau_5} + f_{9-10} \frac{I_9}{\tau_9} - \frac{I_{10}}{T_{10}} \quad (\text{A.10})$$

$$\frac{dI_{11}}{dt} = f_{8-11} \frac{I_8}{\tau_8} + (1 - f_{9-10}) \frac{I_9}{\tau_9} - \frac{\dot{N}^-}{\eta_t f_b} - \lambda I_{11} \quad (\text{A.11})$$

$$\frac{dI_{12}}{dt} = 0 \quad (\text{not simulated}) \quad (\text{A.12})$$

where:

$$\frac{1}{T_i} = \frac{1 + \varepsilon_i}{\tau_i} + \lambda \quad (\text{A.13})$$

Initial conditions on components' inventory:

- $I_i(t = 0) = I_{i,0} = 0$, for $i = 1, 2, \dots, 10$;
- $I_{11}(t = 0) = I_{11}^0$ is the initial start-up inventory.

Table A.3 shows the values of flow rate fractions (f_{i-j}), which indicate the fraction of total outlet flow rate of component i which flows to component j , and tritium processing efficiencies (η_i), e.g. for components such as TES and CPS units. All losses to environment ε_i are set to 10^{-4} arbitrarily. We assume there are no direct losses to the environment from the blanket and PFCs since these components are in the vacuum vessel, and from the storage and fueling system where fuel is stored and processed at low temperature, i.e. $\varepsilon_1 = \varepsilon_3 = \varepsilon_4 = \varepsilon_{11} = \varepsilon_{12} = 0$.

References

- [1] Abdou M.A., Vold E.L., Gung C.Y., Youssef M.Z. and Shin K. 1986 Deuterium–tritium fuel self-sufficiency in fusion reactors *Fusion Technol.* **9** 250–85
- [2] Kuan W. and Abdou M.A. 1999 A new approach for assessing the required tritium breeding ratio and startup inventory in future fusion reactors *Fusion Technol.* **35** 309–53
- [3] Sawan M.E. and Abdou M.A. 2006 Physics and technology conditions for attaining tritium self-sufficiency for the DT fuel cycle *Fusion Eng. Des.* **81** 1131–44
- [4] Abdou M., Morley N.B., Smolentsev S., Ying A., Malang S. and Rowcliffe A.M. 2015 Blanket/first wall challenges and required R & D on the pathway to DEMO *Fusion Eng. Des.* **100** 2–43
- [5] Riva M. 2020 Predictive methods and analysis of time dependent tritium flow rates and inventories in fusion systems *PhD Dissertation UCLA*
- [6] Day C., Butler B., Giegerich T., Ploekl B. and Varoutis S. 2019 A smart three-loop fuel cycle architecture for DEMO *Fusion Eng. Des.* **146** 2462–8
- [7] Abdou M. 2017 Tritium fuel cycle, tritium inventories, and physics and technology R & D challenges for: 1) enabling the startup of DEMO and future power plants and 2) attaining tritium self-sufficiency in fusion reactors *13th Int. Symp. on Fusion Nuclear Technology (ISFNT-13)* (Kyoto, Japan, 25–29 September 2017) (<http://fusion.ucla.edu/abdou/Presentation%20Web%20Page.html>)
- [8] Ni M., Wang Y., Yuan B., Jiang J. and Wu Y. 2013 Tritium supply assessment for ITER and DEMOnstration power plant *Fusion Eng. Des.* **88** 2422–6
- [9] Chen H., Pan L., Lv Z., Li W. and Zeng Q. 2016 Tritium fuel cycle modeling and tritium breeding analysis for CFETR *Fusion Eng. Des.* **106** 17–20
- [10] Pan L., Chen H. and Zeng Q. 2016 Sensitivity analysis of tritium breeding ratio and startup inventory for CFETR *Fusion Eng. Des.* **112** 311–6
- [11] Song Y., Huang Q., Ni M. and Chen X. 2011 Analysis on initial tritium supply for starting up fusion power reactor FDS-II *Fusion Sci. Technol.* **60** 1121–4
- [12] Zheng S., King D.B., Garzotti L., Surrey E. and Todd T.N. 2016 Fusion reactor start-up without an external tritium source *Fusion Eng. Des.* **103** 13–20
- [13] Coleman M., Hörstemsmeier Y. and Cismondi F. 2019 DEMO tritium fuel cycle: performance, parameter explorations, and design space constraints *Fusion Eng. Des.* **141** 79–90
- [14] Day C. and Giegerich T. 2013 The direct internal recycling concept to simplify the fuel cycle of a fusion power plant *Fusion Eng. Des.* **88** 616–20
- [15] Kovari M., Coleman M., Cristescu I. and Smith R. 2018 Tritium resources available for fusion reactors *Nucl. Fusion* **58** 026010
- [16] Abdou M.A. *et al* 1996 Results of an international study on a high-volume plasma-based neutron source for fusion blanket development *Fusion Technol.* **29** 1–57
- [17] Peters B.J. and Day C. 2017 Analysis of low pressure hydrogen separation from fusion exhaust gases by the means of superpermeability *Fusion Eng. Des.* **124** 696–9
- [18] Hernández F., Pereslavtsev P., Kang Q., Norajitra P., Kiss B., Nádas G. and Bitz O. 2017 A new HCPB breeding blanket for the EU DEMO: evolution, rationale and preliminary performances *Fusion Eng. Des.* **124** 882–6
- [19] Palermo I., Rapisarda D., Fernández-Berceruelo I. and Ibarra A. 2016 Tritium production assessment for the DCLL EUROfusion DEMO *Nucl. Fusion* **56** 104001
- [20] Martelli E.A. *et al* 2018 Advancements in DEMO WCLL breeding blanket design and integration *Int. J. Energy Res.* **42** 27–52
- [21] Abdou M. 2019 Lessons learned from 40 years of fusion science and technology research *Keynote Presentation at the Int. Symp. on Fusion Nuclear Technology (ISFNT-14)* (Budapest, Hungary, 22–27 September 2019) (<http://fusion.ucla.edu/abdou/Presentation%20Web%20Page.html>)
- [22] Ying A., Zhang H., Anh M.-Y. and Lee Y. 2015 Tritium transport evolutions in HCCR TBM under ITER inductive operations *Fusion Sci. Technol.* **68** 346–52
- [23] Ying A., Zhang H., Merrill B.J. and Ahn M.-Y. 2016 Advancement in tritium transport simulations for solid breeding blanket system *Fusion Eng. Des.* **109–111** 1511–6
- [24] Ying A., Liu H. and Abdou M. 2013 Analysis of tritium/deuterium retention and permeation in FW/divertor including geometric and temperature operating features *Fusion Sci. Technol.* **64** 303–8
- [25] Zucchetti M., Nicolotti I., Ying A. and Abdou M. 2015 Tritium modeling for ITER test blanket module *Fusion Sci. Technol.* **68** 644–7
- [26] Ying A., Zhang H., Merrill B., Ahn M.-Y. and Cho S. 2018 Breeding blanket system design implications on tritium transport and permeation with high tritium ion implantation: a MATLAB/Simulink, COMSOL integrated dynamic tritium transport model for HCCR TBS *Fusion Eng. Des.* **136** 1153–60
- [27] Riva M., Ying A., Abdou M., Ahn M.-Y. and Cho S. 2019 Impact of outer fuel cycle tritium transport on initial startup inventory for next fusion devices *Fusion Sci. Technol.* **75** 1037–45
- [28] Peeters M.M.W., Magielsen A.J., Stijkel M.P. and van der Laan J.G. 2007 In-pile tritium release behaviour of lithiummetatitanate produced by extrusion-spheroidisation-sintering process in EXOTIC-9/1 in the high flux reactor, Petten *Fus. Eng. Des.* **82** 2318–25
- [29] Demange D., Borisevich O., Gramlich N., Wagner R. and Welte S. 2013 Zeolite membranes and palladium membrane reactor for tritium extraction from the breeder blankets of ITER and DEMO *Fusion Eng. Des.* **88** 2396–9

- [30] Day C., Butler B., Giegerich T., Lang P.T. and Lawless R.B. 2016 Consequences of the technology survey and gap analysis on the EU DEMO R & D programme in tritium, matter injection and vacuum *Fusion Eng. Des.* **109–111** 299–308
- [31] Federici G. *et al* 2019 Overview of the DEMO staged design approach in Europe *Nucl. Fusion* **59** 066013
- [32] Kim K. *et al* 2015 Design concept of K-DEMO for near-term implementation *Nucl. Fusion* **55** 053027
- [33] Scott W. LANL and ITER 2009 Private communication
- [34] Abdou M.A., Maekawa H., Oyama Y., Youssef M., Kumar A.Y.C., Maekawa F., Kosako K., Nakamura T. and Bennett E. 1995 Japan Atomic Energy Research Institute/United States integral neutronics experiments and analyses for tritium breeding, nuclear heating, and induced radioactivity *Fusion Technol.* **28** 5–38
- [35] Youssef M. and Abdou M.A. 1986 Uncertainties in prediction of tritium breeding in candidate blanket designs due to present uncertainties in nuclear data base *Fusion Technol.* **9** 286–307
- [36] Sato S. *et al* 2006 Progress in the blanket neutronics experiments at JAERI/FNS *Fusion Eng. Des.* **81** 1183–93
- [37] Verzilov Y. *et al* 2004 Integral experiments for verification of tritium production on the beryllium/lithium titanate blanket mock-up with a one-breeder layer *JAERI-Research 2004-015*
- [38] Wu Y. and (FDS Team) 2009 CAD-based interface programs for fusion neutron transport simulation *Fusion Eng. Des.* **84** 1987–92
- [39] Palermo I., Rapisarda D., Fernández-Berceruelo I. and Ibarra A. 2017 Optimization process for the design of the DCLL blanket for the European DEMONstration fusion reactor according to its nuclear performances *Nucl. Fusion* **57** 076011
- [40] Angioni C., Fable E., Greenwald M., Maslov M., Takenaga H. and Weisen H. 2009 Particle transport in tokamak plasmas, theory and experiment *Plasma Phys. Control. Fusion* **51** 124017
- [41] Chang C.S. *et al* 2017 Gyrokinetic projection of the divertor heat-flux width from present tokamaks to ITER *Nucl. Fusion* **57** 116023
- [42] de Vries P.C. *et al* 2017 Multi-machine analysis of termination scenarios with comparison to simulations of controlled shutdown of ITER discharges *Nucl. Fusion* **58** 026019
- [43] Dux R., Loarte A., Fable E. and Kukushkin A. 2014 Transport of tungsten in the H-mode edge transport barrier of ITER *Plasma Phys. Control. Fusion* **56** 124003
- [44] Futatani S., Huijsmans G., Loarte A., Baylor L.R., Commaux N.T.C., Fenstermacher M.E., Lasnier C., Osborne T.H. and Pegourié B. 2014 Non-linear MHD modelling of ELM triggering by pellet injection in DIII-D and implications for ITER *Nucl. Fusion* **54** 073008
- [45] Garzotti L. *et al* 2019 Integrated core-SOL modelling of fuelling, density control and divertor heat loads for the flat-top phase of the ITER H-mode D–T plasma scenarios *Nucl. Fusion* **59** 026006
- [46] Hirshman S.P. and Sigmar D.J. 1981 Neoclassical transport of impurities in tokamak plasmas *Nucl. Fusion* **21** 1079
- [47] Horton L.D. *et al* 1999 High fusion power steady state operation in JET DT plasmas *Nucl. Fusion* **39** 993
- [48] Hu Q.M. *et al* 2019 The density dependence of edge-localized-mode suppression and pump-out by resonant magnetic perturbations in the DIII-D tokamak *Phys. Plasmas* **26** 120702
- [49] ITER Organization 2018 ITER Research plan *ITER-18-003 ITER* (https://www.iter.org/doc/www/content/com/Lists/ITER%20Technical%20Reports/Attachments/9/ITER-Research-Plan_final_ITR_FINAL-Cover_High-Res.pdf)
- [50] Ikeda K. 2007 Progress in the ITER physics basis *Nucl. Fusion* **47** S1
- [51] Kaveeva E. *et al* 2020 SOLPS-ITER modelling of ITER edge plasma with drifts and currents *Nucl. Fusion* **60** 046019
- [52] Köchl F. *et al* 2020 *Plasma Phys. Control. Fusion* in preparation
- [53] Kukushkin A.S. *et al* 2002 Basic divertor operation in ITER-FEAT *Nucl. Fusion* **42** 187
- [54] Kukushkin A.S., Pacher H.D., Kotov V., Reiter D. and Pacher G.W.D. 2007 Effect of conditions for gas recirculation on divertor operation in ITER *Nucl. Fusion* **47** 698
- [55] Kukushkin A.S. *et al* 2009 Analysis of performance of the optimized divertor in ITER *Nucl. Fusion* **49** 075008
- [56] Kukushkin A.S., Polevoi A.R., Pacher H.D., Pacher G.W. and Pitts R.A. 2011 Physics requirements on fuel throughput in ITER *J. Nucl. Mater.* **415** S497
- [57] Kukushkin A.S., Pacher H.D., Pacher G.W., Kotov V., Pitts R.A. and Reiter D. 2013 *Nucl. Fusion* **53** 123024
- [58] Kukushkin A.S. and Pacher H.D. 2016 *Nucl. Fusion* **56** 126012
- [59] Loarte A. *et al* 2002 Characteristics and scaling of energy and particle losses during type I ELMs in JET H-modes *Plasma Phys. Control. Fusion* **44** 1815
- [60] Loarte A., Liu F., Huijsmans G.T.A., Kukushkin A.S. and Pitts R.A. 2015 MHD stability of the ITER pedestal and SOL plasma and its influence on the heat flux width *J. Nucl. Mater.* **463** 401
- [61] Loarte A. *et al* 2014 Evolution of plasma parameters in the termination phase of high confinement H-modes at JET and implications for ITER *Nucl. Fusion* **54** 123014
- [62] Loarte A. *et al* 2014 Progress on the application of ELM control schemes to ITER scenarios from the non-active phase to DT operation *Nucl. Fusion* **54** 033007
- [63] Loarte A. *et al* 2016 Evaluation of tungsten transport and concentration control in ITER scenarios *Preprint: 2016 IAEA Fusion Energy Conf.* (Kyoto, Japan, 17–22 October 2016) PPC/2-1 (<https://nucleus.iaea.org/sites/fusionportal/Shared%20Documents/FEC%202016/fec2016-preprints/preprint0506.pdf>)
- [64] Loarte A. and Neu R. 2017 Power exhaust in tokamaks and scenario integration issues *Fusion Eng. Des.* **122** 256
- [65] Maruyama S. *et al* 2012 ITER fuelling and glow discharge cleaning system overview *Proc. 24th Int. Conf. on Fusion Energy* (San Diego, CA, 2012) ITR/P5-24 ([http://www-naweb.iaea.org/napc/physics/FEC/FEC2012/papers/332_ITRP524.pdf](http://www.naweb.iaea.org/napc/physics/FEC/FEC2012/papers/332_ITRP524.pdf))
- [66] Maslov M. *et al* 2018 Observation of enhanced ion particle transport in mixed H/D isotope plasmas on JET *Nucl. Fusion* **58** 076022
- [67] Pitts R.A. *et al* 2019 Physics basis for the first ITER tungsten divertor *Nucl. Mater. Energy* **20** 100696
- [68] Pacher H.D., Kukushkin A.S., Pacher G.W., Kotov V. and Reiter D. 2015 Impurity seeding in ITER DT plasmas in a carbon-free environment *J. Nucl. Mater.* **463** 591
- [69] Pégourié B., Köchl F., Nehme H. and Polevoi A.R. 2009 Recent results on the fuelling and control of plasmas by pellet injection, application to ITER *Plasma Phys. Control. Fusion* **51** 124023
- [70] Polevoi A.R. and Shimada M. 2001 Simplified mass ablation and relocation treatment for pellet injection optimization *Plasma Phys. Control. Fusion* **43** 1525
- [71] Polevoi A.R. *et al* 2003 Pellet injection as a possible tool for plasma performance improvement *Nucl. Fusion* **43** 1072
- [72] Polevoi A.R. *et al* 2008 Assessment of pumping requirements in ITER for pellet fuelling and ELM pace making *35th EPS Conf. Plasma Physics* (Hersonissos, Greece, 9–13 June 2008) P-1.109 (http://epsppd.epfl.ch/Hersonissos/pdf/P1_109.pdf)
- [73] Polevoi A.R. *et al* 2015 Assessment of operational space for long-pulse scenarios in ITER *Nucl. Fusion* **55** 063019

- [74] Polevoi A.R. *et al* 2017 Analysis of fuelling requirements in ITER H-modes with SOLPS-EPED1 derived scalings *Nucl. Fusion* **57** 022014
- [75] Polevoi A.R. *et al* 2018 Integrated simulations of H-mode operation in ITER including core fuelling, divertor detachment and ELM control *Nucl. Fusion* **58** 056020
- [76] Polevoi A.R. *et al* 2018 *45th EPS Conf. Plasma Physics* (Prague, Czech Republic, 2–6 July 2018) P5.1050 (<http://ocs.ciemat.es/EPS2018PAP/pdf/P5.1050.pdf>)
- [77] Pütterich T., Dux R., Janzer M.A., McDermott R.M. and (ASDEX Upgrade Team) 2011 ELM flushing and impurity transport in the H-mode edge barrier in ASDEX Upgrade *J. Nucl. Mater.* **415** S334
- [78] Schmitz O. *et al* 2016 Three-dimensional modeling of plasma edge transport and divertor fluxes during application of resonant magnetic perturbations on ITER *Nucl. Fusion* **56** 066008
- [79] Vincenzi P. *et al* 2015 Fuelling and density control for DEMO *Nucl. Fusion* **55** 113028
- [80] Wiesen S. *et al* 2017 Control of particle and power exhaust in pellet fuelled ITER DT scenarios employing integrated models *Nucl. Fusion* **57** 076020
- [81] Corrigan R. *et al* 2015 Advances in the physics basis for the European DEMO design *Nucl. Fusion* **55** 063003
- [82] Artaud M. *et al* 2013 Particle transport analysis of the density build-up after the L–H transition in ASDEX Upgrade *Nucl. Fusion* **53** 093020
- [83] Combs S.K. and Baylor L.R. 2018 Pellet-injector technology—brief history and key developments in the last 25 years *Fusion Sci. Technol.* **73** 493–518
- [84] Baylor L.R., Parks P.B., Jernigan T.C., Caughman J.B., Combs S.K., Foust C.R., Houlberg W.A., Maruyama S. and Rasmussen D.A. 2007 Pellet fuelling and control of burning plasmas in ITER *Nucl. Fusion* **47** 443
- [85] Plöckl B. and Lang P.T. 2013 The enhanced ASDEX Upgrade pellet centrifuge launcher *Rev. Sci. Instrum.* **84** 103509
- [86] Baylor L.R. *et al* 2003 Comparison of fueling efficiency from different fueling locations on DIII-D *J. Nucl. Mater.* **530** 313–6
- [87] Sakamoto R. *et al* 2001 Impact of pellet injection on extension of the operational region in LHD *Nucl. Fusion* **41** 381
- [88] Lang P.T. *et al* 2001 High-density H-mode operation achieved using efficient plasma refueling by inboard pellet launch *J. Nucl. Mater.* **374** 290–3
- [89] Loarte A. *et al* 2014 Progress on the application of ELM control schemes to ITER scenarios from the non-active phase to DT operation *Nucl. Fusion* **54** 033007
- [90] Baylor L.R. *et al* 2007 Comparison of deuterium pellet injection from different locations on the DIII-D tokamak *Nucl. Fusion* **47** 1598–606
- [91] Matsuyama A., Koechl F., Pégourié B., Sakamoto R. and Yamada H.G. 2012 Modelling of the pellet deposition profile and ∇B -induced drift displacement in non-axisymmetric configurations *Nucl. Fusion* **52** 123017
- [92] Kukushkin A.S. *et al* 2002 Basic divertor operation in ITER-FEAT *Nucl. Fusion* **42** 187
- [93] Valovic M. *et al* 2020 Compatibility of pellet fueling with ELM suppression by RMPs in the ASDEX Upgrade tokamak *Nucl. Fusion* **60** 054006
- [94] Parks P.B. and Turnbull R.J. 1978 Effect of transonic flow in the ablation cloud on the lifetime of a solid hydrogen pellet in a plasma *Phys. Fluids* **21** 1735
- [95] Baylor L.R. *et al* 1997 An international pellet ablation database *Nucl. Fusion* **37** 445
- [96] Combs S.K., Baylor L.R., Meitner S.J., Caughman J.B.O., Rasmussen D.A. and Maruyama S. 2012 Overview of recent developments in pellet injection for ITER *Fusion Eng. Des.* **87** 634–40
- [97] Lang P.T. *et al* 2015 Considerations on the DEMO pellet fuelling system *Fusion Eng. Des.* **96–97** 123
- [98] Frattolillo A. *et al* 2018 Core fueling of DEMO by direct line injection of high-speed pellets from the HFS *IEEE Trans. Plasma Sci.* **46** 1429
- [99] Maruyama S. *et al* 2012 ITER fuelling and glow discharge cleaning system overview *Proc. 24th Int. Conf. on Fusion Energy* (San Diego, CA, 2012) ITR/P5-24 (<https://www-pub.iaea.org/iaameetings/41985/24th-Fusion-Energy-Conference>)
- [100] Valovic M. *et al* 2018 Shallow pellet fueling under conditions of RMP ELM mitigation or divertor detachment in ASDEX Upgrade *45th EPS Conf. Plasma Physics* (Prague, Czech Republic, 2–6 July 2018) P2.1075 (<https://www.eps.org/blogpost/739454/293322/45th-Conference-on-Plasma-Physics-EPS-2018>)
- [101] Garzotti L. *et al* 2019 Integrated core-SOL modelling of fuelling, density control and divertor heat loads for the flat-top phase of the ITER H-mode D–T plasma scenarios *Nucl. Fusion* **59** 026006
- [102] Frattolillo A. *et al* 1996 High-speed repeating hydrogen pellet injector for long-pulse magnetic confinement fusion experiments *Rev. Sci. Instrum.* **67** 1834
- [103] US Department of Energy 2015 *Tritium Handling and Safe Storage*
- [104] US Department of Energy 1996 *Safety of Magnetic Fusion Facilities: Requirements—DOE Technical Standards Program*
- [105] US Department of Energy 1996 *Safety of Magnetic Fusion Facilities: Guidance - DOE Technical Standards Program*
- [106] Abbott M.L. and Wenzel D.R. 1993 Dose calculations for routine airborne releases of ITER activation products *EGG-EEL-11108* Idaho National Engineering
- [107] Humrickhouse P.W. and Merrill B.J. 2018 Tritium aspects of the fusion nuclear science facility *Fusion Eng. Des.* **135** 302–13
- [108] IRSN 2017 *Nuclear Fusion Reactors //safety and radiation protection considerations for demonstration reactors that follow the ITER facility*
- [109] Nakamura H., Sakurai S., Suzuki S., Hayashi T. and Tobita K.M. 2006 Case study on tritium inventory in the fusion DEMO plant at JAERI *Fusion Eng. Des.* **81** 1339–45
- [110] Malo M., Valle F.J., Jiménez F.M., Moroño A. and Moreno C. 2017 Isotope thermo-diffusion in structural materials *Fusion Eng. Des.* **124** 924–7
- [111] Ali-Khan I., Dietz K. J., Waelbroeck F.G. and Wienhold P. 1978 The rate of hydrogen release out of clean metallic surfaces *J. Nucl. Mater.* **76–77** 337–43
- [112] Steward S.A. 1983 Review of hydrogen isotope permeability through materials <https://doi.org/10.2172/5277693>
- [113] Reiter F., Forcey K.S. and Gervasini G. 1993 *A Compilation of Tritium-Material Interaction Parameters in Fusion Reactor Materials* Commission of the European Communities
- [114] Serra E., Benamati G. and Ogorodnikova O.V. 1998 Hydrogen isotopes transport parameters in fusion reactor materials *J. Nucl. Mater.* **255** 105–15
- [115] Causey R.A., Karnesky R.A. and San Marchi C. 2012 4.16-Tritium barriers and tritium diffusion in fusion reactors *Compr. Nucl. Mater.* ed R.J.M. Konings (Oxford: Elsevier) pp 511–49
- [116] Hatano Y. 2017 Permeation and permeation barrier *Tritium Fuel Fusion React.* ed T. Tanabe (Berlin: Springer) pp 207–29
- [117] Shimada M. 2020 Tritium transport in fusion reactor materials *Ref. Module Mater. Sci. Mater. Eng.* (Oxford: Elsevier)
- [118] Völkl J. and Alefeld G. 1975 Hydrogen diffusion in metals *Dif-fus. Solids Recent Dev.* ed A S Nowick and J J Burton (New York: Academic) pp 231–302

- [119] Wampler W.R. 1991 Surface-limited release of deuterium from tantalum *J. Appl. Phys.* **69** 3063–7
- [120] Serra E. and Perujo A. 1995 The surface rate constants of deuterium in the martensitic steel DIN 1.4914 (MANET) *J. Nucl. Mater.* **223** 157–62
- [121] Serra E. and Perujo A. 1997 Influence of the surface conditions on permeation in the deuterium-MANET system *J. Nucl. Mater.* **240** 215–20
- [122] Esteban G.A., Perujo A., Sedano L.A. and Mancinelli B. 2000 The surface rate constants of deuterium in the reduced activating martensitic steel OPTIFER-IVb *J. Nucl. Mater.* **282** 89–96
- [123] Perujo A., Douglas K. and Serra E. 1996 Low pressure tritium interaction with inconel 625 and AISI 316 L stainless steel surfaces: an evaluation of the recombination and adsorption constants *Fusion Eng. Des.* **31** 101–8
- [124] Esteban G.A., Perujo A., Sedano L.A., Legarda F., Mancinelli B. and Douglas K. 2002 Diffusive transport parameters and surface rate constants of deuterium in incoloy 800 *J. Nucl. Mater.* **300** 1–6
- [125] Altunoglu A.K., Blackburn D.A., Braithwaite N.S.J. and Grant D.M. 1991 Permeation of hydrogen through nickel foils: surface reaction rates at low temperatures *J. Less Common Met.* **172–174** 718–26
- [126] Grant D.M., Cummings D.L. and Blackburn D.A. 1987 Hydrogen in 304 steel: diffusion, permeation and surface reaction *J. Nucl. Mater.* **149** 180–91
- [127] Hatano Y., Busnyuk A., Livshits A., Homma H. and Matsuyama M. 2007 Correlation between hydrogen isotope permeation through niobium and bulk oxygen concentration: possible influence of oxygen on tritium recovery from Pb–Li by vacuum permeator *Fusion Sci. Technol.* **52** 990–4
- [128] Hatano Y., Busnyuk A., Alimov V., Livshits A. and Matsuyama M.Y. 2008 Influence of oxygen on permeation of hydrogen isotopes through group 5 metals *Fusion Sci. Technol.* **54** 526–9
- [129] Anderl R.A., Holland D.F., Longhurst G.R., Pawelko R.J., Trybus C.L. and Sellers C.H. 1992 Deuterium transport and trapping in polycrystalline tungsten *Fusion Technol.* **21** 745–52
- [130] Merrill B.J., Jones J.L. and Holland D.F. 1986 TMAP/Mod 1: Tritium migration analysis program code description and user's manual EG and G Idaho Inc. Idaho Falls, USA (<https://osti.gov/biblio/6472488-tmap-mod-tritium-migration-analysis-program-code-description-user-manual>)
- [131] Longhurst G.R. 2008 TMAP7 user manual Idaho National Laboratory (INL) <https://doi.org/10.2172/952013>
- [132] Longhurst G.R. and Ambrosek J. 2005 Verification and validation of the tritium transport code TMAP7 *Fusion Sci. Technol.* **48** 468–71
- [133] Franza F., Ciampichetti A., Ricapito I. and Zucchetti M. 2012 A model for tritium transport in fusion reactor components: the FUS-TPC code *Fusion Eng. Des.* **87** 299–302
- [134] Ugorri F.R. *et al* 2017 Tritium transport modeling at system level for the EUROfusion dual coolant lithium–lead breeding blanket *Nucl. Fusion* **57** 116045
- [135] Ni M., Song Y., Huang Q. and Wu Y. 2009 Development of tritium analysis system TAS 1.0 *Chin. J. Nucl. Sci. Eng.* **29** 355–61
- [136] Shimada M. *et al* 2011 First result of deuterium retention in neutron-irradiated tungsten exposed to high flux plasma in TPE J. *Nucl. Mater.* **415** S667–71
- [137] Zhang S.-Y., Jin S., Zou D.-R., Cheng L., Hou Q. and Lu G.-H. 2017 The effect of inert gas pre-irradiation on the retention of deuterium in tungsten: a TMAP investigation combined with first-principles method *Fusion Eng. Des.* **121** 342–7
- [138] Franza F., Boccaccini L.V., Ciampichetti A. and Zucchetti M. 2013 Tritium transport analysis in HCPB DEMO blanket with the FUS-TPC code *Fusion Eng. Des.* **88** 2444–7
- [139] Merrill B.J. *et al* 2004 Safety assessment of two advanced ferritic steel molten salt blanket design concepts *Fusion Eng. Des.* **72** 277–306
- [140] Aiello A., Ciampichetti A. and Benamati G. 2004 An overview on tritium permeation barrier development for WCLL blanket concept *J. Nucl. Mater.* **329–333** 1398–402
- [141] Song Y., Huang Q., Wang Y. and Ni M. 2009 Analysis on tritium controlling of the dual-cooled lithium lead blanket for fusion power reactor FDS-II *Fusion Eng. Des.* **84** 1779–83
- [142] Nie B., Jiang M. and Wu Y. 2015 A dynamic modeling 3H transfer to the environment under accidental release from the fusion reactor *J. Fusion Energy* **34** 739–45
- [143] Hollenberg G.W., Simonen E.P., Kalinin G. and Terlain A. 1998 Tritium/hydrogen barrier development *Fusion Eng. Des.* **28** 190–208
- [144] Perujo A. and Forcey K.S. 1995 Tritium permeation barriers for fusion technology *Fusion Eng. Des.* **28** 252–7
- [145] Xiang X., Wang X., Zhang G., Tang T. and Lai X. 2015 Preparation technique and alloying effect of aluminide coatings as tritium permeation barriers: a review *Int. J. Hydrog. Energy* **40** 3697–707
- [146] Gilbert E.R. *et al* 1992 Tritium permeation and related studies on barrier treated 316 stainless steel *Fusion Technol.* **21** 739–44
- [147] Esteban G.A., Perujo A., Legarda F., Sedano L.A. and Riccardi B. 2002 Deuterium transport in SiCf/SiC composites *J. Nucl. Mater.* **307–311** 1430–5
- [148] Sato R., Chikada T., Matsuzaki H., Suzuki A. and Sugiyama K.T. 2014 Measurement of hydrogen isotope concentration in erbium oxide coatings *Fusion Eng. Des.* **89** 1375–9
- [149] Conrad R., Debarberis L., Coen V. and Flament T. 1991 Irradiation of liquid breeder material Pb–17Li with *in-situ* tritium release measurements in the LIBRETTO 2 experiment *J. Nucl. Mater.* **179–181** 875–8
- [150] Proust E., Leroy P. and Franenberg H.W. 1992 Preliminary interpretation of the LIBRETTO-2 experimental results in terms of tritium permeation barrier efficiency *J. Nucl. Mater.* **191–194** 186–9
- [151] Conrad R., Fütterer M.A., Giancarli L., May R. and Sample T.A. 1994 LIBRETTO-3: performance of tritium permeation barriers under irradiation at the HFR Petten *J. Nucl. Mater.* **212–215** 998–1002
- [152] Magielsen A.J. *et al* 2002 In-pile performance of a double-walled tube and a tritium permeation barrier *J. Nucl. Mater.* **307–311** 832–6
- [153] Zheng G., Carpenter D., Dolan K. and Hu L.-w. 2019 Experimental investigation of alumina coating as tritium permeation barrier for molten salt nuclear reactors *Nucl. Eng. Des.* **353** 110232
- [154] Tanabe T. 2012 Tritium issues to be solved for establishment of a fusion reactor *Fusion Eng. Des.* **87** 722–7
- [155] Glugla M. *et al* 2007 The ITER tritium systems *Fusion Eng. Des.* **82** 472–87
- [156] Taylor N. *et al* 2017 Materials-related issues in the safety and licensing of nuclear fusion facilities *Nucl. Fusion* **57** 092003
- [157] Day C. and Giegerich T. 2014 Development of advanced exhaust pumping technology for a DT fusion power plant *IEEE Trans. Plasma Sci.* **42** 1058–71
- [158] Day C. *et al* 2016 Consequences of the technology survey and gap analysis on the EU DEMO R & D programme in tritium, matter injection and vacuum *Fusion Eng. Des.* **109–111** 299–308

- [159] Hörstemsmeier Y.N., Butler B., Day C. and Franza F. 2018 Analysis of the EU-DEMO fuel cycle elements: intrinsic impact of technology choices *Fusion Eng. Des.* **136** 314–8
- [160] Lawless R., Butler B., Hollingsworth A., Camp P. and Shaw R. 2017 Tritium plant technology development for a DEMO power plant *Fusion Sci. Technol.* **71** 679–86
- [161] Giegerich T. *et al* 2016 Advanced design of the mechanical tritium pumping system for JET DTE2 *Fusion Eng. Des.* **109–111** 359–64
- [162] Luo A. *et al* 1997 Applications of superpermeable membranes in fusion: the flux density problem and experimental progress *J. Nucl. Mater.* **241–243** 1203–9
- [163] Peters B.J. and Day C. 2017 Analysis of low pressure hydrogen separation from fusion exhaust gases by the means of superpermeability *Fusion Eng. Des.* **124** 696–9
- [164] Peters B.J., Hanke S. and Day C. 2018 Metal foil pump performance aspects in view of the implementation of direct internal recycling for future fusion fuel cycles *Fusion Eng. Des.* **136** 1467–71
- [165] Hanke S. *et al* 2020 Progress of the R & D programme to develop a metal foil pump for DEMO *Fusion Eng. Des.* (unpublished)
- [166] Scannapiego M. and Day C. 2017 Experimental investigation on charcoal adsorption for cryogenic pump application *IOP Conf. Ser.: Mater. Sci. Eng.* **278** 012160
- [167] Schwenzer J. *et al* 2020 Start-up and operational tritium inventories in the EU-DEMO fuel cycle *Fusion Eng. Des.* (in preparation)
- [168] Coleman M., Hörstemsmeier Y. and Cismondi F. 2019 DEMO tritium fuel cycle: performance, parameter explorations, and design space constraints *Fusion Eng. Des.* **141** 79–90
- [169] Wilson J., Becnel J., Demange D. and Rogers B. 2019 The ITER tokamak exhaust processing system design and substantiation *Fusion Sci. Technol.* **75** 794–801
- [170] Tosti S., Bruni G., Incelli M. and Santucci A. 2017 Ceramic membranes for processing plasma enhancement gases *Fusion Eng. Des.* **124** 928–33
- [171] Serra E., Ciora R.J., De Meis D. and Richetta M. 2019 Plasma enhancement gases (PEGs) separation using a carbon molecular sieve (CMS) membrane *Fusion Eng. Des.* **146** 2438–41
- [172] Heung L.K., Sessions H.T. and Xiao X. 2011 TCAP hydrogen isotope separation using palladium and inverse columns *Fusion Sci. Technol.* **60** 1331–4
- [173] Neugebauer C., Hörstemsmeier Y. and Day C. 2020 Technology development for isotope rebalancing and protium removal in the EU DEMO fuel cycle *Fusion Sci. Technol.* **76** 215–20
- [174] Spagnolo D.A. and Miller A.I. 1995 The CECE alternative for upgrading/detrification in heavy water nuclear reactors and for tritium recovery in fusion reactors *Fusion Technol.* **28** 748–54
- [175] Cristescu I. 2016 Enhanced configuration of a water detrification system; impact on ITER isotope separation system based cryogenic distillation *Fusion Eng. Des.* **109–111** 1404–7
- [176] Rozenkevich M., Pak Y., Marunich S., Bukin A., Perevezentsev A. and Lepetit L. 2016 Main features of the technology for air detrification in scrubber column *Fusion Sci. Technol.* **70** 435–47
- [177] Boniface H.A., Gnanapragasam N.V., Ryland D.K., Suppiah S. and Perevezentsev A. 2017 Water detrification system for ITER—evaluation of design parameters *Fusion Sci. Technol.* **71** 241–5
- [178] Lozada-Hidalgo M., Hu S., Marshall O., Mishchenko A., Dryfe R.A.W., Radha B., Grigorieva I.V. and Geim A.K. 2016 Sieving hydrogen isotopes through two-dimensional crystals *Science* **351** 68–70
- [179] Cismondi F. *et al* 2020 Progress of the conceptual design of the European DEMO breeding blanket, tritium extraction and coolant purification systems *Fusion Eng. Des.* **157** 111640
- [180] Day A., Frattolillo A., Incelli M. and Tosti S. 2017 The coolant purification system in DEMO: interfaces and requirements *Fusion Eng. Des.* **124** 744–7
- [181] Siviero F. *et al* 2019 Characterization of ZAO sintered getter material for use in fusion applications *Fusion Eng. Des.* **146** 1729–32
- [182] Sartori R.A., Karnesky R.A. and San Marchi C. 2012 Tritium barriers and tritium diffusion in fusion reactors *Compr. Nucl. Mater.* **4** 511–49
- [183] Vála L., Kordač M., Melichar T. and Utili M. 2018 Numerical analyses for conceptual design of an irradiation PbLi capsule for testing of protective coatings for the European DEMO breeding blanket project *Fusion Eng. Des.* **136** 797–802
- [184] Santucci A. *et al* 2020 The issue of tritium in DEMO coolant and mitigation strategies *Fusion Eng. Des.* **158** 111759
- [185] Bornschein B., Day C., Demange D. and Pinna T. 2013 Tritium management and safety issues in ITER and DEMO breeding blankets *Fusion Eng. Des.* **88** 466–71
- [186] Utili M. *et al* 2019 Status of Pb–16Li technologies for European DEMO fusion reactor *Fusion Eng. Des.* **146** 2676–81
- [187] D’Auria V. *et al* 2017 Design of a permeator-against-vacuum mock-up for the tritium extraction from PbLi at low speed *Fusion Eng. Des.* **121** 198–203
- [188] Okino F., Calderoni P., Kasada R. and Konishi S. 2016 Feasibility analysis of vacuum sieve tray for tritium extraction in the HCLL test blanket system *Fusion Eng. Des.* **109–111** 1748–53
- [189] Frattolillo A. *et al* 2018 Core fueling of DEMO by direct line injection of high-speed pellets from the HFS *IEEE Trans. Plasma Sci.* **46** 1429
- [190] Lang B., Day C., Frattolillo A., Igitkhanov Y., Pégourié B. and Zohm H. 2017 Matter injection technology for DEMO, state of the art *Fusion Eng. Des.* **123** 186
- [191] Giegerich T. and Day C. 2014 The KALPUREX-process—a new vacuum pumping process for exhaust gases in fusion power plants *Fusion Eng. Des.* **89** 1476–81
- [192] Pearson R.J., Antoniazzi A.B. and Nuttall W.J. 2018 Tritium supply and use: a key issue for the development of nuclear fusion energy *Fusion Eng. Des.* **136** 1140–8
- [193] Miyamae K. *et al* 2020 Fuel flow and stock during deuterium-deuterium start-up of fusion reactor with advanced plasma model *Fusion Eng. Des.* **160** 111794
- [194] Konishi S., Kasada R. and Okino F. 2017 Myth of initial loading tritium for DEMO—Modelling of fuel system and operation scenario *Fusion Eng. Des.* **121** 111–6